Université Catholique de Louvain
Faculté des Sciences
Ecole de Biologie

Université de Namur
Faculté des Sciences
Département de Biologie

Influence of experimental *in situ* shading on *Posidonia oceanica* (L.) Delile biology

Adrien Luyckx

Mémoire présenté en vue de l'obtention du diplôme de Master en Biologie des Organismes et Ecologie

Promoteurs : Dr. Jonathan Richir (ULiège)
Prof. Stanley Lutts (UCLouvain)

Lecteurs: Alberto Borges (ULiège), Michèle Leduc (STARESO), Stanley Lutts (UCLouvain), Muriel Quinet (UCLouvain) and Jonathan Richir (ULiège)

Année académique 2019–2020

Acknowledgments

The first person I would like to sincerely thank is **Jonathan Richir**, my principal supervisor. His supervision of my master thesis was precious all along. On one hand, he helped me a lot with the practical work, not always entertaining, which enabled me to get a considerable amount of various data. On the other hand, I am grateful for his intellectual help, particularly for the statistics and environmental data analysis, but also for giving good advice and helping me redact and interpret the data. I keep in mind the "Good laboratory practices" for my future!

I also specially want to thank Prof. **Stanley Lutts**, my co-supervisor at UCLouvain, who was of precious help for the coordination between ULiège and GRPV laboratory at UCLouvain, where I carried out most of the practical work. I also thank him for the interesting reflexions and advice on pigments and carbohydrates. He was also an important actor for my integration in this research group, for instance by giving me the opportunity to present one of the laboratory's seminars.

I was given the opportunity to extract pigments at Prof. **Fabrice Franck** laboratory (Bioenergetics lab, ULiège). I thank him for that. Moreover, **Amélie Corato**, PhD student in this lab, was of great help for theoretical and practical aspects of pigment extraction. I am grateful to her. Pigments extracts were analyzed by HPLC at the Chemical Oceanography Unit (ULiège), of which I thank Prof. **Alberto Borges**, head of the lab. This experiment was succesfully completed thanks to the precious help of Prof. **Jean-Pierre Descy** and his HPLC. A last person that contributed to pigment analysis is **Erhard Pfündel** (Walz). His advice for solvant choice were greatly useful; I thank him.

I would like to warmly thank all the members of the Research Group in Plant Physiology (GRPV, UCLouvain). They welcomed me kindly with my exotic species, far from the agricultural and phytoremediation species they usually work with. Thank you for allowing me to use all the equipment. I am sure they will forever remember the delicate odour emanating from *P. oceanica* samples! I am particulary grateful to **Brigitte Vanpee** for precious technical help on carbohydrates extraction, **Servane Bigot** for her advice (particularly for carbohydrates analysis) and her enthusiastic interest in my project, **Marie-Eve Renard** on whom I always could rely on for technical issues and Prof. **André Lejeune** for his help with starch hydrolysis.

Joseph Nader (FYMO research group, UCLouvain) made a grinder available to me in his lab, I am sincerely grateful to him !

Most of the sample work in Corsica in 2018 was done with the help of STARESO staff. I thank them for this precious help, particularly **Michèle Leduc**.

The Diving-PAM fluorimeter was a loan from Walz, Germany. I thank **Stéphane Walz** for this.

I also thank **Lisa Buche** for her help with page layout in LaTeX.

I thank Alberto Borges (ULiège), Michèle Leduc (STARESO), Stanley Lutts (UCLouvain), Muriel Quinet (UCLouvain) and Jonathan Richir (ULiège) for accepting to be in my jury and for evaluating my work.

Eventually, I would like to thank my family and my friends for their support.

Résumé

Influence de l'ombrage expérimental *in situ* sur la biologie de *Posidonia oceanica* (L.) Delile

Posidonia oceanica est une espèce ingénieur de magnoliophyte marine endémique de la mer Méditerranée. Elle forme des herbiers monospécifiques denses, de la surface à 40-45 m de profondeur. Cet écosystème est très productif, fournissant un grand nombre de services écosystémiques. Cependant, les herbiers à *P. oceanica* sont menacés par diverses causes environnementales et anthropiques. Parmi elles, la réduction de lumière est un problème majeur qui devrait s'aggraver dans le futur, particulièrement à cause de l'eutrophisation et des sédiments remis en suspension. Ce travail vise à comprendre comment *P. oceanica* répond à un stress d'ombrage faible à moyen pendant sa période principale de production primaire, du printemps à l'été.

Des écrans de différentes tailles de maillage (ombrages approximatifs de 15, 30 et 60% en comparaison au contrôle) ont été installés au-dessus d'un herbier à *P. oceanica* en bon état écologique, à 15 m de profondeur en Corse. L'expérience s'est déroulée entre avril et août 2018. Les pigments (chlorophylles et xanthophylles) ont été dosés dans les feuilles par HPLC. L'activité photosynthétique a été mesurée *in situ* par Diving-PAM (courbes rapides, courbes photosynhtèse/irradiance et rendement quantique). La biométrie des faisceaux et la production primaires ont été évaluées par dissection des pousses. Enfin, les concentrations en sucres solubles et amidon ont été dosés par spectrophotométrie dans les rhizomes.

Les résultats montrent une capacité remarquable de *P. oceanica* à maintenir sa teneur en pigments ainsi qu'à adapter son activité photosynthétique de manière dynamique à l'ombrage. Cependant, une adaptation durable de l'appareil photosynthétique n'est pas observée. L'accumulation de glucides dans les rhizomes au cours du temps est impactée négativement par l'ombrage. Malgré cela, aucun effet sur la croissance de la plante n'est détecté.

La grande résistance des pousses de *P. oceanica* dans un herbier en bon état de conservation à un stress d'ombrage de cinq mois est souligné. En outre, les conséquences potentielles pour la survie de la plante en envisageant un ombrage à plus long terme, au vu de son impact sur l'accumulation de glucides, est discuté. Ces résultats sont comparés à d'autres études *in situ* et à des travaux réalisés le long du gradient bathymétrique, en insistant sur la différenciation génétique et l'adaptation des pousses de *P. oceanica* à une profondeur donnée (c'est à dire à un environnement lumineux donné) qui en découle.

Abstract

Influence of experimental *in situ* shading on *Posidonia oceanica* (L.) Delile biology

Posidonia oceanica is a keystone seagrass species indigenous to the Mediterranean Sea. It forms dense monospecific meadows from the surface to depths of 40-45 m. The meadows are highly productive and provide many valuable goods and services. However, *P. oceanica* meadows are threatened by several environmental and anthropogenic stressors. Among these, light deprivation is a major problem that is expected to worsen in the future, particularly because of eutrophication and sediment resuspension. This work aims to understand how *P. oceanica* responds to environmentally relevant shading during its spring to summer important period of primary productivity.

Screens of different transparency (nominal reduction of 15, 30 and 60% compared to control) were deployed on a healthy meadow at a depth of 15 m, in Corsica. The experiment took place between April and August 2018. Pigments content (chlorophylls and xanthophylls) in leaves was analyzed with HPLC; photosynthetic activity (rapid light curves, photosynthesis/irradiance curves and quantum yield) was monitored with a Diving-PAM; biometry and primary production were estimated after dissection of shoots; starch and soluble carbohydrates content in rhizomes was investigated by spectrophotometry.

Results show a remarkable capacity of *P. oceanica* to maintain its pigment content, as well as to adapt dynamically its photosynthetic activity to the light reduction. However, an adaptation over the experiment period of the photosynthetic apparatus is not observed. Carbohydrates accumulation in rhizomes over time is negatively impacted by shading treatments, resulting in a lower content at the end of summer. In spite of that, light deprivation does not reduce shoots growth.

The high resistance of healthy *P. oceanica* shoots to a five months experimental *in situ* light deprivation stress is underlined. Furthermore, the potential consequences for the plant survival under a longer shading period, in light of the decrease in reserve carbohydrates content, is discussed as well. These results are compared to bathymetric studies and other *in situ* shading experiments, emphasizing the genetic differentiation along the depth gradient and the resulting adaptation of *P. oceanica* shoots to a given depth, i.e., to a given light environment.

Contents

List of Figures

List of Tables

List of abbreviations

α	Initial slope of light curves
AF	Absorption factor
AIC	Akaike information criterion
Chl a/b	Chlorophyll a/b
DA	Dark adapted
DW	Dry weight
e^{-1}	Electron
ETC	Electron transport chain
ETR($_m$)	(Maximal) electron transfer rate
F_v/F_m	Maximal quantum yield
FW	Fresh weight
HPLC	High performance liquid chromatography
I_k	Saturating irradiance
LA	Light adapted
LHC	Light harvesting complex
NADP(H)	Nicotinamide adenine dinucleotide phosphate
NPQ	Non photochemical quenching
PAR	Photosynthetically active radiation
P/I curve	Photosynthesis/Irradiance curve
PSI/PSII	Photosystem I/II
qP	Photochemical quenching
rETR	Relative electron transport rate
RBP	Ribulose-1,5-bisphosphate
RLC	Rapid light curve
ROS	Reactive oxygen species
RPPC	Reductive pentose phosphate cycle
VAZ	Violaxanthin/ Antheraxanthin/ Zeaxanthin
Y(II)	Effective quantum yield

1

Introduction

1.1 Seagrass meadows

Seagrass beds are major coastal ecosystems found worldwide. They are usually made up of a monospecific – sometimes a few species – community of seagrass (Tussenbroek et al. (2006)). Seagrass is a polyphyletic group of angiosperm species that belong to 4 families: *Cymodoceaceae*, *Hydrocharitaceae*, *Posidoniaceae* and *Zosteraceae* (Jayathilake and Costello (2018)), all classified in Alismatales (The Angiosperm Phylogeny Group (2016)). As these plants are restricted to shallow waters (because they need light and anchorage), they account for a small percentage of ocean's surface. On the basis of a model, the total surface of seagrass has been estimated to be about 1.6 million km^2 (Jayathilake and Costello (2018)). However, this value is probably overestimated because of some missing data (e.g. substrate nature). Mediterranean Sea is home to 6 indigenous seagrass species (*Posidonia oceanica*, *Cymodocea nodosa*, *Zostera marina*, *Zostera noltii*, *Ruppia cirrhosa* and *Ruppia maritima*), of which *P. oceanica* is by far the most abundant (Boudouresque et al. (2009)).

1.2 *Posidonia oceanica*

1.2.1 *P. oceanica* meadows description

Posidonia oceanica (L.) Delile – whose vernacular name is "Neptune grass" – is a seagrass endemic to the Mediterranean Sea (Guiry and Guiry (2019)). First classified in *Posidoniaceae* family, the latest update of the Angiosperm Phylogeny Group (APG IV) suggests the inclusion of this family within *Jundcaginaceae*, along with other plant families with similar ecology (e.g. *Zosteraceae* and *Cymodoceaceae*) (The Angiosperm Phylogeny Group (2016)). The genus *Posidonia* includes 9 species, of which 8 are native to southern Australia, *P. oceanica* being completely isolated from its sisters species (Gobert et al. (2006)).

P. oceanica is found in monospecific beds. The species is estimated to cover about 1.2 million ha (less than 0.5% of Mediterranean Sea surface) (Telesca et al. (2015)). As shown on figure 1.1, current available data reveals that *P. oceanica* is found along most of the northern Mediterranean coastline and absent in the eastern-most region. The species does not grow near the main rivers mouths because of sediments and fresh water (it can not tolerate salinities under 33 ppt) (Gobert et al. (2006) and Telesca et al. (2015)). The plant has a subtidal distribution because it does not tolerante dessication; it can grow between the surface and about 40-45 meters depth (Gobert et al. (2006) and Procaccini et al. (2017)).

The EU Habitat Directive considers *P. oceanica* meadows as a priority habitat (Personnic et al. (2014)).

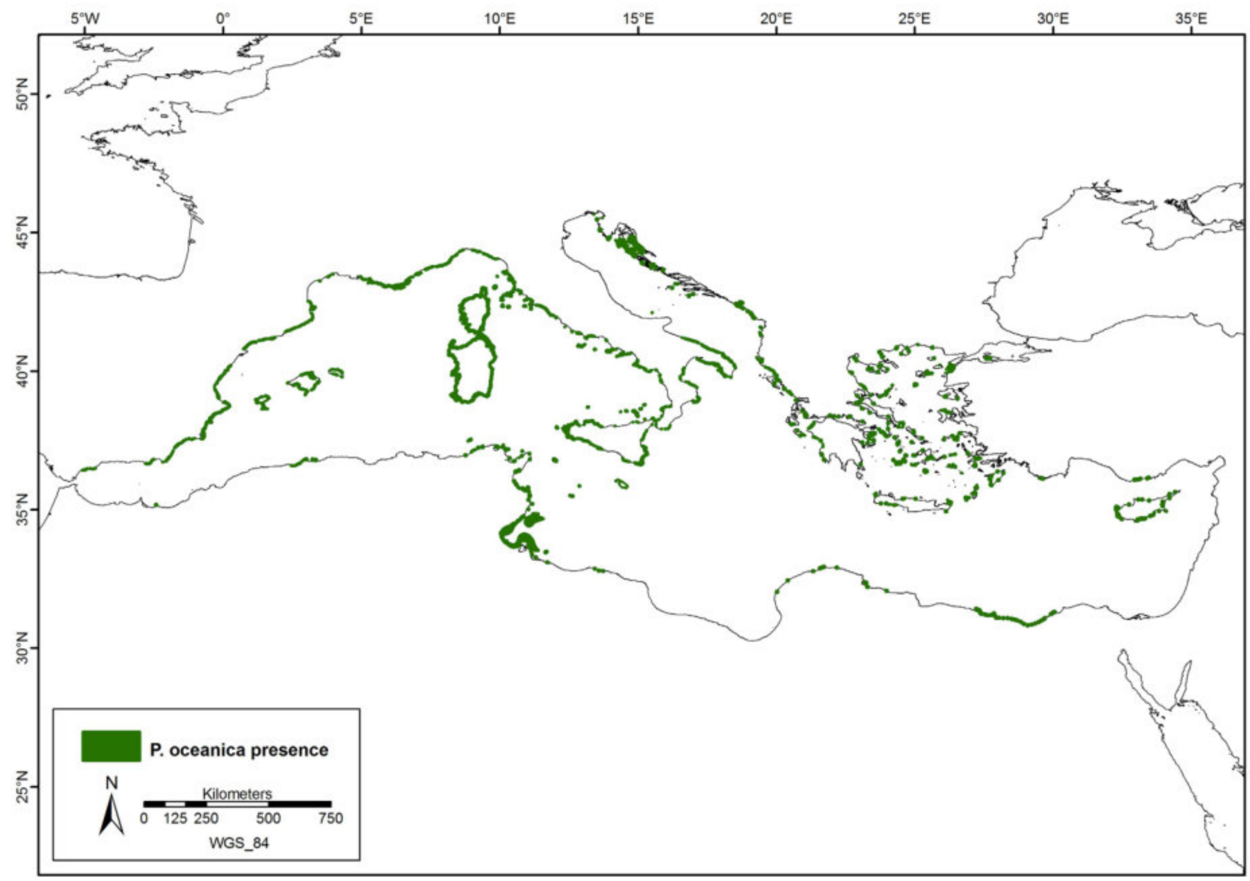

Figure 1.1: **Distribution of *P. oceanica* in 2015.**

Regions with an apparent absence of *P. oceanica* have to be considered carefully, since it could be the result of a lack of investigation and cartography (e.g. Africa coastline). From Telesca et al. (2015).

Morphology *P. oceanica* can be divided into two main parts: leaves and the roots-rhizomes system. There is no true shoot since leaves are directly fixed on the rhizomes (sessile leaves), but 'shoot' is often used in the literature to describe a bundle of leaves and the rhizome tip on which the leaves are anchored (Personnic et al. (2014)). Leaves are linear. Three leaf development stages are described by Giraud (1979): adult, intermediates and juveniles leaves. Adult leaves are made up of two distinct sections. The tough basal region, a few centimeters long, is the sheath (also called "sheathed petiole" or "scales"). The main part of the leaf is the lamina (or "leaf blade"). The boundary between these two structures is called the ligula (Giraud (1979)). Juvenile and intermediates leaves, however, do not have a petiole. Juveniles leaves are distinguishable from intermediates ones by their length (<5 cm). For each shoot, each new leaf grows between the two previous ones, resulting in an alternate leaf layout with the youngest leaf at the center of the shoot. The meristem is located at the leaf's basal region (acropetal growth) (Boudouresque et al. (2012)). Leaves have a long lifespan, up to 7-12 months (Gobert et al. (2006)). The important longevity allows the plant to limit leaf renewal, and therefore limit nutrients requirements (S. Gobert et al. (2002)). Unlike dead leaf blades that break away from shoots (whose fate is detailed in section 1.2.2), leaf sheaths persist on rhizomes for many years. Rhizomes, on which roots are anchored, grow either horizontally (called plagiotropic rhizomes) or vertically (orthotropic rhizomes). In the empty spaces between them, the sediment accumulates through time. Therefore, the deepest and oldest roots-rhizomes die, buried in the sediment. They are protected from decay and can remain untouched for a long time. That is why *P. oceanica* meadows are considered as carbon sinks (see section 1.2.2). All roots and rhizomes (live and dead) with old sheaths are called 'matte' (Boudouresque et al. (2009) and Giraud (1979)). Given the persistence of the matte, analysis of annual cyclic variations in size of dead leaf sheaths and rhizomes (lepidochronology, Pergent et al. (1989)) is used to assess past environmental conditions to which the plant has been exposed (e.g. Pergent et al. (1997a) and Tomasello et al. (2016)).

Phenology Old leaves necrose and decay regularly (Gobert et al. (2006)), with a peak in the end of summer (Pergent and Pergent-Martini (1991)). New juvenile leaves grow continuously throughout the seasons with a peak in autumn (Pergent and Pergent-Martini (1991) and Buia et al. (1992)). About 6-9 leaves are produced every year on each shoot (Personnic et al. (2014)). Orthotropic rhizomes grow at a maximal rate of 7 cm per year. Its longevity is important; the plant can be many tens years old (Gobert et al. (2006)). Both growth rate and biomass are maximal in early summer (figure 1.2, Alcoverro et al. (2001)).

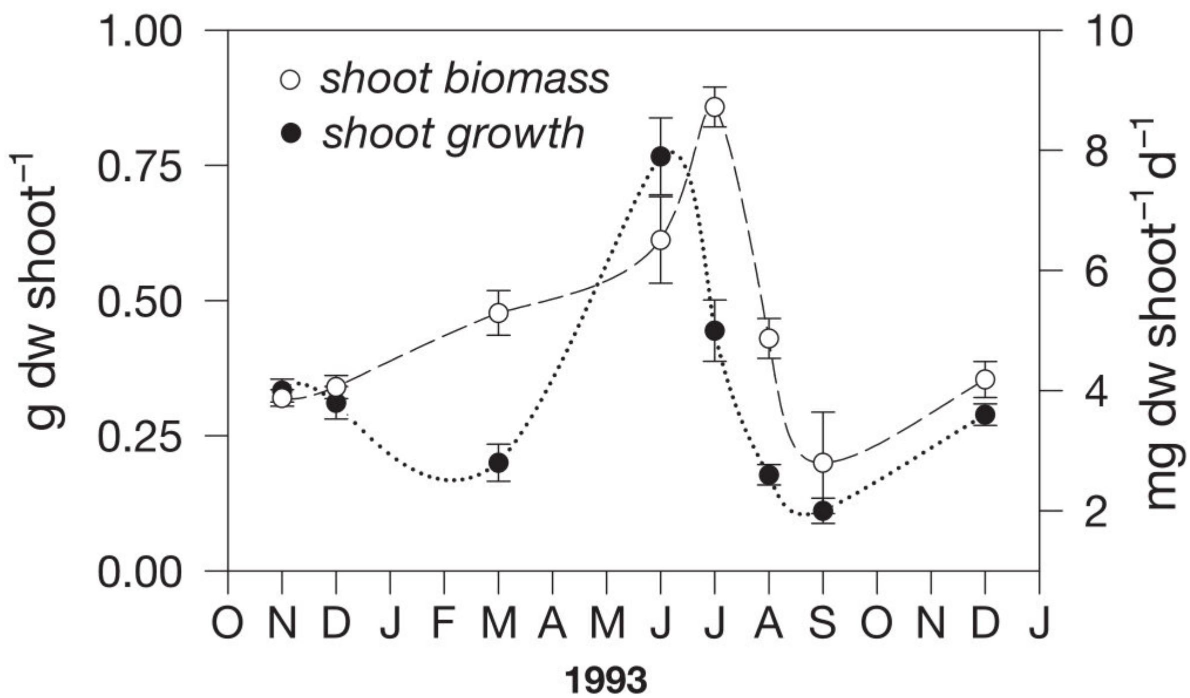

Figure 1.2: **Shoot biomass (left y-axis) and growth rate (right y-axis) of a meadow at 5 m depth, near Medes Islands (western Mediterranean Sea).**

From Alcoverro et al. (2001).

Reproduction Reproduction occurs mainly by asexual clonal propagation. Sexual reproduction (hermaphroditic flowers on a cymose inflorescence, protandry (Ackerman (2006))), despite its important role in adaptation and dispersal, is scarce and rarely abundant. Flowers appear in the autumn, a little earlier near the surface compared to more important depths, when photoperiod decreases and water temperature drops (Buia and Mazzella (1991)). Reproduction events are thought to be dependent on many life-history, environmental and genetic factors (Ruiz et al. (2017)). Pseudoviviparity (development of asexual plantlets in flowers) has been observed once in north-west Mediterranean Sea; it is supposed to contribute to short-distance dispersal (Ballesteros et al. (2005)).

Epiphytes Epiphytes are an important component of *P. oceanica* meadows ecology, accounting for 660 species[1] on leaves and/or on rhizomes (Piazzi et al. (2016)), whose biomass can reach 30% of total canopy biomass (Lepoint et al. (1999)). Since leaves lifetime is long, many organisms can grow on their surface before leaves decay (Alcoverro et al. (1997)). Macrophytes (brown algae and red algae, of which mostly species in *Corallinaceae* family), animals (Bryozoa and Hydrozoa) and bacteria (e.g. cyanobacteria) are the main taxons found among *P. oceanica* epiphytes (Casola

[1] All the species are not found in the entire Mediterranean Sea, there are some geographical gradients (Piazzi et al. (2016)).

et al. (1987) and Jacquemart and Demoulin (2006)). They can be classified into two main groups: epifauna (sessile animals) and epiflora (algae). Macroalgae are by far the dominant group over animals. However, the epiflora/epifauna ratio varies between meadows (Piazzi et al. (2016)). Among epiflora, two layers – encrusting and upright – are described (Mazzella et al. (1989)).

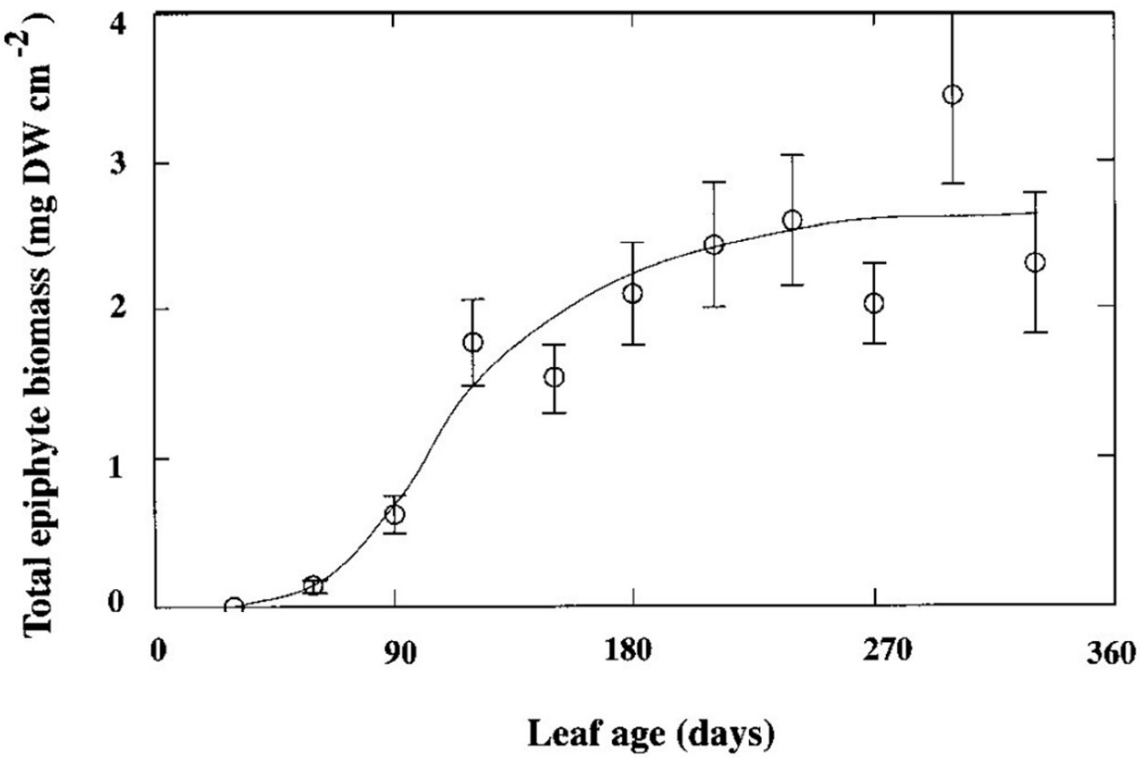

Figure 1.3: **Accumulation of epiphytes on *P. oceanica* leaves with increasing leaf age. From Cebrián et al. (1999).**

Epiphyte distribution, biomass and taxonomic composition is far to be homogeneous on leaves and through the meadow. An epiphytes gradient is observed across the leaf blade, from the basal region to the apex (Casola et al. (1987), Cebrián et al. (1999), and Personnic et al. (2014)). Epiphyte biomass increases towards the leaf apex. The dominant taxon changes through time. Indeed, brown algae grow fast, being dominant over red algae, and reach their maximal size at leaves half-lifespan. Afterwards, encusting red algae keep growing, resulting in a shift in dominance toward red algae when leaves are old. Furthermore, old leaves carry more epiphytes than young leaves. The accumulation of epiphytes on leaves through the year follows a sigmoid curve (figure 1.3). The plateau is explained by an equilibrium between epiphytes growh and herbivory (Cebrián et al. (1999)). The maximal biomass is observed in June, whereas the minimal one occurs in December (Lepoint et al. (1999)).

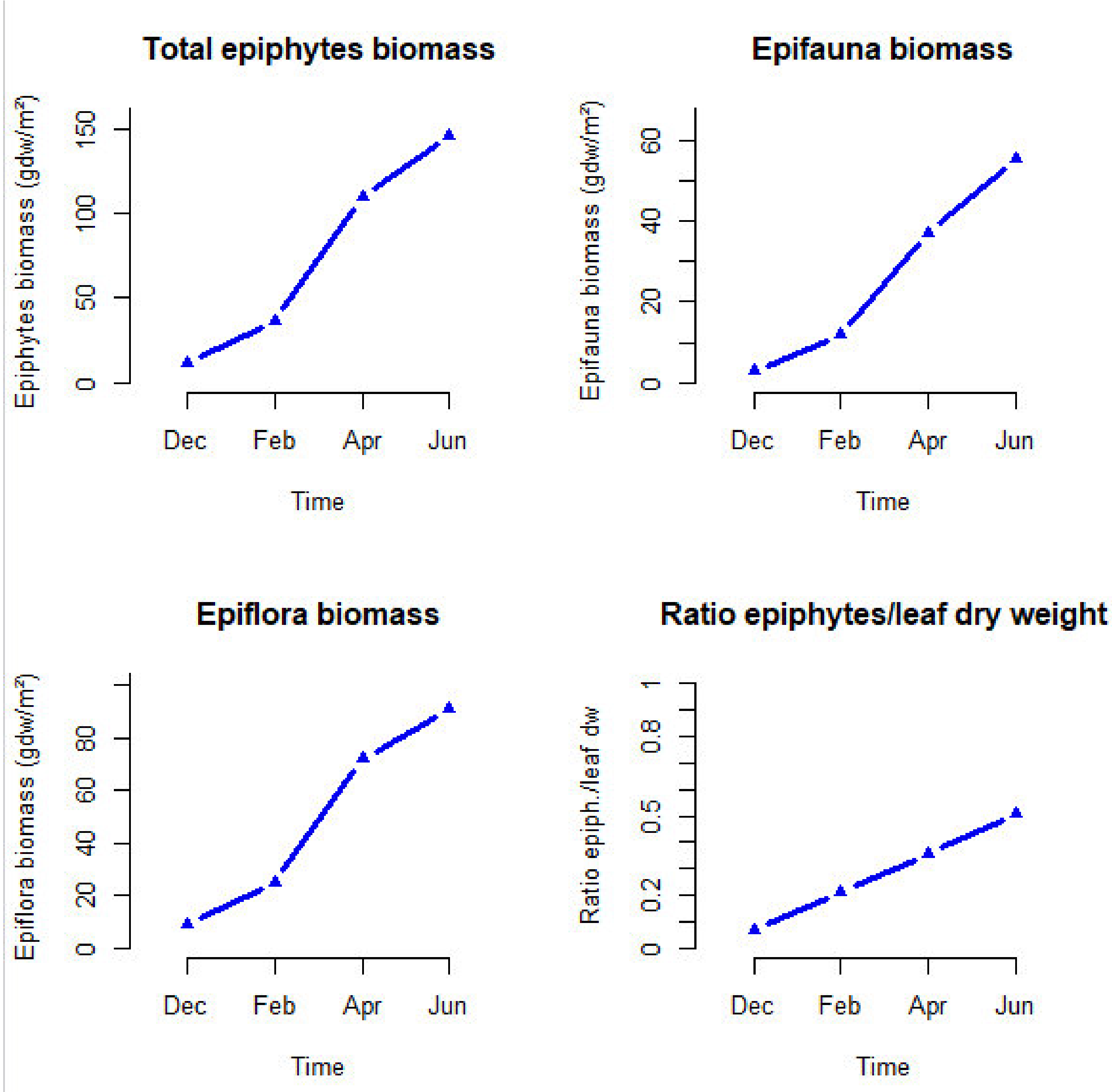

Figure 1.4: **Variation in *P. oceanica* epiphytes biomass between december 1993 and june 1994 in the meadow next to STARESO (Corsica).**

Drawn with data from Lepoint et al. (1999).

Epiphytes composition and abundance on leaves is changing through seasons (figure 1.4). Both epifauna and epiflora biomass increase through spring and summer. The ratio between epiphytes and leaves biomass also rises (Lepoint et al. (1999)). *P. oceanica* leaves epiphytes are an important source of food for herbivores. That is the main reason for grazers to eat leaves tips (where epiphytes biomass is maximal), since leaves themselves are not much palatable (Alcoverro et al. (1997)).

The epiphyte layer is not without consequences on *P. oceanica*. Physical contact (the anchorage in plant tissues differs between species) and shading can affect the plant fitness. On one hand, physical contact causes oxidative stress. On the other hand, shading decreases photosynthesis and thus primary productivity, but also reduces photodamage and reactive oxygen species (ROS) production that result from an excess of light (Costa et al. (2015)).

Depth gradient Since *P. oceanica* grows between the surface and 45m depth, it is exposed to strongly different environmental conditions. Indeed, several environmental parameters change along the depth gradient, of which the most important is light quantity and quality (considerations about light are detailed in section 1.3). This results in gradual changes in several measurements with depth, like foliar index (total leaf surface per ground surface area), leaf size and biomass, epiphytes biomass, shoot density and estimation of herbivory (A coefficient), as shown on figure 1.5 (Gobert (2002)). Epiphyte taxonomic composition also varies with depth.

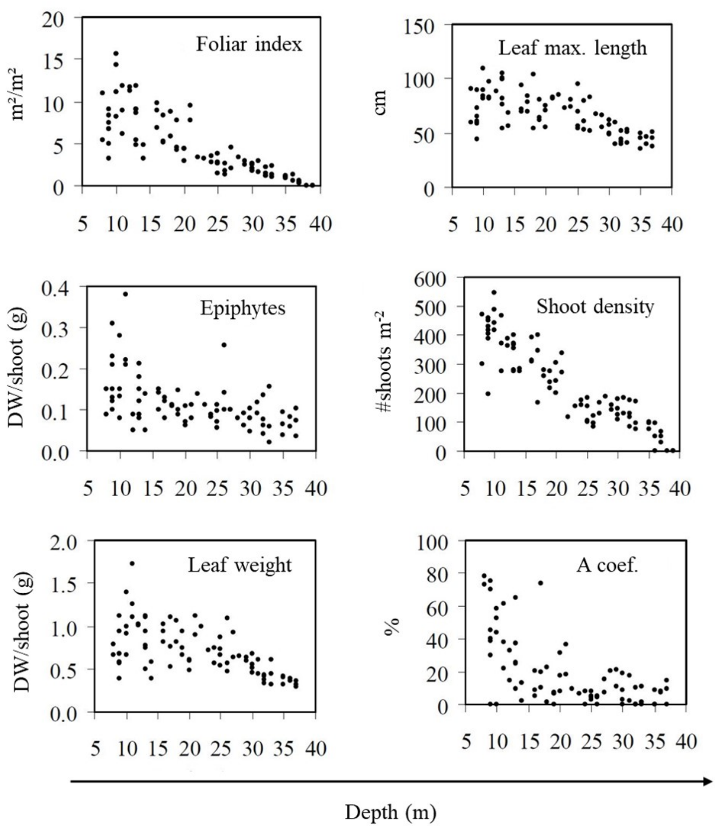

Figure 1.5: ***P. oceanica* morphological parameters along the depth gradient**
DW: dry weight. Data collected in Revellata bay (Corsica) in june 1993. From Gobert (2002).

1.2.2 Ecology

P. oceanica, as well as many other seagrass species, is an engineer species that is the main element of an rich climax ecosystem (Boudouresque et al. (2009)). It requires a stable substrate enriched in organic matter, conditions that can be provided by colonization of some pioneer plant and algae species like *Caulerpa prolifera*, *Cymodocea nodosa* or *Zostera* sp. (Gobert et al. (2006)).

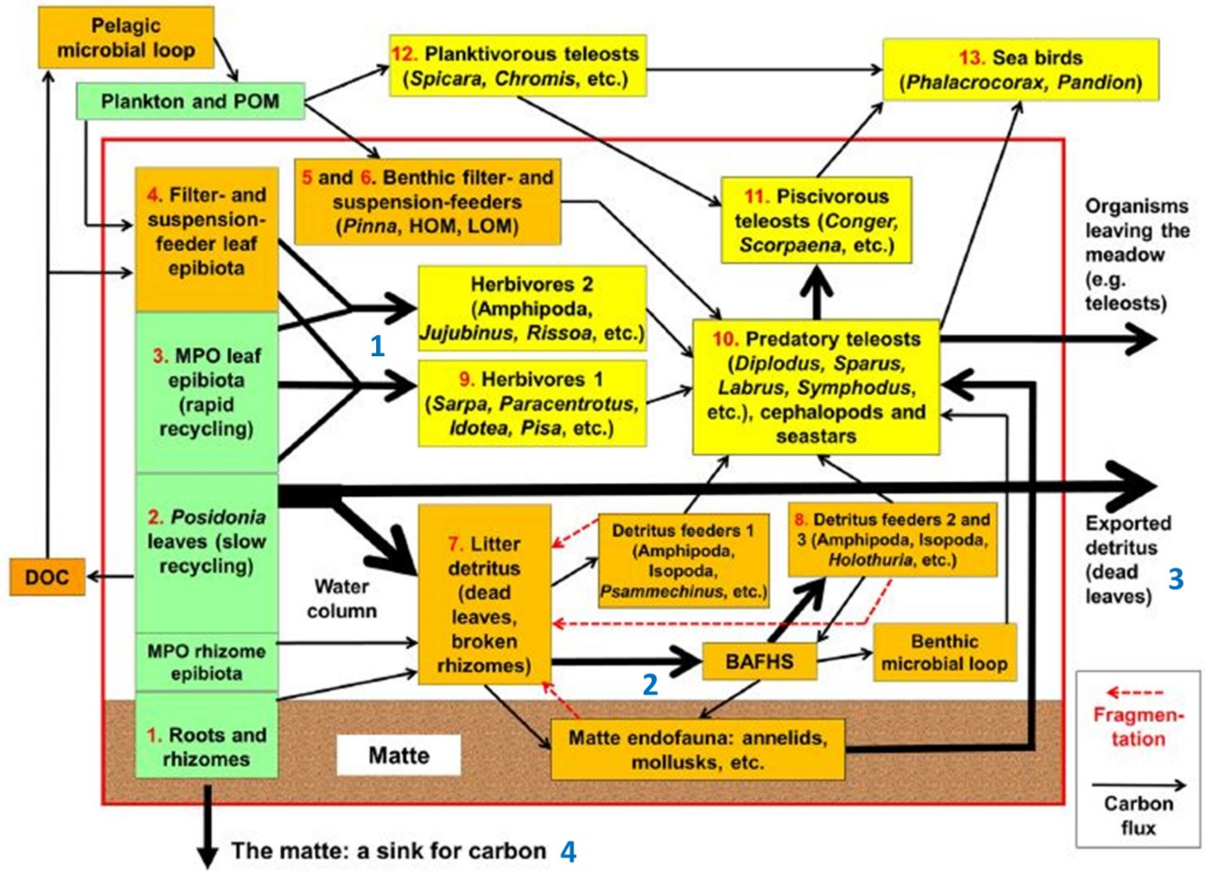

Figure 1.6: **Model of a *P. oceanica* ecosystem**
POM: Particulate Organic Matter; DOC; Dissolved Organic Carbon; MPO: Multicellular Photosynthetic Organisms; BAFHS: *Bacteria*, *Archaea*, Fungi and Heterotrophic Stramenophiles. Blue numbers show the four main fates of *P. oceanica* leaves: (1) Consumption by herbivores; (2) *in situ* decomposition; (3) Exportation outside the meadow; (4) Long-term storage in the matte. From Personnic et al. (2014).

Several ecosystems are associated with *P. oceanica*. The living meadows is the central one and the most diversified. Besides that, dead matte and accumulation of exported biomass can be considered as other ecosystems.

The living meadow With the aim of developing a biotic indice that would provide some insight into *P. oceanica* ecosystem health, it has been divided into many functional compartments (Personnic et al. (2014), figure 1.6). The central component of their model is living *P. oceanica*, itself divided into 4 sub-compartments: roots and rhizomes system (matte), leaves, and their associated epifauna (filter- and suspension-feeders on rhizomes, belonging to Bryozoa, Hydrozoa, Porifera, Annelida, Tunicata, Gastropoda and Bivalva) and epiflora (figure 1.6, in green). Primary production of *P. oceanica* has four main fates: three for leaf and rhizomes that necrose and break apart (litter detritus) and one for living leaves (Pergent et al. (1997b)). Necrosed biomass is either exported outside the meadow (see next paragraph), eaten by pelagic or benthic detritivores (e.g.

Holoturia), or recycled *in situ* by unicellular and multicellular decomposers (BAFHS, benthic and pelagic microbial loops) (see figure 1.6 caption). Furthermore, fresh leaves and/or their epiphytes are directly grazed by very few herbivorous species, themselves eaten by primary and secondary (even more) predatory animals (Teleostea, Asteroidea, Cephalopoda, Aves), sometimes leaving the ecosystem. An amount of this biomass can come back in the meadow through excrements. Some organic matter is relased in the water column as dissolved organic matter (DOC) or particular organic matter (POM) that is consumed by filter- and suspension- feeder organisms like plankton or *P. oceanica* epiphytes (Personnic et al. (2014)). The relative amount of these four ways does dependent on hydrodynamic forces and therefore on depth. Extrapolation of local data leads to an estimation of 1.2 million tons of exported carbon and 1.1 million tons of recycled carbon each year (Pergent et al. (1997b)). Exported carbon is estimated to account for about 6-50% of the net primary production of *P. oceanica* (Personnic et al. (2014)).

Other ecosystems Leaves that continuously die are torn away from rhizomes and exported, in part, to unvegetated areas (e.g. sand patches) where they accumulate with other dead biomass (e.g. macroalgae). Such accumulations shelter microorganisms (bacteria, fungi, diatoms) and invertebrates that contribute to organic matter decomposition and are thus considered as – despite temporary – real ecosystems. In these litter accumulations, invertebrates are dominated by copepodes and nematodes, those accounting for more than 50% of total individuals (Mascart et al. (2015)). Many other organisms are found to a lesser extent. The relative amount of individuals of different taxons varies throughout the year, which makes sense since *P. oceanica* dead leaves production is not constant (Pergent et al. (1997b)). Biomass can be exported to deep waters, where it provides energy for food webs (C. F. Boudouresque et al. (2016))

When shoots die – resulting from a natural disaster (e.g. strong currents or waves) or from anthropogenic pressure –, the matte becomes unprotected and is colonized by many organisms. The species diversity of motile macroinvertebrates even seems to be higher in a dead matte environment compared to a living meadow's matte. The additional species are mainly detritivores. The different species composition could also be explained by differences in light intensity at the surface of the matte. However, this ecosystem goes toward degradation because of the lack of photosynthetic primary production (Borg et al. (2006)). Moreover, recolonization of a bare matte by *P. oceanica* is often impossible, because of (1) changes in sediment chemistry that takes place in the matte without shoots (Abadie et al. (2016)) and (2) prior recolonization by competitive species like the alien invasive species *Caulerpa cylindracea* (Kiparissis et al. (2011)).

1.2.3 Ecosystem services and regression of *P. oceanica* meadows

Ecosystem services are defined as *the aspects of ecosystems utilized (actively or passively) to produce human well-being* (Fisher et al. (2009)). Nordlund et al. (2016) have summarized several services provided by seagrass, including the use in agriculture and as food source, the production of valuable chemicals, water purification, use for biomonitoring and diverse other cultural/society benefits (tourism, recreation, spirituality). Vassallo et al. (2013) hightlighted four main ecosystem services provided by *P. oceanica* meadows: nursery, coastline protection, primary production and carbon sequestration. As a nursery for fishes, they contribute to fish stocks. The large leaves catch sediments and break waves, resulting in shoreline protection. Moreover, dead leaves accumulate on beaches and play also a role of protection (Campagne et al. (2015)). *P. oceanica* and its photosynthetic epiphytes provide fresh biomass through photosynthesis, as well as releasing oxygen in the water column. They also underline the highly efficient carbon sequestration in the matte.

Some authors estimate the value of this ecosystem to be about 170€ m^{-2} $year^{-1}$, mainly because of sediment trapping (Vassallo et al. (2013)). This value must be considered carefully, since several methods are used to assess ecosystemic services value. For example, Campagne et al. (2015) have rather estimated that a *P. oceanica* meadow is worth between 0.0284€ and 0.0514€ m^{-2} $year^{-1}$, much less than Vassallo et al. (2013).

Despite providing those valuables ecosystem services, *P. oceanica* meadows are threatened by anthropogenic pressure. Excess nutrients and organic matter inputs can decrease the plant's fitness, especially because of light attenuation caused by phytoplankton blooms that result from eutrophication (see section 1.4). Coastal erosion, mechanical impacts (e.g. destruction of meadows with anchoring and trawling) and climate change (figure 1.7, Marbà et al. (2014)). Some meadows are currently extending, but many are quickly shrinking, the net area at the scale of the whole Mediterranean Sea decreases. Changes (often regressions) in shallow and deep depth limits are often observed (Marbà et al. (2014)).

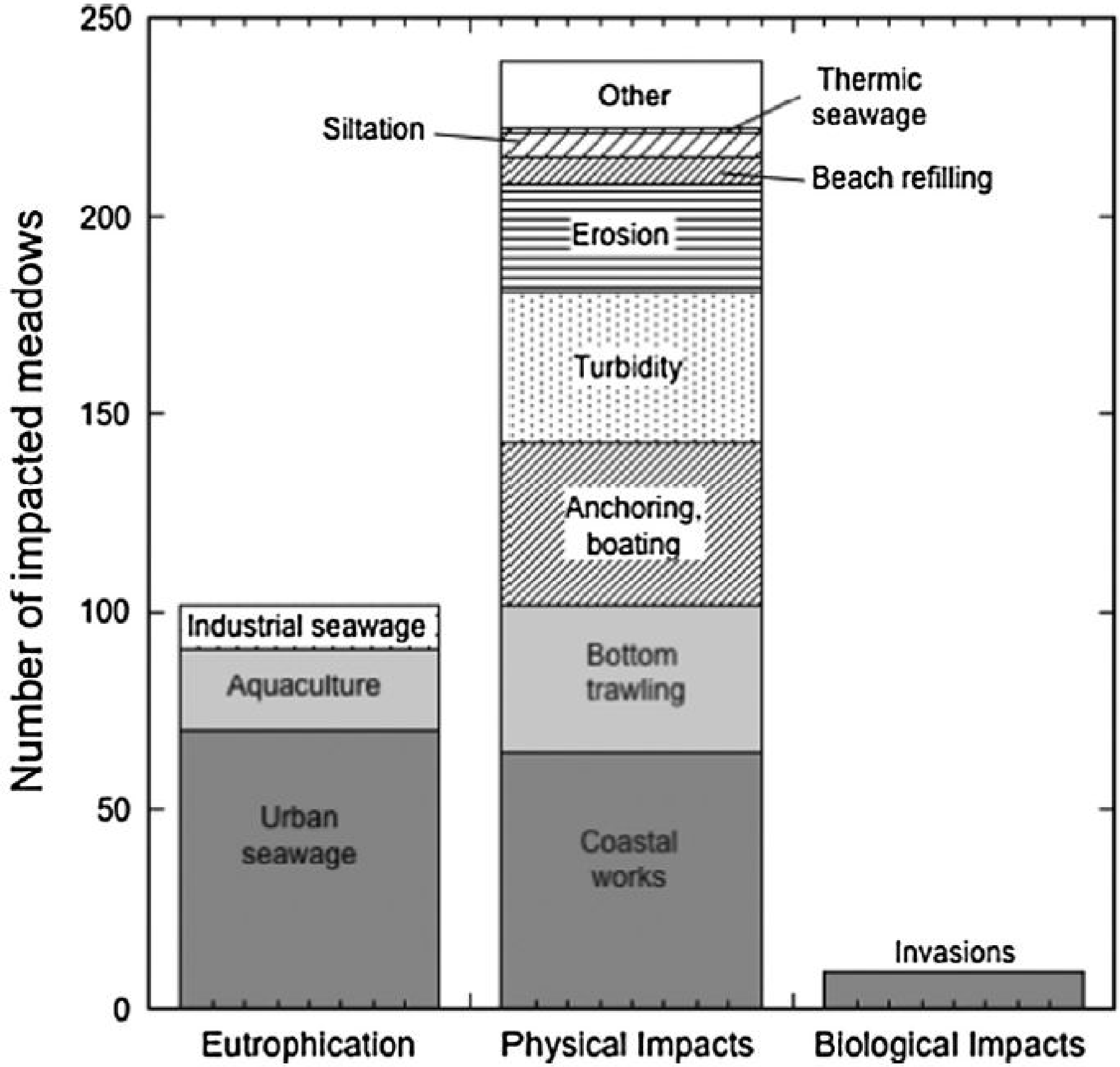

Figure 1.7: **Main threats to which *P. oceanica* is exposed.**
From Marbà et al. (2014).

1.3 Photosynthesis and primary production

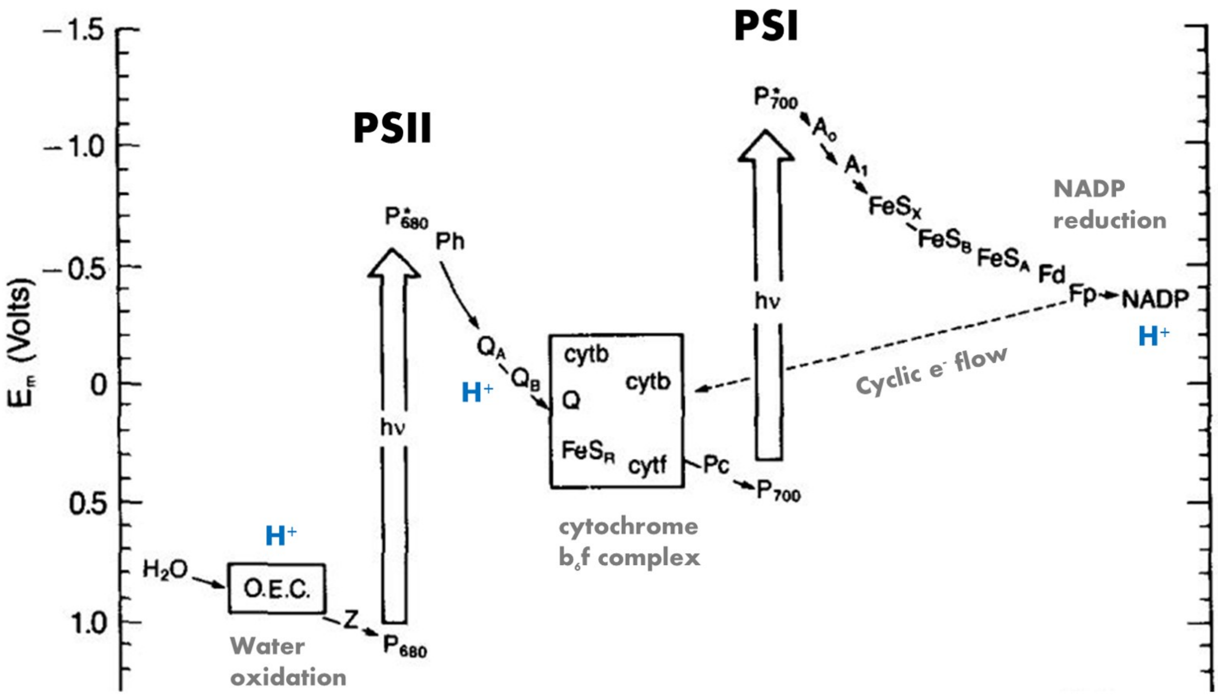

Figure 1.8: **Overview of the oxygenic photosysnthesis electron transport chain**
Water is oxidized at the oxygen-evolving complex (O.E.C). Chl a in PSII is then oxidized with light energy (hν). The electrons go through the cytochrome b_6f complex before a second chl a oxidation in PSI. After several intermediates, $NADP^+$ is reduced. Blue H^+ are steps involved in the proton gradient. Adapted from Blankenship and Prince (1985).

1.3.1 The basics of photosynthesis

Photosynthesis takes place in thylakoids, within chloroplasts. It is divided into two main steps: **light reactions** and **carbon reaction**.

Light reactions First, photons are absorbed by photosystems, that are complexes of proteins and pigments located in the thylakoid membrane of chloroplasts. Two different photosystems – with roughly the same structure but differing in wavelength absorption spectra – working in series are found in plants. Photosystem II (PSII) is the site of water oxidation and the maximal absorption of its reaction center (two chlorophyll molecules) is at 680 nm (red). On the other hand, photosystem I (PSI) reaction center absorbs light with a maximum at 700 nm (far-red) and works after PSII in electron transfer. Cytochrome b_6f complex is another important complex that carries the electrons between PSII and PSI (figure 1.8). A photosystem is made up of a **reaction center** – in which chlorophyll oxidation takes place – surrounded by a **light-harvesting**

complex (or **antenna complex**) – which consists of many pigments that bring light energy to the reaction center (two chl a molecules), associated with proteins –. In higher plants, light-harvesting complexes (LHC) contain between 200 and 300 chlorophylls (chl a and chl b) associated to each reaction center (LHCII for PSII and LHCI for PSI) besides other pigments, like lutein that contributes to excitation energy transfer, or other xanthophylls involved in non-photochemical quenching (see paragraph **Xanthophyll cycles**) and proteins that can bind these pigments. The pigments are not arranged randomly. The maximum absorption wavelength of pigments close to the reaction center is higher (excitation energy is thus lower) than the one of pigments that are more distant from the RC. Close to the RC are found chl a and carotenoids whereas the periphery is made up of chlorophylls a and b (Demmig-Adams and Adams (1996)). Therefore, energy transfer is thermodynamically favorable toward the reaction center and not backwards.

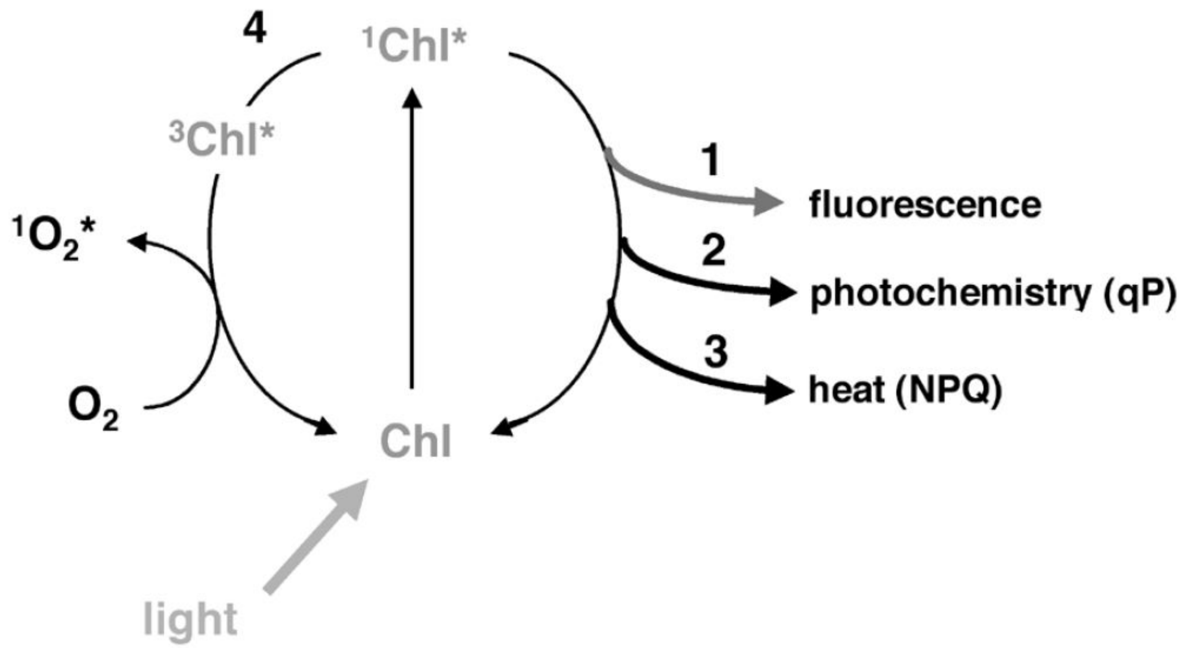

Figure 1.9: **Fates of the energy released by excited chlorophyll molecules**
From Muller (2001).

When a chlorophyll molecule is excited by a photon, some electrons switch to a higer energy level (single-state, ^{1}Chl*). When they come back to the ground state, the energy is released, following four feasible fates (Ralph and Gademann (2005), Taiz et al. (2015), and Muller (2001)). First, fluorescence can be emitted (figure 1.9 (1)). Otherwise, the energy could be transferred to an adjacent molecule by FRET (**F**örster **r**esonance **e**nergy **t**ransfer). Photochemistry can be triggered in the reaction center if the energy reaches it through resonance transfer between many pigments. It is called **photochemical quenching** (qP) (figure 1.9 (2)). Another fate is heat dissipation, mainly through the xanthophyll cycle (**non-photochemical quenching**, NPQ) (figure 1.9 (3)).

Finally, excited chlorophyll can shift to another excited state (triplet-state, $^3Chl^*$) that is a strong reactant that produces singlet oxygen ($^1O_2$), a higly reactive ROS (1.9 (4)). Non-photochemical quenching will be detailed in section 1.3.2. If an excited electron leaves a chlorophyll, it is replaced with another coming from a neighbouring pigment (or from water at the beginning of the process, in PSII) (Taiz et al. (2015)).

After PSII, electrons are carried through the electron transport chain (ETC). They are first loaded on membrane-bound plastoquinones that are intermediates before the cytochrome b_6f complex. Then, electrons are transported to PSI by plastocyanin, a soluble protein. In PSI, $NADP^+$ is reduced to NADPH with electrons that come originally from water oxidization. The ETC electron carriers have increasing redox potentials through the chain. This model is called 'Z-scheme', in reference to the shape of the variations in redox potential (figure 1.8). Besides carrying electrons, some ETC intermediates also transport protons through the thylakoid membrane, from the stroma to the lumen (figure 1.8). The resulting proton gradient is used by ATP synthases as a source of energy to phosphorylate ADP. NADPH and ATP pools are the source of energy for the carbon reaction of photosynthesis.

The reductive pentose phosphate cycle The first step of carbon reactions is the reductive pentose phosphate cycle (RPPC). NADPH and ATP, synthetized at the end of the light reactions, are used to reduce CO_2 to carbohydrates. In seagrass, CO_2 mainly comes from HCO_3^- dissolved in water (Beer et al. (2014)). First, CO_2 is fixed on a ribulose-1,5-bisphosphate (RBP) molecule. This reaction is catalyzed by the enzyme ribulose-1,5-bisphosphate carboxylase-oxygenase (RuBisCO). Throughout the RPPC, many intermediate metabolites are involved, consuming ATP and NADPH. For each 3 CO_2 molecule that enters the cycle, a triose phosphate leaves the cycle. Meanwhile, metabolites that remain in the cycle are recycled to RBP through many steps (Taiz et al. (2015)). Unlike all photosynthesis steps that occur in chloroplasts, synthesis of diverse carbohydrates using trioses phosphate (synthetized in RPPC) takes place in various compartments. Statch is synthesized in chloroplasts, whereas sucrose is produced in the cytosol (Taiz et al. (2015)).

1.3.2 Regulation of photosynthesis

A fine regulation of photosynthesis is required since light conditions under which plants develop are not constant. They have to cope with changing irradiance through seasons. Furthermore, light intensity variations occur at a much smaller scale. It can suddenly decrease or increase because of a quick and short change in local conditions (e.g., a cloud shading the sun, leaves shaded by other leaves because of their movement). Furthermore, tides and waves are short-term fluctuations specific to the marine environment. Some seagrass species are intertidal, thus daily exposed to direct light and light attenuated by water (that is not true for *P. oceanica*, which is strictly subtidal, Beer et al. (2014)). Therefore, seagrass need to be able to quickly cope with such stochastic and rapid light fluctuations (through photoacclimation) (Ralph et al. (2002)). Besides light quantity, its quality also matters for plants. Along the depth gradient, a change in light spectrum is observed, with a decrease in red photons (strongly absorbed by water) and an increase in blue photons proportion (Beer et al. (2014)). Moreover, light intensity decreases quickly with depth.

Photosynthesis, as a master metabolic pathway, shows an important long- and short-term plasticity. When light irradiance is under saturation, energy is mostly dissipated through photochemical quenching (photochemistry). However, when light intensity exceeds saturation, the excessive energy must be dissipated. Fast changes include **photoinhibition**, that is the decrease in photosynthesis efficiency through decrease of chlorophyll quantum yield and increase in non-photochemical quenching (heat dissipation) in PSII. These mechanisms protect the photosynthetic apparatus from damage induced by high light irradiances (Ralph (1999)). In contrast, the long-term plasticity relies on the regulation of pigments contents, which is a slow acclimatization process in response to permanent changes in light irradiance (Ralph et al. (2002)).

Non-photochemical quenching When a plant is exposed to a light intensity higher than what can be used by the carbon reaction, excess energy must be dissipated, otherwise it could damage some structure. It is mainly dissipated through the xanthophyll cycles that converts the excess energy into heat. Two xanthophyll cycles have been described in vascular plants so far (figure 1.10, Jahns and Holzwarth (2011) and García-Plazaola et al. (2007)). They both dissipate excessive light energy in PSII through de-epoxidation of xanthophylls. The VAZ cycle involves 3 xanthophylls that target excited singlet chlorophyll (^{1}Chl*) deactivation. The other one involves lutein, which desactivates excited triplet chlorophyll (^{3}Chl*).

The VAZ xanthophyll cycle This xanthophyll cycle is the main way of non-photochemical quenching in vascular plants. It is made up of three xanthophyll carotenoids (**v**iolaxanthin, **a**ntheraxanthin and **z**eaxanthin) that target excited singlet chlorophyll (^{1}Chl*) deactivation. Under high irradiance, violaxanthin can be converted to zeaxanthin by two steps of de-epoxidation, with antheraxanthin as an intermediate metabolite (figure 1.10). These reactions are catalyzed by violaxanthin de-epoxidase (Demmig-Adams and Adams (1996) and Taiz et al. (2015)). Conversely, antheraxanthin is converted back to violaxanthin by epoxidations under low irradiance conditions, by zeaxanthin epoxidase. The conversions need ascorbate as a cofactor and protons are consumed for the conversion from violaxanthin to zeaxanthin (Taiz et al. (2015)). Low lumen pH is the consequence of a high electron transport activity and thus high light absorption. Thereby, the xanthophyll cycle is regulated by the protein PsbS (that interact with some LHCII proteins), itself regulated by protons as a function of light irradiance. This prevents light to be dissipated in low-light conditions (Demmig-Adams and Adams (1996) and Jahns and Holzwarth (2011)). The cycle is regulated through changes in (1) total VAZ xanthophylls concentration and (2) conversion rates, regulated by lumen pH (which is an indicator of the ETC activity) and ascorbate among other factors (Eskling and Åkerlund (1998)).

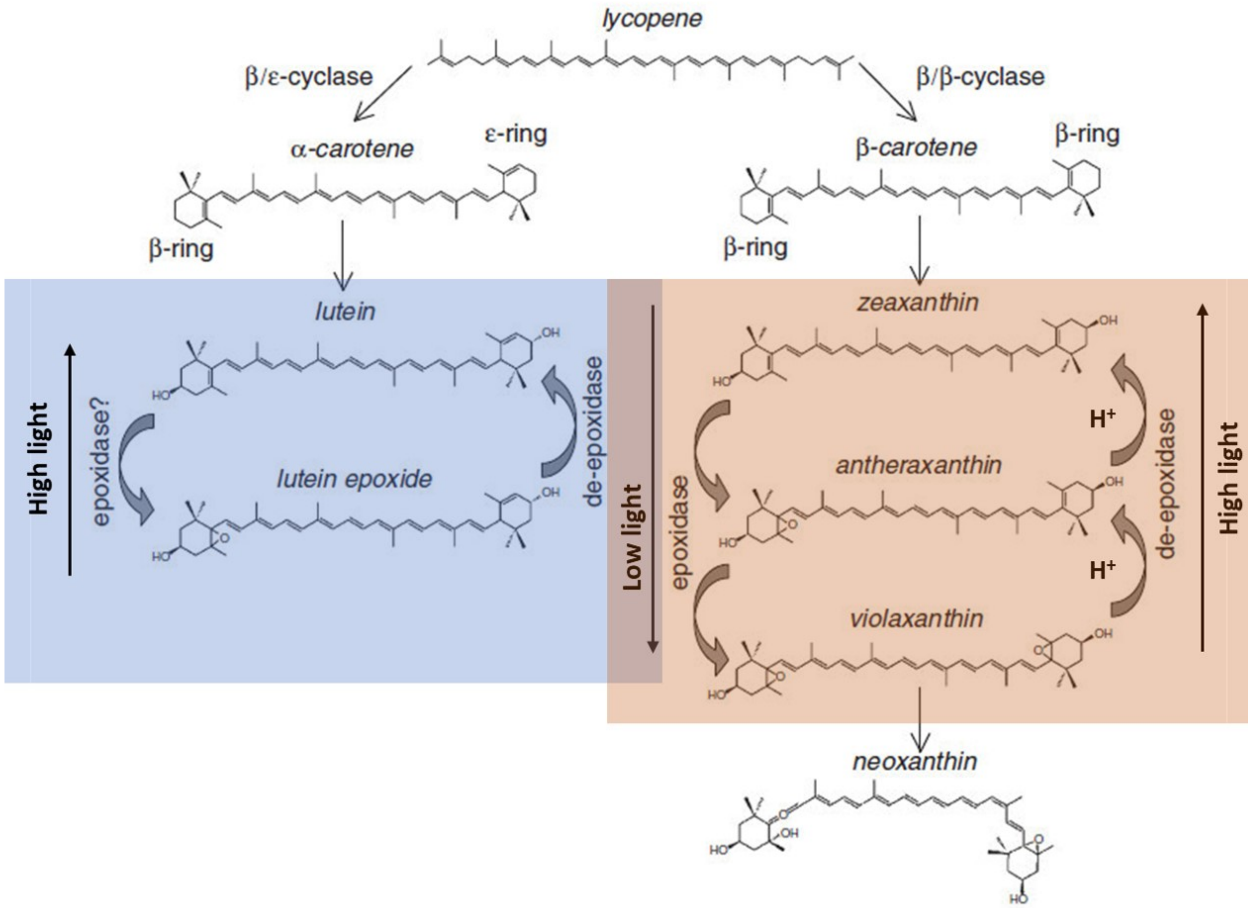

Figure 1.10: **An overview of lutein (blue) and VAZ (red) xanthophyll cycles.** Adapted from García-Plazaola et al. (2007).

The lutein cycle In the same way of the VAZ cycle, epoxidized lutein is associated with low ligh, whereas the carotenoid is de-epoxidized with high irradiance (Jahns and Holzwarth (2011)). Interconversion is probably catalyzed by the same enzymes as those of the VAZ cycle (violaxanthin de-epoxidase and zeaxanthin epoxidase). This carotenoid is probably able to play a role in NPQ (quenching of ^{1}Chl*) (García-Plazaola et al. (2007)). Contrary to the VAZ cycle, it is not found in all plant species (Esteban et al. (2009)).

1.3.3 Analysis of photosynthesis by fluorimetry

Since chl *a* fluorescence is inversely proportional to photochemistry, its analysis by fluorimetry provides some valuable information (Silva et al. (2009)). It is a powerful and non destructive method used to assess the photosynthetic apparatus state (White and Critchley (1999), Schreiber

(2004), and Ralph and Gademann (2005)). Chl *a* fluorescence is emitted mainly by PSII (Muller (2001)). The technique is based on the measurement of fluorescence intensity induced by exposition of the plant sample (a leaf usually, at least a photosynthetic organ) to light. This can be carried out on samples adapted to dark or adapted to light. Measurements obtained on these two kinds of samples are to be interpreted in a different way because the photosynthesis apparatus gets acclimated to light intensity.

Fluorimetry enables to obtain instantaneous measurements of photosynthesis quantum yield (maximal yield for dark-adapted tissues or effective yield for light-adapted tissues), to realize **P/I curves** (**P**hotosynthesis-**I**rradiance curves) and **RLC** (**R**apid **L**ight **C**urves) to estimate several parameters of photochemical and non-photochemical quenching. This method is convenient and easy for *in situ* measurements, in contrast to oxygen-based measurement approaches that have been used for a long time (Silva et al. (2009)).

Quantum yield Among many parameters unraveled by fluorimetry, chlorophyll quantum yield of PSII (Φ_{PSII} or **Y(II)**) is of great interest[2]. It is the fraction of absorbed light that is re-emitted as fluorescence (see figure 1.9 and section 1.3.1). That is a good proxy for the proportion of open PSII reaction centers (Ralph et al. (2002)).

Chlorophyll quantum yield can be quickly measured by exposing the photosynthetic tissue to a short sequence of light flashs. First, a very weak light ($\approx$ 0.1 µmol photons $m^{-2}.s^{-1}$) illuminates a dark-adapted sample. This is used to measure the minimal chlorophyll fluorescence intensity F_0, without inducing photosynthesis (light intensity is too weak) (Ralph and Gademann (2005) and Schreiber (2004)). In this situation, all photosystems are oxidized and therefore fully available for electrons transport. Then, a short saturating pulse ($\approx 10^4$ µmol photons $m^{-2}.s^{-1}$) closes all photosystems (they switch to reduced state). The resulting fluorescence intensity F_m is maximal; total fluorescence is quenched only by non-photochemical quenching because photochemical quenching is prevented by PSII closure (Ralph and Gademann (2005) and Schreiber (2004)). Figure 1.11 shows the variation of chlorophyll fluorescence intensity in a measurement of chlorophyll quantum yield. The difference between maximal fluorescence (F_m) and minimal fluorescence (F_0) of samples adapted to darkness is written F_v. The ratio F_v/F_m is the maximal quantum yield, calculated with equation 1.1.

$$Max\,yield = \frac{F_m - F_0}{F_m} \tag{1.1}$$

The effective quantum yield of samples adapted to light is given by equation 1.2 (Ralph and Gademann (2005)).

$$Y(II) = \frac{F'_m - F}{F'_m} \tag{1.2}$$

[2]It is also possible to measure a quantum yield for all light reactions steps (Beer et al. (2014)), but it will not be described in this work.

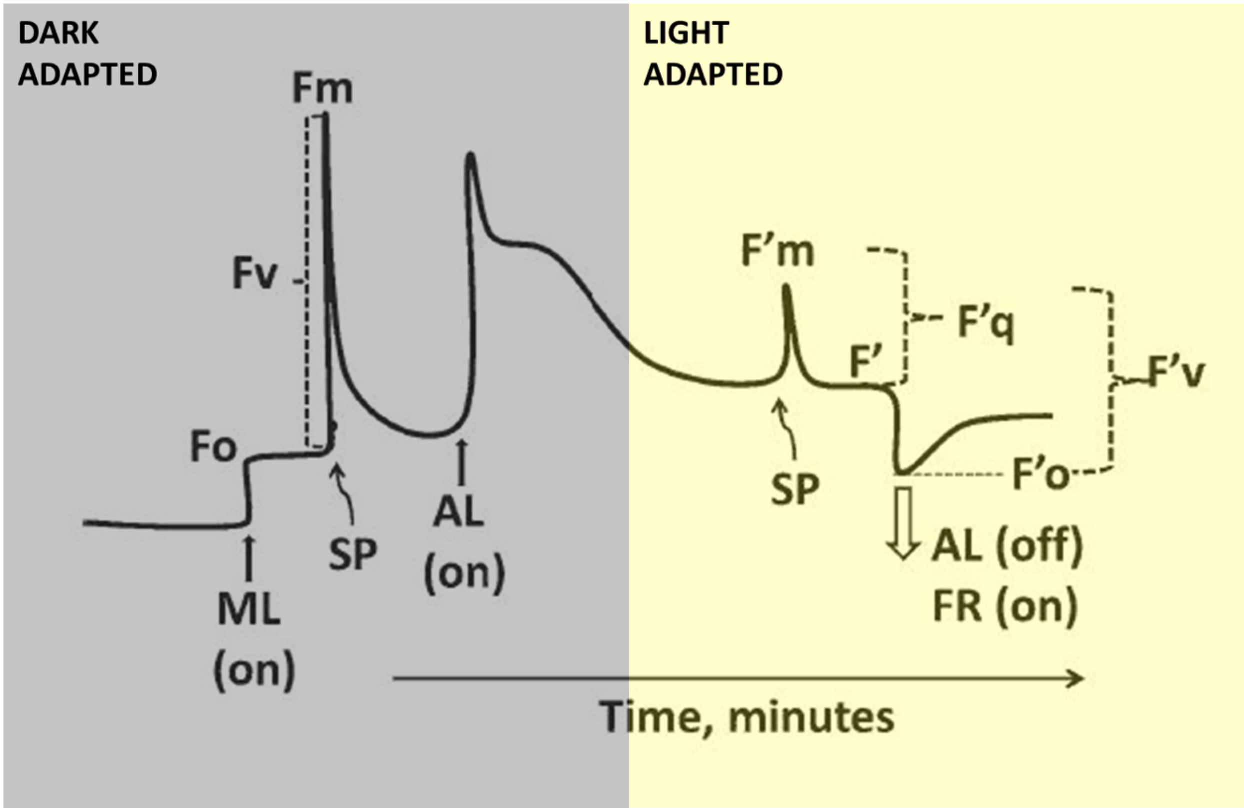

Figure 1.11: **Variation in chlorophyll fluorescence during a measurement of chlorophyll quantum yield.**

ML : weak modulating light; SP: saturating pulse; AL : actinic light; FR : far red light; F_0 : fluorescence minima (DA); F_m : fluorescence maxima (DA); F' : fluorescence minima (LA); F_m' : fluorescence maxima (LA). From Mishra (2018).

Quantum yield in seagrass Photosynthesis acclimatization in response to varying light irradiances has been investigated in some seagrass species, like *Zostera marina*. Ralph et al. (2002) revealed the dynamics of fluorescence parameters and of the VAZ xanthophll cycle in this species (figure 1.12). NPQ and maximal quantum yield are proportional and inversely proportional to irradiance, respectively (A-B). Moreover, light induces the conversion of violaxanthin to antheraxanthin and zeaxanthin (C-D). Experimental transfer from high light to low light and the opposite show the same patterns fluorescence parameters and xanthophyll pigments in relation to light (Ralph et al. (2002)).

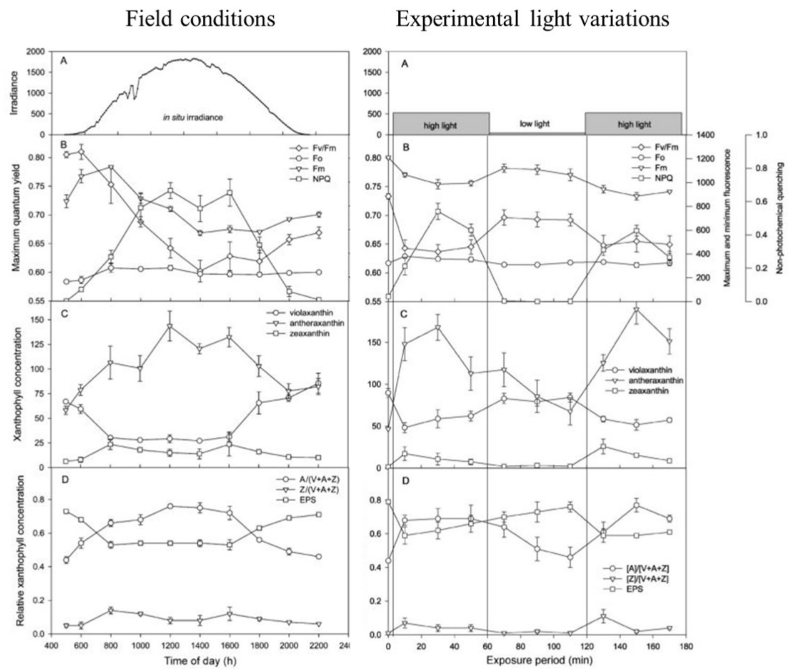

Figure 1.12: **Variations in chla a fluorescence parameters and VAZ xanthophylls concentration in *Z. marina*.**

(A) Irradiance (μmol photons m^{-2}.s^{-1}); (B) Chl a fluorescence parameters; (C) VAZ concentration; (D) Relative VAZ concentration (EPS=(Z+0.5A)/(V+A+Z)). From Ralph et al. (2002).

P/I curves and RLC

Besides the one-time measurement of chlorophyll quantum yield, analysis of its evolution while the photosynthetic tissue is exposed to increasing light intensities interspersed with saturating pulses gives additional information on the photosynthetic apparatus. Two kinds of curves are used that differ by the time interval length between each saturating pulse. In the case of P/I curves, the time interval is long (typically several minutes). This allows acclimatization of the photosynthetic apparatus before each new saturating pulse. Their interpretation allows to assess the plant ability to perform photosynthesis on a broad range of light intensities (Ralph and Gademann (2005)). On the other side, saturating pulses frequency is high (a few seconds between each pulse) for RLCs. As a consequence, the plant does not have enough time to become acclimated to the increasing light intensity before the next saturating pulse. Thus, these curves rather give information about photosynthetic apparatus ability to cope with rapid light intensity fluctuations (Ralph and Gademann (2005)). However, the interval length must be long enough so that each saturating pulse has no impact on the next fluorescence measurement (Ralph and Gademann (2005)). Figure 1.13 illustrates the evolution of chlorophyll fluorescence intensity through a RLC and figure 1.14 shows an example of RLC.

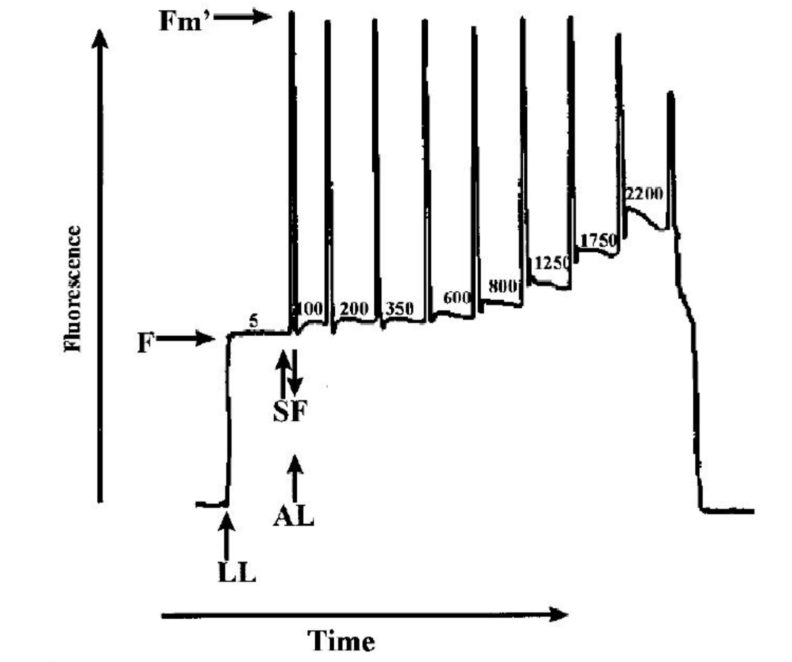

Figure 1.13: **Example of a RLC on a light-adapted leaf.**

LL : low-intensity light; SF: saturating flah (pulse); AL : actinic light; F_m' : maximal fluorescence (light-adapted). Values written at the base of each fluorescence intensity peak are increasing actinic light intensities. Frequency of saturating pulses is 0.1 Hz. From White and Critchley (1999).

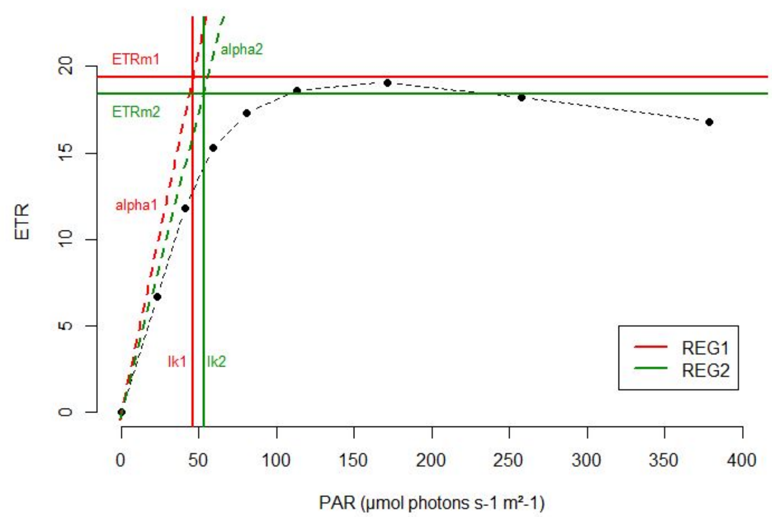

Figure 1.14: **Example of a RLC on a *P. oceanica* leaf in the 15% shading treatement of the experiment of this master thesis, on 6 April 2018.**

On the x-axis, PAR values; on the y-axis, electron transfer rate. α, I_k and ETR_m parameters are drawn for two regression models (REG1 and REG2).

After recording of the values of Y(II) on the defined PAR scale (**p**hotosynthetically **a**ctive **r**adiation, that is the light intensity only for wavelengths used in photosynthesis; also called PPFD (**p**hotosynthetic **p**hoton **f**lux **d**ensity)), the electron transfer rate (ETR) is estimated on the basis of Y(II) and PAR, with equation 1.3. AF is the absorption fraction, that is the fraction of photons absorbed by the leaf. It varies among species (White and Critchley (1999)) and is sometimes difficult to assess. In the latter case, the relative ETR (rETR) is calculated with equation 1.3 from which AF and 0.5 are removed (Ralph and Gademann (2005) and Beer et al. (2014)). 0.5 assumes that 2 photons are required for each electron (Ralph (1999)).

$$ETR = Y(II) * PAR * 0.5 * AF \tag{1.3}$$

RLC and P/I curves can be modelled using non-linear regression. Two models have been described, initially on phytoplankton. A first one assumes the existence of photoinhibition (i.e. decreasing of chlorophyll quantum yield at high irradiances) (REG1, described by Platt et al. (1980)) whereas another does not rely on this assumption (REG2, Jassby and Platt (1976)). Then, several parameters are calculated on the basis of the RLC regression curves.

α is the curve initial slope, which corresponds to the relation between photosynthesis efficiency (whose proxy is ETR) and PAR, when light is still the limiting factor for photosynthesis. ETR_m is the maximal electron transfer rate reached, before its decrease due to photoinhibition. I_k (also called E_k) is the minimal saturating light intensity, which matches with light intensity value at the intersection between ETR = α and ETR = ETR_m * PAR.

RLCs are particularly adapted to investigate seagrass photosynthesis, since these species are exposed to important and rapid light variations, as explained earlier. These curves can reveal how fast they can cope with light variations (Ralph and Gademann (2005)). For example, RLCs has been used to investigate *Z. marina* photosynthesis from dawn to dusk (Ralph et al. (2002)). ETRm is not maximal when light irradiance reachs its maximal value, but rather with intermediate irradiance values (figure 1.15). That illustrates light-saturation of photosystems and therefore non-photochemical quenching.

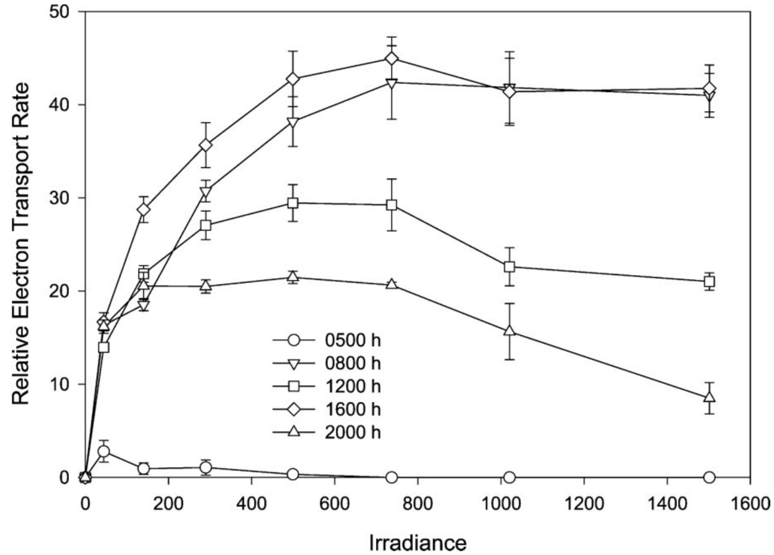

Figure 1.15: **RLCs on *Z. marina* leaves throughout the day.**
From Ralph et al. (2002).

1.3.4 Products of photosynthesis and primary production

Allocation of carbohydrates In low-light conditions (to which *P. oceanica* is usually exposed), the carbon balance between inputs from photosynthesis and outputs through respiration has to be tightly regulated. Moreover, allocation to the various plant organs must be optimal with the available carbohydrates (Burke et al. (1996)). As underlined by Alcoverro et al. (2001), the understanding of carbohydrates allocation is crucial to have a grasp of seasonal plant dynamics and response to various environmental factors. *P. oceanica* is furthermore a plant whose the majority of biomass is underground and therefore not photosynthetic; the carbon balance of this biomass is always negative. It has been shown that carbon allocation is the highest in rhizomes (Alcoverro et al. (2001)).

Maximal nonstructural carbohydrates values in all organs are found through summer, whereas the minimal values are in spring.

Primary productivity of *P. oceanica* Several approaches are used to study primary productivity in seagrass (either the seagrass only or the whole meadow ecosystem). Lepidochronology, as mentioned earlier, is a powerful tool that provide some valuable information on the seagrass past growth dynamics (Pergent et al. (1989)). Otherwise, primary production can be estimated by marking the leaf at the base and measuring, after a certain time of growth, the distance between the mark and the new base (that is possible since leaf growth is acropetal) (Zieman (1974)). Quantification of the net community production on the basis of O_2 production is used for the whole ecosystem, therefore including macro- and microalgae, photosynthetic epiphytes and phytoplankton besides *P. oceanica* (used e.g. in Champenois and Borges (2012) and Champenois and

Borges (2018)). Regarding *P. oceanica* only, the gain in carbon (by photosynthesis) is close to zero through winter (global carbon balance being negative) and is maximal in summer (Alcoverro et al. (2001)).

A survey of 10 years of the meadow primary productivity at 10 m in Revellata Bay (Corsica) was carried out by Champenois and Borges (2018). They show that the meadow is a net producer of biomass (net primary productivity is 23 ± 23 mol O_2 $m^{-2}.y^{-1}$) and its gross primary productivity is 87.7 ± 18.4 mol O_2 $m^{-2}.y^{-1}$. They observed an important variability between years, essentially explained by solar radiation. Duarte et al. (2010) reviewed primary productivity data of several seagrass species. The mean of all species is about 80 mol O_2 $m^{-2}.y^{-1}$, even if the mean for temperate species only is lower (about 60 mol O_2 $m^{-2}.y^{-1}$).

Seagrass beds are estimated to contribute to about 1-10% of net primary production in oceans, with a productivity of 394-449 g carbon $m^{-2}.yr^{-1}$ (Duarte (2017)). Assuming the total *P. oceanica* surface of 1.2 million ha estimated by Telesca et al. (2015), the species would produce between 4.7 and 5.4 million tons of biomass each year.

Given the accumulation of organic matter in the matte, the meadow ecosystem is a carbon sink. The stored carbon originates from photosynthetic tissues production as well as organic carbon particles trapped from the water column by leaves (Kennedy et al. (2010)). It is estimated to account for about 15-30% of the net primary production of this species (Personnic et al. (2014), see section 1.3.4).

1.4 Light attenuation on *P. oceanica*

Decrease of light intensity is one of the main threats to which *P. oceanica* is exposed. This seagrass is particularly sensitive to eutrophication since its meadows are *low nutrients high chlorophyll* ecosystems (the Mediterranean Sea is overall oligotrophic) (S. Gobert et al. (2002)). It means that the plant is adapted to grow in a water poor in nutrients and, despite that, yielding a high biomass. However, eutrophication causes phytoplankton blooms (whose frequency has steadily increased for more than 25 years) and a more important epiphytes load, both factors that decrease light availablity for the plant's photosynthesis (Alcoverro et al. (2001)). The Mediterranean Sea is today subjected to eutrophication that results from industrial waste, sewage and agriculture runoff (Karydis and Kitsiou (2012)). As mentioned earlier, light seems to be an important factor for *P. oceanica* primary production (Champenois and Borges (2018)). Growth rate and epiphytes biomass have been observed to decrease in shading experiments (e.g. Ruiz and Romero (2001)). A decrease in light intensity could cause a shift in seagrass meadows from autotrophic to heterotrophic ecosystems because the primary productivity would not be enough to balance the respiration rate (Gacia et al. (2012) and Alcoverro et al. (2001)).

Two kinds of surveys from which conclusions about the effect of light on *P. oceanica* can be

Reference	Depth	K_d	% I_s above screens	Shading	% I_s below screens
Ruiz and Romero (2001)	9.5 m	0.11 m^{-1}	35	70%	**10.40**
				40%	**16.7**
Serrano et al. (2011)	5 m	/	/	99%	1
				90%	**10**
				80%	**20**
Gacia et al. (2012)	6 m	0.093 m^{-1}	57	98%	1.14
				88%	**6.87**
				81%	**10.87**
				79%	**12.02**
				69%	**17.74**
				24%	43.50
				18%	46.93
				8%	52.66
This work	15 m	0.10 m^{-1}	22	60%	8.93
				30%	15.62
				15%	18.97

Table 1.1: **Review of shading levels used in three *P. oceanica* light deprivation experiments. K_d: light attenuation coefficient; I_s: Surface irradiance. Values in bold are similar to the shading levels tested in this work. K_d for STARESO was assumed to be 0.1.**

draw have been performed so far. Either the meadow is experimentally shaded *in situ* at a given depth, or parameters are studied along the bathymetric gradient.

1.4.1 *In situ* shading experiments

Other experiments that has aimed to shade *P. oceanica* meadows were not performed at the same depth (see data in table 1.1). Our experimental shading was installed deeper than the shading that has been tested so far (5 m, 6 m , 9.5 m), at 15 m (usually the reference depth for ecophysiological studies, Personnic et al. (2014)). Aquatic plants display depth-related adaptations, especially towards light and temperature (Genot et al. (1994)). Therefore, different physiological and primary production responses are expected for similar shading provided at different depths.

Two hypotheses can be formulated regarding light adaptation.

1. Deep-growing shoots are strongly adapted to low light conditions. Then, a decrease in light intensity would be less harmful than for plants adapted to high light conditions.

2. Deep-growing plant are, although better adapted to low light than shallow-growing plants, close to the compensating irradiance, thus more sensitive to light deprivation. This leads to a second question. Regarding comparaison of shading experiments conducted at different depths, is it more relevant to consider shading (1) as the relative decrease in light intensity for a given depth or (2) as the absolute irradiance to which plant are exposed? In the first

case, a 40% shading at 5 m is considered to be similar to a 40% shading at 15 m, even tough the incident irradiance is much higher at 5 m. In the latter, a 40% shading at 5 m will be considered similar to a much lower shading at 15 m, given the strong exponential decrease in light intensity with depth especially at shallow depths.

Comparison of our results with these three studies conducted at different depths could be informative. Table 1.1 lists the shading levels used in the three experiments, expressed as % of surface irradiance. These results are discussed in the discussion sections.

1.4.2 Bathymetric studies

Some research has been conducted on several seagrass species along the bathymetric gradient (e.g., Via et al. (1998), Silva and Santos (2003), Collier et al. (2008), and Dattolo et al. (2013)). Results showed variations in shoot density and biomass, photosynthetic surface, pigments content, epiphytes cover, photosynthesis and variation in many genes expression. Light intensity is the main driver of this gradient. Via et al. (1998) describes three kinds of gradients that affect light availability in water, particularly for benthic organisms.

1. Light is absorbed by water; its intensity decreases exponentially with depth (Beer et al. (2014)).

2. Light spectrum changes because some wavelengths are more absorbed by water than others. High wavelengths photons are the most absorbed by water, their availability is thus strongly reduced in increasing depths. Light quality is associated with variations in antenna pigment content (Via et al. (1998) and Croce and Amerongen (2014)).

3. Besides the water absorption-related decrease in light intensity, variations in shoot density along the gradient modulate autoshading of shoots (i.e. leaves shaded by other leaves) (Via et al. (1998)).

Furthermore, other parameters than light shape the depth gradient.

1. Temperature, that is a key parameter for respiration and photosynthesis rates (Champenois and Borges (2012)), decreases with depth.

2. Waves cause more disturbances in shallow meadows, promoting dead organic matter exportation and therefore decreasing the respiration rate (as a consequence of organic matte decay) in the meadow (Mateo and Romero (1997)) The absence of storms in autumn/winter period has been linked to a decrease in primary production as a consequence of organic matter accumulation that shades the meadows-associated primary producers and promotes respiration (Champenois and Borges (2012)).

3. Shoots show some local genetic adaptation along the depth gradient (Procaccini et al. (2017) and Jahnke et al. (2018))

The experiment conducted for this work is free of these confounding factors since all light treatments were applied at the same depth (15 m).

There is seemingly a lack of information about *P. oceanica* (and other seagrass) response to low shading. Duration of the experiment is variable between papers, with several month for Ruiz and Romero (2001) and Serrano et al. (2011) whereas Gacia et al. (2012) carried out the experiment on three weeks. To my knowledge, among the feasible combinations between shading intensity and experiment duration, low shading on a long period of time has not been investigated yet.

1.5 Objectives of this work

This study was conducted in the framework of a hypothetical future global decrease of light intensity in the Mediterranean Sea (Boudouresque et al. (2009)). It aims at understanding how *P. oceanica* responds to low to moderate light deprivation over its seasonal growth cycle. The response to shading treatment was monitored through the analysis of several biomarkers: pigments content, photosynthetic activity, carbohydrates, shoot biometry and primary production are analyzed. To reach this objective, nine square meters of healthy *P. oceanica* meadow in Corsica were shaded with screens at several shading levels (0%, 15%, 30% and 60%) between April and August 2018 over the almost overall growing cycle of the plant.

2

Materials and methods

2.1 Experimental site

The experiment was carried out in the *Posidonia oceanica* meadow that spreads next to STARESO (**Sta**tion de **Re**cherches **S**ous-Marines et **O**céanographiques) oceanography station located at the north-west of Corsica, at the end of Revellata Cape, in the Gulf of Calvi (42.5804°N, 8.72407°E) (Fig. 2.1).

This *Posidonia* meadow is described as dense – 400-430 shoots m^{-2} at 10 m depth (Richir et al. (2013) and Champenois and Borges (2018)) – and productive. Waters in th Gulf of Calvi are clear and oligotrophic water (S. Gobert et al. (2002)). The marine environment of the Gulf of Calvi is considered as in a good state of conservation (Gobert et al. (2009)).

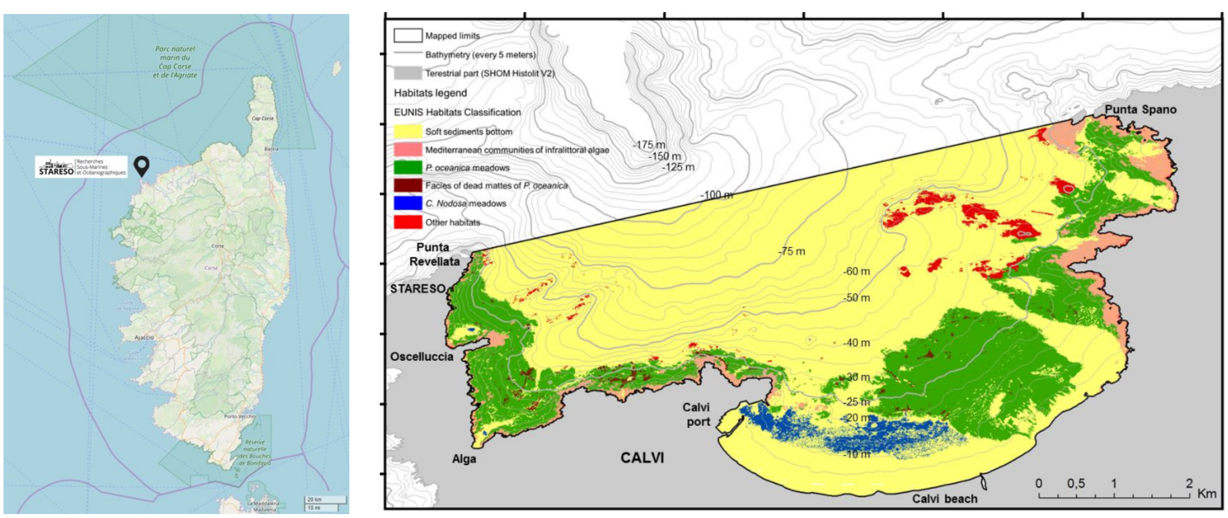

(a) (b)

Figure 2.1: **Localization of STARESO.**
From Openstreetmap (left) and Gobert et al. talk, 2015 (right)

2.2 Study area

The meadow was shaded with white plastic screens (n = 1 by treatment). Three squares by 3x3 m were cut in polyethylene screens of different transparency (Alphatex by multimailles, *ConsoRex white*, *SupraTex white* and *EdiTis white*). About 85%, 70% et 40% of incident light crosses the screens, respectively. They were deployed at 15 m depth, maintained at 2 m above the sediment with eight vertical metal poles and four horizontal ones (fig. 2.2). A non-shaded portion of meadow was used as control. The 15 m depth is assumed to be representative of the whole depth gradient of *P. oceanica* habitat, and is considered as the optimal depth for growing for this species in the north-west Mediterranean Sea (Personnic et al. (2014)).

Weekly to fortnightly, the screens were cleaned of the epiphytes (handly brushed) that rapidly grew on it, in order to keep the shading level at a constant value. Plastic nets were replaced twice by new ones.

2.3 Experimental design and field work

The experiment was carried out between April 2018 and August 2018. Measurements and samplings were carried out monthly, once or three times on 10 days, depending on the parameter. Samples were taken back at STARSEO, transported in black plastic bags and stored at -20°C. Biochemical and biometry analyses were further conducted in Belgium, at the University of Liège (Chemical Oceanography Unit and Bioenergetics lab) and the University of Louvain-la-Neuve (Research Group in Plant Physiology). Biochemical (except carbohydrates) and photosynthetic activity analyses were performed on the middle section of the 3^{rd} intermediate leaf. Biometry

Figure 2.2: **Screen used to shade the meadow**
©J. Richir

analyses were performed on the whole shoots.

2.4 Environmental parameters

PAR was recorded contiuously (every minute) during the experiment, with a miniPAR logger (PME, Inc.) for photosynthetic active radiation at the control treatment. Light under experimental shading treatments was recorded with Odyssey loggers (Odyssey Submersible Photosynthetic Active Radiation Logger, Dataflow Systems Ltd) every 10' and calibrated against the miniPAR logger. HOBO loggers (HOBO Pendant Temperature/Light Data Logger, Onset Computer Corporation) recorded continuously (every 10') the temperature and light intensity (Lux) under each screen and at the control. Only the temperature and light data corresponding to the 11:00 - 14:00 time window, i.e., corresponding to around midday photosynthetic activity measurements, were considered and averaged. Loggers were located at the center of the nine m^2 shaded area, fixed just above the meadow canopy on vertical metal poles.

2.5 Laboratory and *in situ* analyses

2.5.1 Pigments

About 50 mg of fresh leaves was cut into small pieces into capped tubes. After addition of an iron ball, the tubes were frozen in liquid nitrogen and ground in a mixer mill (MM 400, Retsch GmbH) at 25 Hz for 5 minutes. 1.5 mL of 100% acetone was then added to ground samples. After homogenisation, the iron balls were removed from capped tubes. The tubes were put on a shaker for 45 minutes for pigment extraction. After centrifugation (17,000 g, 5 minutes), the supernatant was removed and stored at -28°C. Grinding and extraction were performed a second time, but with small-sized glass balls in 1.5 mL 100% acetone. After centrifugation, the second supernatant was pooled with the first one. The extract was stored at -80°C until HPLC analysis. All previous steps were performed either on ice or in a cold room and always in light conditions as low as possible to prevent pigment degradation. Pigments were analyzed by high performance liquid chromatography (HPLC). The reverse-phase HPLC used for the pigment analysis is made up of a Waters pump 600E, an autosampler Waters 717, a Waters 2996 photodiode array detector and a Waters fluorescence detector (Waters Corporation, The Netherlands). The column used is Nova Pack C18 HPLC. Three solvants were sequentially used: methanol 80%/ammonium acetate 20 %, acetonitrile 90 %/water 10 % and then ethyl acetate. 10 µL of 100% acetone extract were injected. Retention time and absorbance spectrum were analyzed for peaks identification. Concentration of pigments were determined from previous calibration curves of reference samples. Chlorophylls *a* and *b*, lutein, $\beta\beta$-carotene, zeaxanthin, antheraxanthin and violaxanthin were quantified. Concentrations are expressed as mg.kg^{-1} fresh weight.

2.5.2 Photosynthesis

Photosynthetic activity measurements were performed, either *in situ* in the meadow for Y(II), F_v/F_m and RLC or on samples brought back to the station facilities for PI curves. The Diving-PAM II (Heinz Walz GmbH, Germany) was used for all photosynthetic activity measurements. At dawn (05h00 - 06h00), F_v/F_m of overnight dark-adapted leaves samples was measured *in situ* (n = 6) and these leaves were cut close to the base with cisors and taken back in the laboratory for P/I curves (n = 3). The time interval of each light step (between 0 and 400-800 µmol photons $m^{-2}.s^{-1}$, before photoinhibition) was set to 3 minutes. Around midday, Y(II) (n = 3) of light-adapted leaves was measured *in situ* (also on the middle section of the third leaf), as well as rapid light curves (n = 3). The time interval of each light step (between 0 and 400-500 µmol photons $m^{-2}.s^{-1}$, before photoinhibition) was set to 30 seconds. The measurements of Y(II) and RLC were performed on leaves in their natural position in the water column, i.e., at the vertical. The leaves used for P/I curves and RLC were frozen (-20°C) for further pigment analysis. The measurements of photosynthetic activity were replicated 3 times for each treatment each month. Three parameters are derived from RLC and PI curves, plotted as ETR against irradiance (α, ETR_m and I_k).

2.5.3 Carbohydrates

About 100-150 mg of fresh growing rhizome tip (n = 6) was cut into small pieces and ground in capped tubes with an ceramic ball in a mixer mill (MM 400, Retsch GmbH) at 30 Hz for 4 minutes (30 Hz, 8 x 30" with freezing in liquid nitrogen between each 30" run). Soluble carbohydrates were extracted successively in 10, 5 and 5 mL 80% ethanol, respectively, at room temperature for 15'. Each extract was centrifugated (6654 g, 10') and the three supernatants were pooled. The pellet was stored at -20°C for starch extraction. 200 µL of 5% w/v phenol and 1 mL of 95% sulphuric acid were added to 200 µL of extract. These reactants transform soluble carbohydrates into yellow-orange furan derivatives that are stable with phenol (Nielsen (2010) and DuBois et al. (1956)). The solutions were homogenized, left at room temperature for 10', then homogenized again. Coloration developed for 30'. Total soluble sugars concentration was quantified spectrophotometrically (UV-1800, Shimadzu Corporation) at 490 nm, on the basis of a calibration curve of D(+)-glucose $\cdot$ $1H_20$ (0-150 $mg.L^{-1}$, fig. 6.2). Each sample was read three times; the mean of these values was kept. Starch in pellets was hydrolyzed with 8 mL 1M HCl for 2 hours in a 95°C shaking water bath and homogenized every 20 minutes out of the water bath. Extracts were cooled in room temperature water, then neutralized with NaOH (10, 1 and 0.1M) in a 25 mL becher using a pH-meter. Neutralized extracted volume was adjusted to 25 mL with deinonized water, then centrifugated (6654 g, 10'). 10 mL of supernatant were removed and stored in the fridge at 4°C. Starch was measured as soluble carbohydrates through spectrophotometry on the basis of the same protocol as for soluble carbohydrates.

2.5.4 Biometry

Once a month, *P. oceanica* shoots were sampled in each treatment (twice in April, at t_0 and 7 days later; n=6/10). Samples were analyzed for biometry according to the method of Giraud (1979). For each shoot, leaves were detached from the rhizome, separated and counted, then sorted from the oldest (outside the shoot) to the youngest (inside the shoot). The developmental stage of each leaf was identified (juvenile if $<$50 mm length, intermediate if $>$50 mm without a marked base, adult if $>$50 mm with a distinct petiole). For each leaf, total length, width and petiole length, if present, was measured. Total leaf surface was estimated with equation 2.1.

$$Surface = mean(width) * \sum length_i \tag{2.1}$$

The A coefficient was calculated as the frequency of torn or grazed apexes. Epiphytes were removed on both sides with a razor blade (Dauby and Poulicek (1995)). Shoot samples for biometry has been marked for primary production measurements. Each month, a hole was pierced through all leaves, a few milimeters above the ligula (Zieman (1974)); these shoots were identified with capped tubes used as floats. When leaves were sorted during dissection, the distance between the original hole location (estimated fot the oldest leave, that did not grow) and the new hole location for growing leaf tissue was measured. Growing distances, i.e., new tissue produced, correspond to the net primary production of shoot leaves during the past month. These monthly primary production segments of all leaves were pooled for each shoot. Dissected tissues, i.e, epiphytes, primary production leaf segments and remaining leaf tissue, were transferred to suitable pre-weighted glass or plastic vials. They were dried at 60°C for at least 48 hours and weighted again for dry weight determination. Presence of dead matte was checked at the end of the experiment (August 2018) and in spring (May) and winter (December) of year 2019.

2.6 Statistical analyses

Relationships between response variables: pigments, photosynthetic activity, biometry and carbohydrates were explored using Spearman's rank correlation coefficient (Pearson (2001) and Schober et al. (2018)). The interpretation of the meaning of the Spearman's rank correlation coefficients was from Fowler and Cohen (1990). Relationships between response variables and potential explanatory variables time and treatment where analysed using median linear regression (quantile regression, Cade and Noon (2003)) and restricted cubic spline regression (Gauthier et al. (2019)). Predictions from models of response variables over time are plotted on graphs with their 95% confidence interval. Model selection is based on the knowledge of *P. oceanica* ecophysiological cycle, fitting of response variable predictions and comparaisons of model AIC values.

Quantile (including median) regression presents several advantages for environmental data: it is robust to outliers; avoids parametric distribution assumptions; estimates rates of change in all parts of the response variable distribution and is invariant to monotonic transformations (Koenker and Bassett (1978); Cade and Noon (2003)). Cubic spline is essentially a piecewise cubic polynomial. Cubic polynomials have been found to have nice properties with good ability to fit sharply curving shapes. Cubic spline is made to be smooth at the join points, called knots. A restricted cubic spline has the additional property that the curve is linear before the first knot and after the last knot. The number of knots used in the spline is determined by the user, but in practice five or fewer knots are sufficient (Gauthier et al. (2019) and Harrel (2015)). In the present study, we used 3-4 knots either as free parameters, either fixed a priori on the basis of the natural annual cycle of parameters (with the help of others works on the ecophysiology of *P. oceanica* conducted over more than 1 year if available or use of the control treatment of this experiment).

P. oceanica third leaves collected for pigment analysis were sampled either at dawn, during F_v/F_m measurements, either at midday, during Y(II) and RLC measurements. Student's t-test or Wilcoxon signed-rank test (depending on normality and homoscedasticity) conclude that difference between light- and dark-adapted samples strongly depend on time and shading level. The difference in pigments content is particularly marked in June. Because most (72%) tests were non-significant, pigment concentrations could be grouped by date and treatment regardless of the time of day.

Finally, two grouping methods permitting the information synthesis contained in all response variables were performed: principal component analysis (PCA) and ascendant hierarchical classification (cluster analysis). Samples were clustered using Ward's method (Euclidean distance between objects as measure of similarity) (Zar (2010)).

The significance level alpha was set to 1% to reduce Type I error.

The statistical analyses was performed in RStudio version 1.2.5019 (RStudio Team 2016), using R's base functions and functions of packages 'quantreg' (Koenker) and 'rlm' (Harell)

Values are presented as mean ± standard deviation, replicates number is precised in figure captions. All variables are plotted in superposition to PAR.

3

Results

3.1 Environmental parameters

Overall, there is a steady temperature increase between April and August of about 0.10°C day^{-1}. Maximal temperature was reached on 9th and 10th August, with 28.4°C in all treatments. Minimal temperature was recorded on 5th and 6th May, with 13.8-13.9° in all light conditions. There is no difference in temperature throughout the studied period between treatments (fig. 3.1); the mean over the experiment period is 20.9°C.

Light intensity (in lx, fig. 3.1) and photosynthetically active radiation (µmol photons m^{-2}.s^{-1}, fig. 3.1) both follow a concave curve, with maxima of 13376 lx on 30st June (control), 12170 lx on 26st July (shading 15%), 8295 lx on 17st June (shading 30%), 554 lx on 17st June (shading 60%) for HOBO records. Maximal values for PAR are 505 µmol photons m^{-2}.s^{-1} on 30st June (control), 444 µmol photons m^{-2}.s^{-1} on 18st June (15% shading), 303 µmol photons m^{-2}.s^{-1} on 18st June (30% shading), 239 µmol photons m^{-2}.s^{-1} on 18st June (60% shading).

Mean light intensity over the season was calculated; values are reported in table 3.1. It turns out that, relative to control, theoretical 60% shading treatment is 54-56% (PAR and lx respectively) shading, 30% shading is 43-40% and 15% shading is 31-14% shading. The 31% average shading for 15% shading treatment was corrected using calibration of 30% and 60% shading loggers (see fig. 3.1 and table 3.1). A shading of 14% was estimated, close to the expected 15% shading. Despite these small differences between the theoretical and measured light intensity, the shading levels will be considered further as nominal shading factors 15%, 30% and 60%.

Figure 3.1: **Environmental parameters.**
(Top) Temperature and light intensity [lx] recorded by HOBO loggers; (Bottom) Photosynthetically active radiation (PAR) recording by Odyssey loggers (except a PME logger for control treatment) (µmol photons $m^{-2}.s^{-1}$). Recorded data for the 15% treatment are in dotted lines, recalibration of the logger with the other ones is in solid lines. Each daily point is the mean over the 11h00-14h00 period.

	Light intensity (lx, $cd.sr.m^{-2}$)		PAR (µmol photons $m^{-2}.s^{-1}$)	
Treat.	Mean	Shad. %	Mean	Shad. %
Control	2850	0%	117	0%
Shading 15%	2457	14%	99	(31%) 15%
Shading 30%	1699	40%	66	44%
Shading 60%	1252	56%	52	55%

Table 3.1: **Expected and observed shading levels.**
Light intensity and PAR values are means over the experiment. They are expressed as raw data and percentage of control treatment. The PAR shading percentage in 15% shading (31%) was corrected using calibration of the Odyssey loggers used in the other treatments.

3.2 Pigments

All pigment concentrations decrease throughout the experiment period, except for antheraxanthin, for which the amount of null concentrations (50-60% of measurements in every treatments) makes data difficult to understand (fig. 3.2). The most abundant pigments are chlorophylls with several thousands of mg.kg$^{-1}_{FW}$ (minimum and maximum of chlorophyll *a* concentrations are 1131 ± 94 mg.kg$^{-1}_{FW}$ in August, 15% and 3226 ± 544 mg.kg$^{-1}_{FW}$ in April, 30% respectively; minimum and maximum of chlorophyll *b* concentrations are 548 ± 52 mg.kg$^{-1}_{FW}$ in August, 15% and 1467 ± 234 mg.kg$^{-1}_{FW}$ in April, 30% respectively) whereas antheraxanthin was detected at concentrations less than 5 mg.kg$^{-1}_{FW}$ (between 0 mg.kg$^{-1}_{FW}$ (many dates and treatments) and 3.12 ± 1.73 mg.kg$^{-1}_{FW}$ in April, 30%). Zeaxanthin was never detected. Violaxanthin concentrations range between 35 ± 5.4 mg.kg$^{-1}_{FW}$ (July, control) and 128 ± 21 mg.kg$^{-1}_{FW}$ (April, 30%). Total VAZ concentrations are similar to violaxanthin concentrations because zeaxanthin was not detected and antheraxanthin is more than ten times less concentrated. Lutein concentrations are between 121 ± 3 mg.kg$^{-1}_{FW}$ (August, 15%) and 325 ± 59 mg.kg$^{-1}_{FW}$ (April, 30%). $\beta\beta$-carotene concentrations range between 33.6 ± 10 mg.kg$^{-1}_{FW}$ (June, 60%) and 101 ± 36 mg.kg$^{-1}_{FW}$ (April, 15%). Difference between treatments are rarely significant, with a few exceptions (weak difference of 60% shading for chl *b* and lutein, see table 6.3). The temporal rate of decrease of the Chl a/Chl b ratio seems to differ slightly between treatments.

There is a global trend for a higher content in pigments in leaves sampled at midday compared to those sampled at dawn, with the exception of violaxanthin and antheraxanthin.

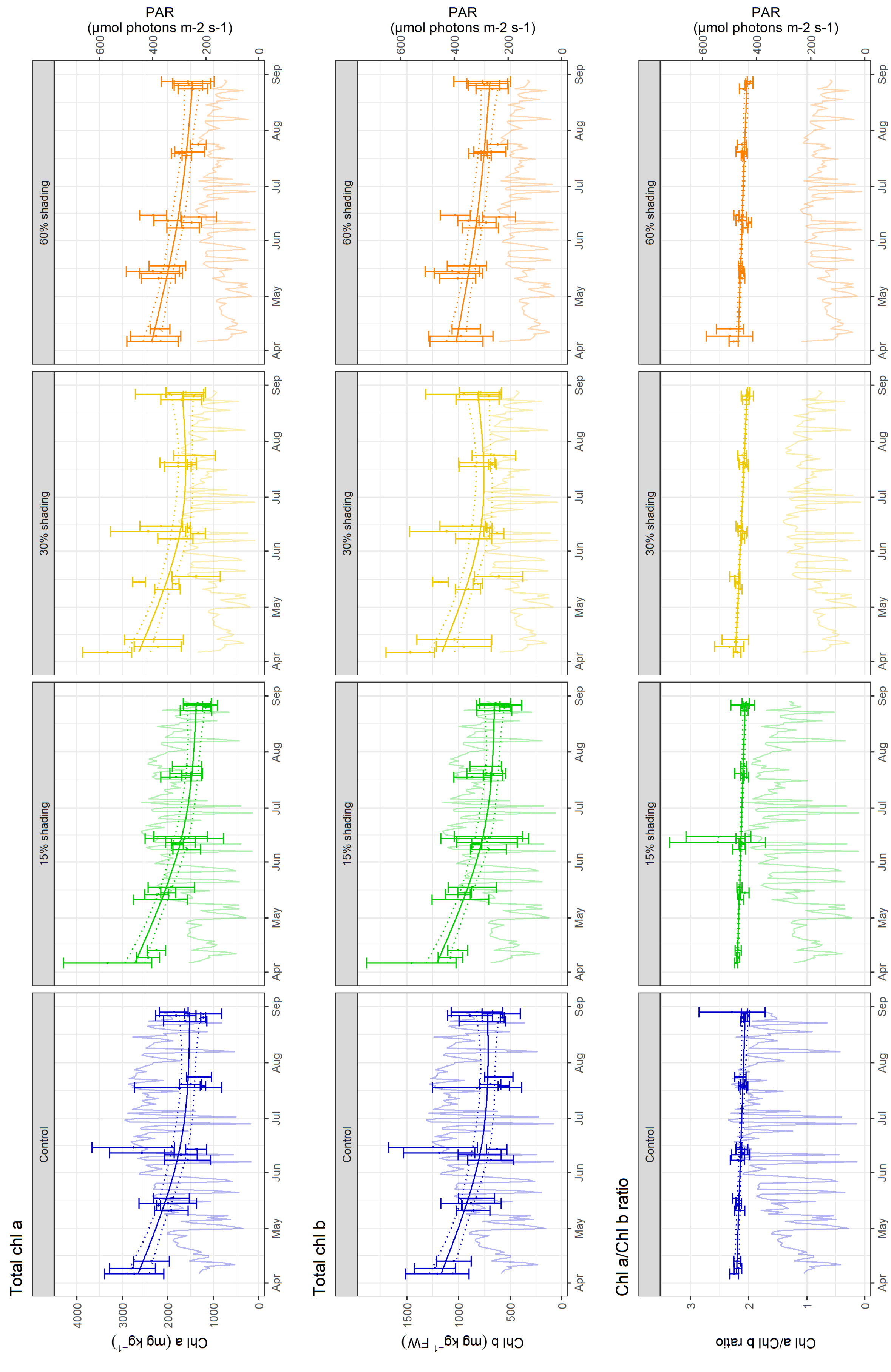

Figure 3.2: **Pigments content**
(Top) Chl *a*; (Middle) Chl *b*; (Bottom) Chl *a*/chl *b* ratio. n = 6

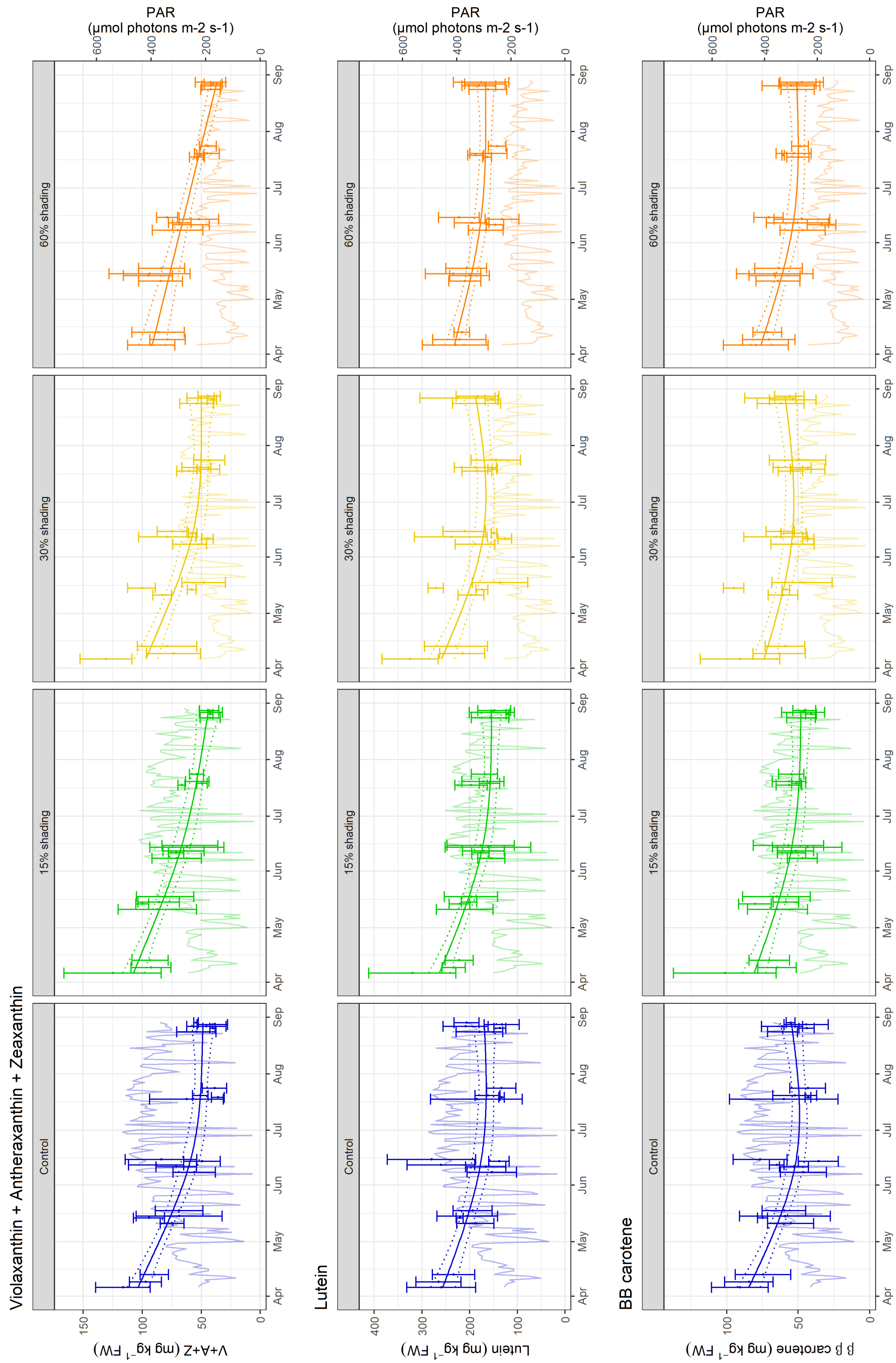

Figure 3.2: **Pigments content (cont.).**
(Top) Total VAZ xantophylls (violaxanthin, antheraxanthin, violaxanthin); (Middle) Lutein; (Bottom) $\beta\beta$-carotene. n = 6.

3.3 Photosynthetic activity

3.3.1 Photochemical quantum yield

Figure 3.3 shows that F_v/F_m is roughly constant (between 0.72 ± 0.00 on 24 August, 15% shading and 0.80 ± 0.0037 on 9 April, 60% shading) throughout the growing period. Y(II), however, follows a convex curve (fig. 3.3, $p < 0.01$ for time effect), with a minimum in summer (20 July, control treatment). The curve becomes progressively flatter with increasing shading level (showing a similarity with light intensity pattern). 30% and, to a lesser extent, 60% shading treatments are statistically different from the others ($p = 0.059$ for the increasing segment, $p = 0.080$ for the decreasing one). F_v/F_m does not show any difference between treatments.

3.3.2 Photosynthesis-Irradiance curves

P/I curves are similar between treatments throughout the experimental period (fig. 3.3) for all parameters. Alpha increases slowly from April to August, from 0.2 to 0.3 µmol e^{-1} µmol photons^{-1}, but the slopes are not significantly different from 0 (fig. 6.5). I_k shows a maximal value in summer ($p = 0.082$ for the first restricted cubic spline segment, $p = 0.088$ for the second one), which is particularly marked for 15% and 30% shading treatments, whereas ETR_m shows a steady increase (but not significantly different from a slope of 0) until its maximum in July before decreasing in August (not significant as well). I_k ranges between 30 and 90 µmol photons s^{-1} m^{-2} and ETR_m ranges between 10 and 35 µmol e^{-1} s^{-1}.

3.3.3 Rapid light curves

The shading treatments seem to have slightly influenced RLC parameters (fig. 3.3), but no significantly (table 6.5). Alpha increases towards a stronger shading but is roughly constant through time within a treatment (no significant differences, $p > 0.8$ for both slopes of segments predicted by restricted cubic spline). I_k values show a maximum in June, with the exception of the strongest shading, for which the maximum occurs earlier, in May ($p < 0.001$ for time effect, but no differences between treatments). ETR_m is higher under higher irradiances ($p < 0.001$ for time effect, no shading effect). In comparison to P/I parameters, RLC parameters are larger. RLC alpha ranges from 0.25 to 0.45 µmol e^{-1} s^{-1} µmol photons s^{-1} m^{-2}, I_k ranges from 25 to 250 µmol photons s^{-1} m^{-2}, ETR_m ranges from 10 to 70 µmol e^{-1} s^{-1}.

3.4 Correlations within and between pigments and photosynthetic parameters

On one hand, pigment contents correlate strongly to each other (often > 0.9, Spearman's rho coefficent), for dark-adapted samples as well as for light-adapted samples (figs. 6.6, 6.7), with the exception of antheraxanthin that shows no correlation in light-adapted samples. F_v/F_m, alpha and ETR_m do slightly correlate with lutein and chlorophylls in dark-conditions. However, only ETR_m and I_k shows a correlation with these pigments in light conditions.

The correlation circles (outputs of a principal component analysis) show that, for both light- and dark-adapted samples, pigments are grouped together except for antheraxanthin that, moreover, does not explain much variance (figs. 6.8, 6.9). RLC parameters are orthogonal to pigments. I_k and ETR_m are together, anti-correlated to Y(II) in light-adapted samples, whereas ETR_m, I_k and alpha are roughly toegether in dark-adapted samples, against F_v/F_m that explains few variance.

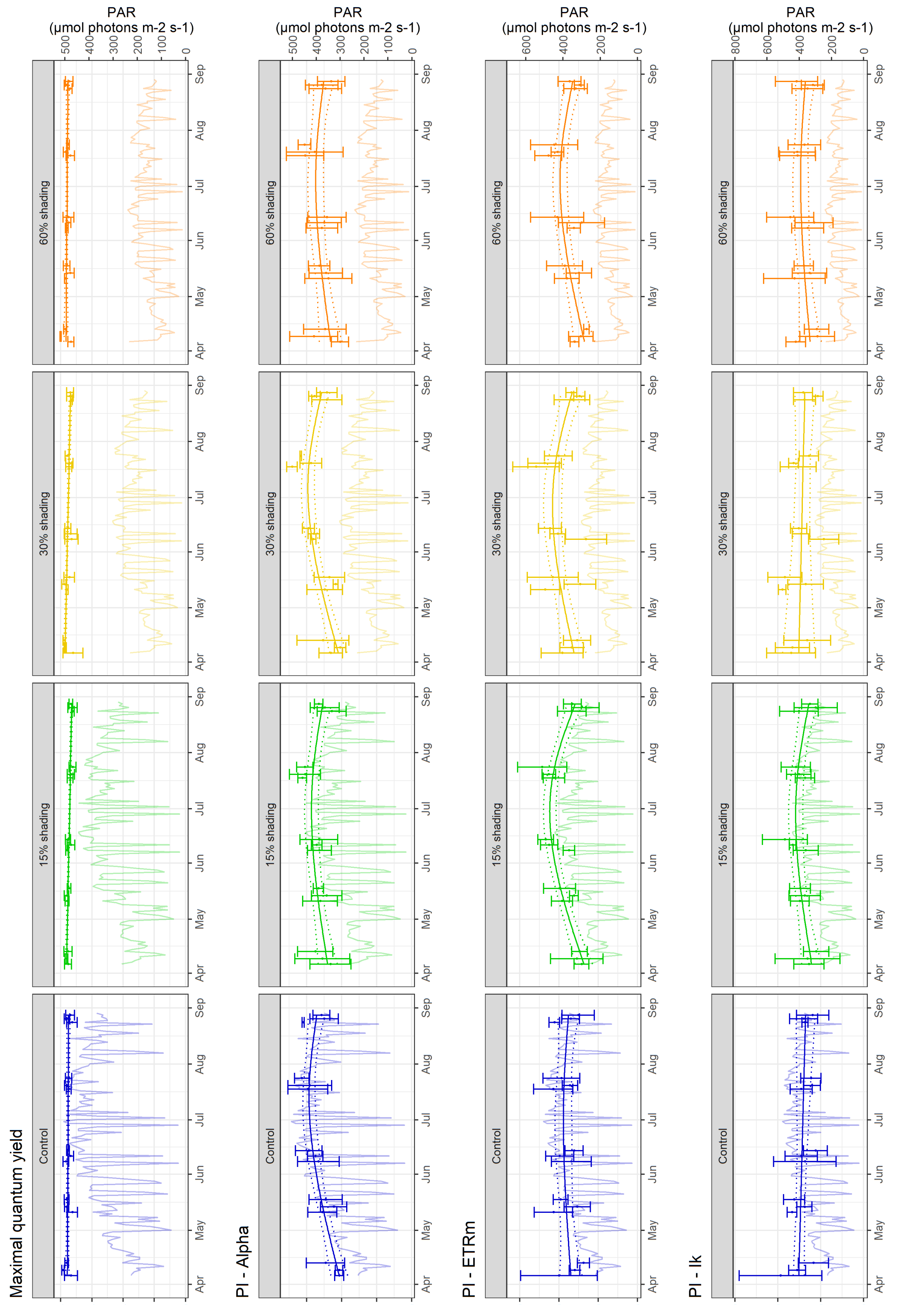

Figure 3.3: **Photosynthetic activity (Diving-PAM).** Maximal photochemical yield and P/I parameters. From top to bottom: F_v/F_m, alpha, ETR_m and I_k are shown. n = 3.

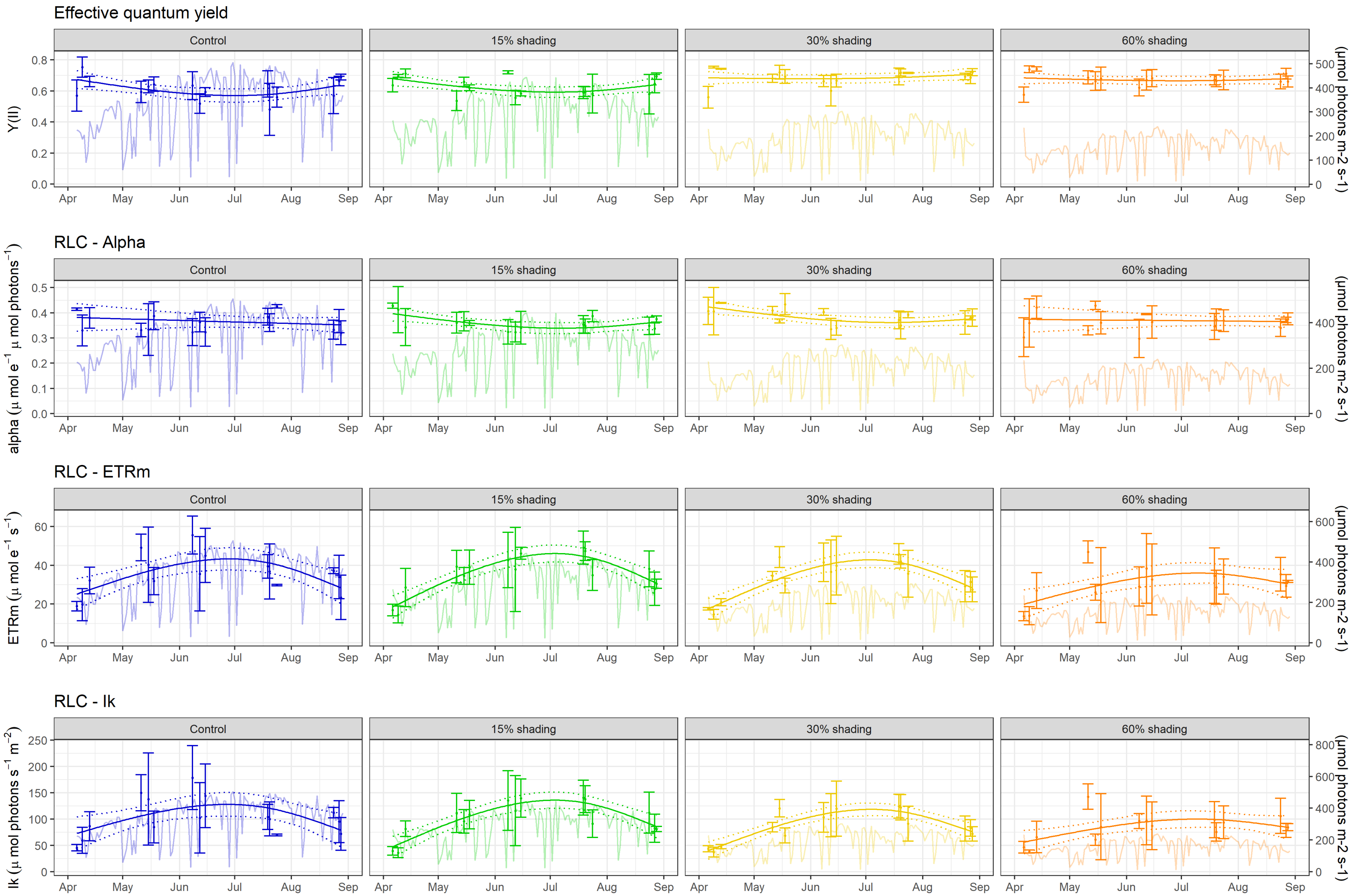

Figure 3.3: **Photosynthetic activity (Diving-PAM) (cont.).**
Effective photochemical yield and RLC parameters. From top to bottom: Y(II), alpha, ETR_m and I_k are shown. n = 3.

3.5 Carbohydrates

Soluble carbohydrate concentrations in rhizomes keeps roughly constant in April until an increase in May/June, then a sharp increase in August, except in the 15% treatment (fig. 3.4). The slope between June an August is progressively smaller toward increasing shading (restricted cubic spleen, $p < 0.001$). Concentrations range from 2 mg.g_{FW}^{-1} to 93 mg.g_{FW}^{-1}[1]. Starch steadily accumulates in rhizomes from April to August in control and 15% shading treatments but decreases from July in 30% and, to a lesser extent, 60% shading (restricted cubic spline, $p < 0.006$ and $p = 0.936$, respectively). Concentrations range from 25 to 250 mg.g_{FW}^{-1}. Interestingly, the rate of carbohydrates accumulation over time seems to be proportional to relative light intensity, particularly for starch whose concentration decrease in late summer in 30% and 60% shading treatments (see fig. 3.4). Soluble carbohydrates peak in August is also lower in the two most shaded treatments, but the accumulation throughout the experimental period keeps increasing however.

[1]With the exception of a negative value.

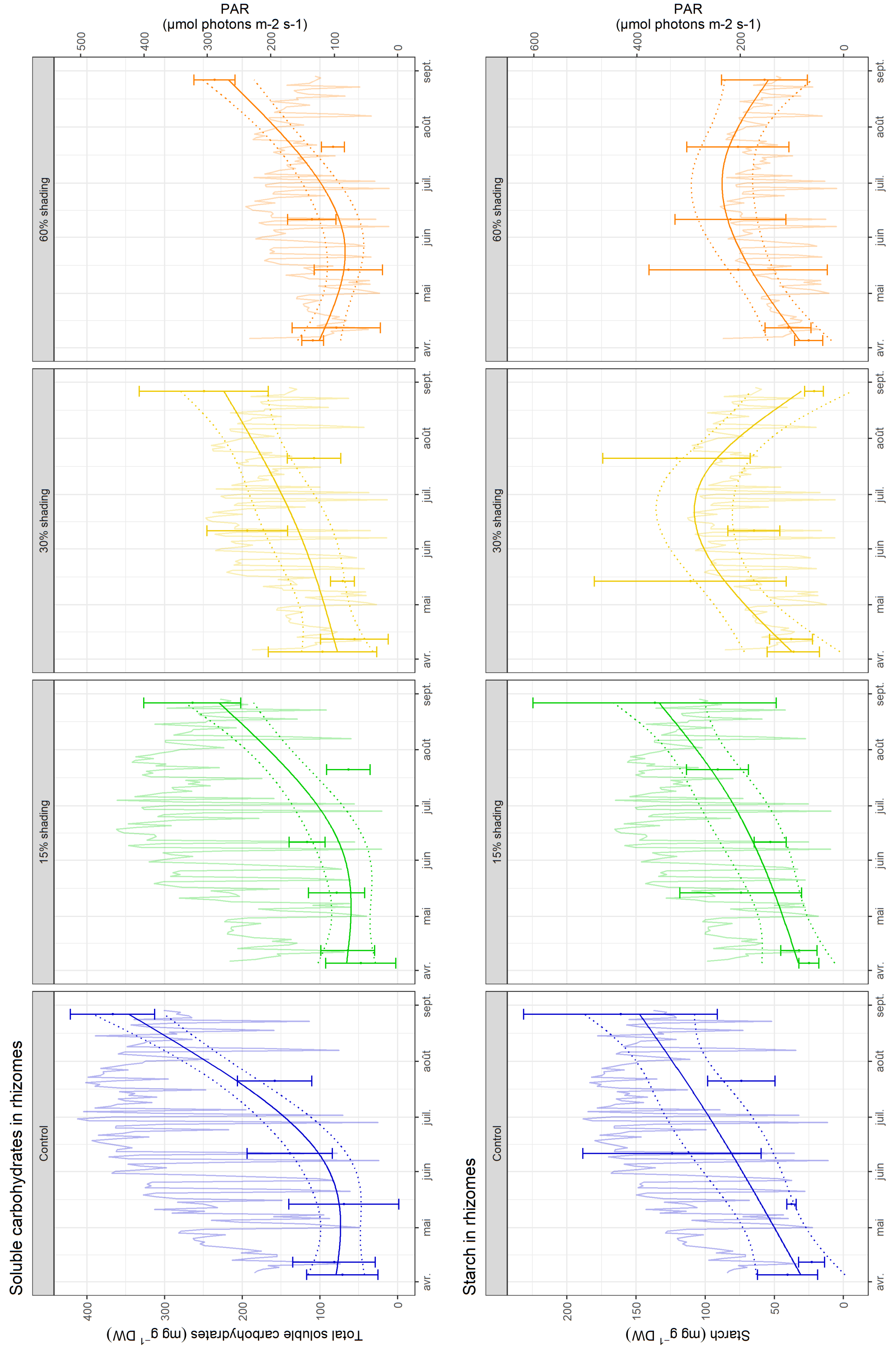

Figure 3.4: **Carbohydrates**
(Top) Total soluble carbohydrates; (Bottom) Starch. n = 6.

3.6 Biometry

Globally, shoot development phenology is not influenced by shading treatments (fig. 6.3). Shoot dry weight is minimal in June, in 30% treatment (0.82 ± 0.23 mg_{DW}) and increases from April to July (maximum in control treatment with 1.30 ± 0.41 mg_{DW}) then drops in August, at least for control and 15% shading treatments (fig. 3.5). The dry shoot biomass in the 30% shading treatment, however, decreases in spring until it reaches a minimum in June before rising until August. The growing pattern in the most shaded treatment seems to be similar to what is observed in the 30% shading treatment, but the minimum is less marked. Total foliar surface follows a similar trend, but the maximum is reached in June (337 ± 58.9 cm^2 in control) and the minimum in August (239 ± 68.3 cm^2 in 60% shading) (fig. 6.4).

Primary production dry weight decreases between May and August, but not significantly (quantile regression, $p = 0.085$). No difference between treatments are detected neither. This lack of temporal evolution is confirmed by total shoot dry weight ($p = 0.12$), that also shows no differences among shading levels.

Epiphytes biomass decreases through time from May to August, in a similar way in all treatments (fig. 3.5). Maximal dry biomass relative to foliar surface is reached in May in 15% shading (11.9 ± 1.62 $mg_{DW}.m^{-2}$) and minimal value is observed in August, 30% shading (3.19 ± 0.48 $mg_{DW}.m^{-2}$). The same trend is observed for total epiphytes biomass.

The longest leaf length for each shoot continuously increases throughout the growing season, from 621 ± 74 cm in April, 15% shading to 1030 ± 148 cm in August, 60% shading (fig. 3.5). The growing pattern is similar in all treatments. Total foliar surface, however, shows a slight concave curve in control and 60% shading (maximum of 337 ± 59 cm^2 observed in June, control) whereas it is roughly constant through time in 15% shading and shows a concave trend in 30% shading (minimum in June) (fig. 3.5). Overall, the minimal foliar surface is reached in August, 60% shading (239 ± 68 cm^2). The total shoot surface/shoot dry weight ratio was not affected either (fig. 3.5).

The A coefficient (percentage of damaged leaves) increases between April and July, then drops in August (fig. 3.5). It is minimal in April, 30% shading (9.3 ± 11 % of leaves whose apex is damaged) and maximal in July, 30% shading (53 ± 17 % of leaves are damaged).

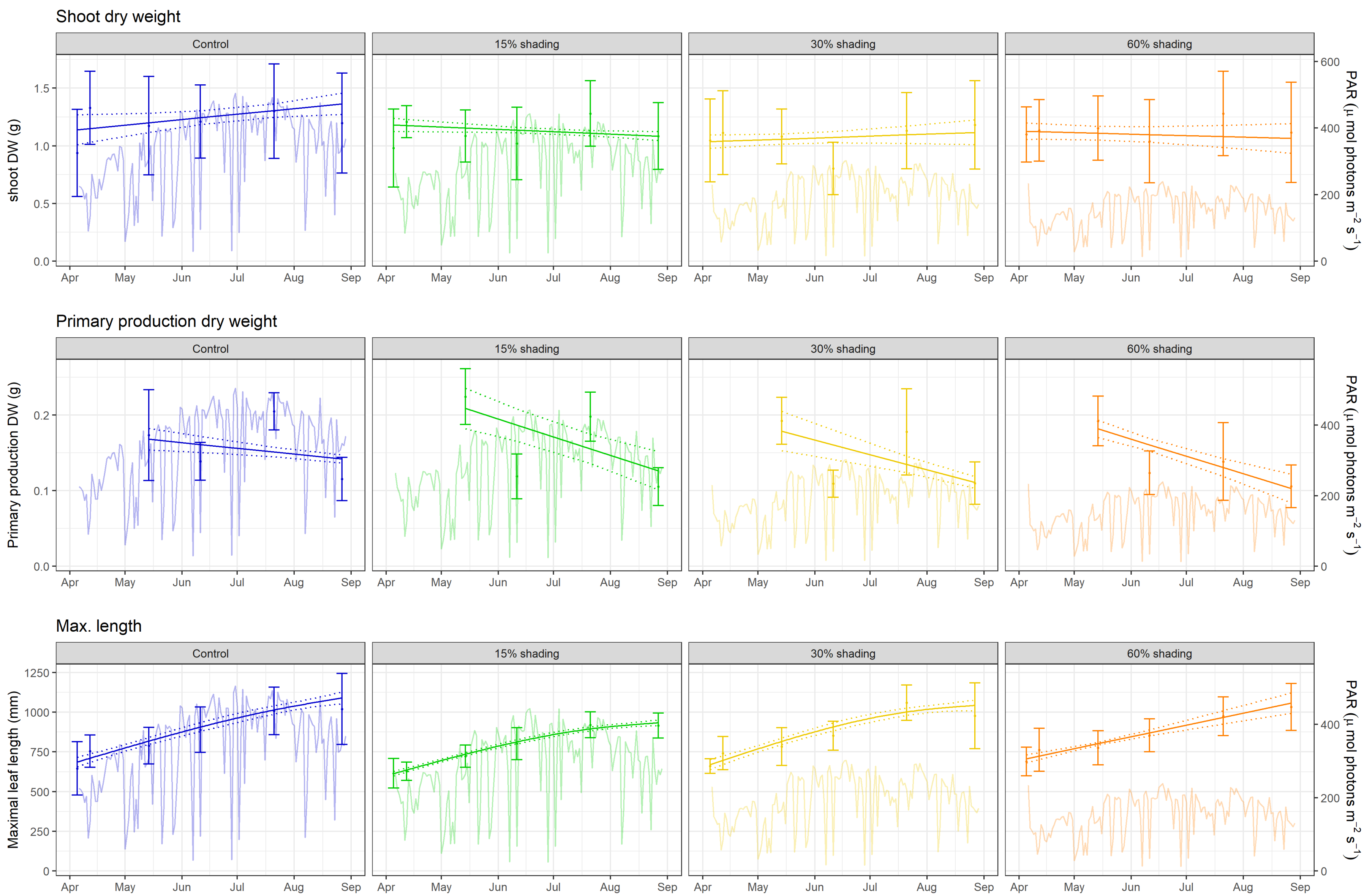

Figure 3.5: **Biometry**
(Top) Shoot dry weight; (Middle) Primary production dry weight; (Bottom) Leaves maximal length. n = 10

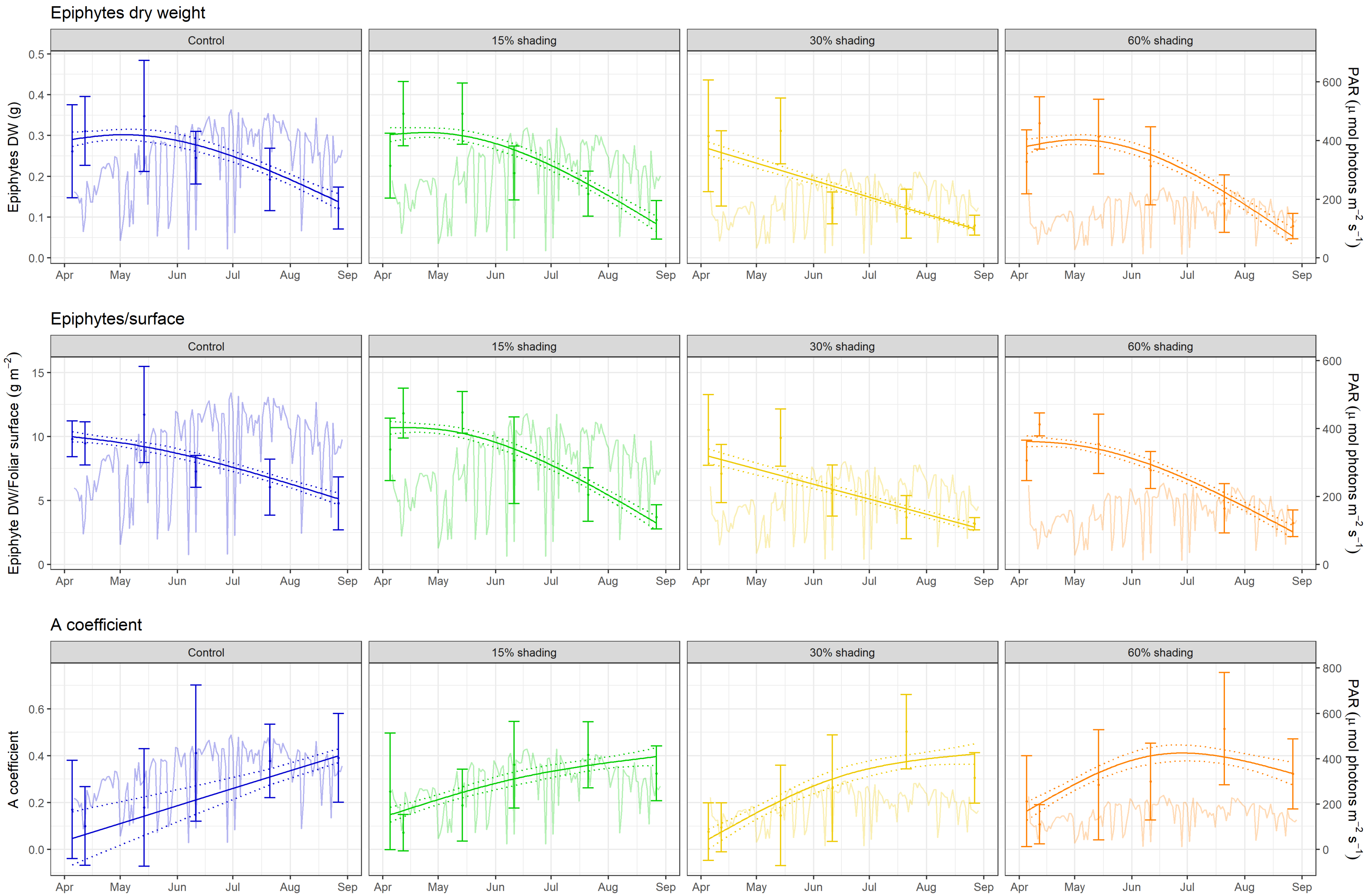

Figure 3.5: **Biometry (cont.).**
(Top) Maximum leaves length; (Middle) Epiphytes dry weight relative to total foliar surface; (Bottom) A coefficient. n = 10

4

Discussion

The aim of this work was to investigate *Posidonia oceanica* response to a low to moderate light deprivation.

Experimental shading without confounding factors is important to understand the effects of sole shading. But in reality, shading will certainly not come alone. Eutrophication is probably one of the main shading causes (Calleja et al. (2007)). Phytoplankton blooms will, on one hand, intercept some light. On the other hand, these cell proliferations will result in an excess of organic matter, that accumulates in the roots/rhizomes system and promotes bacterial growth, leading to oxygen depletion.

Nevertheless, it is necessary to understand how *P. oceanica* responds to variations in a sole parameter with controlled experimental approaches.

4.1 Environmental parameters

Light, in every treatment, reaches its maximum intensity in end June/early July whereas temperature does not reach a plateau earlier than August (fig. 3.1) because of the inertia of water towards temperature.

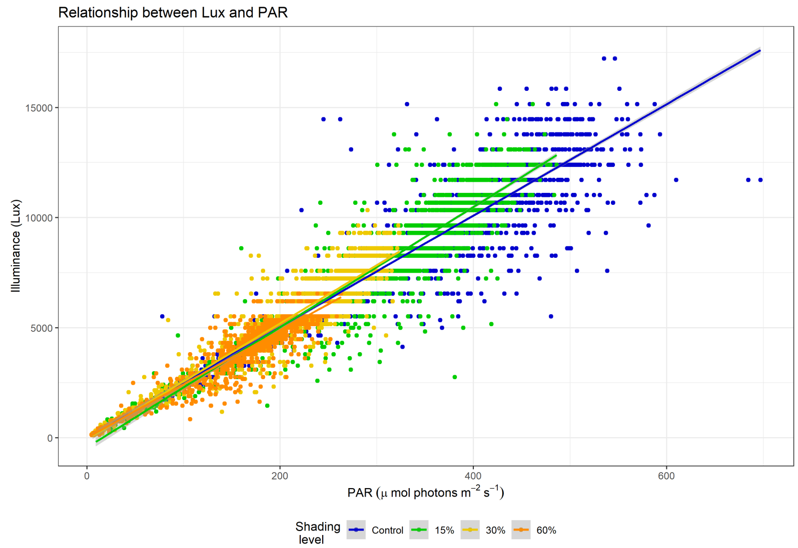

Figure 4.1: **Relationship between PAR and illuminance (lx).**

The screens fixed above the meadow aimed to decrease light intensity only, without shift in its spectrum. A method to check this is to analyze the correlation between PAR and illuminance measurements for each treatment. If spectra are different (i.e., filtration of some wavelength in the PAR range), slopes of PAR/illuminance relationships could be modified among treatments. As shown on fig. 4.1, slopes are similar.

4.2 Pigments and Photosynthesis

4.2.1 Pigments

No zeaxanthin, the most efficient pigment of the VAZ xanthophyll for light dissipation (Jahns and Holzwarth (2011)), was detected in any sample. Some peaks identified after chromatography were close to the theoretical retention time, but absorption spectra did not match zeaxanthin spectrum enough to be considered as this. Dattolo et al. (2014) detected very low zeaxanthin content as well in *P. oceanica*, either at 5 m or at 25 m. A high irradiance treament (1200 μmol photons m^{-2} s^{-1}) induced a dramatic increase in this pigment content but, surprisingly, no change in zeaxanthin epoxidase (involved in conversion of zeaxanthin to antheraxanthin, Taiz et al. (2015)) expression between both depths. Marín-Guirao et al. (2013) also did not detected zeaxanthin in *P. oceanica* samples collected at 5-7 m in April whereas an experimental exposure to a high light irradiance (600 μmol photons m^{-2} s^{-1}, namely 20% more than the maximal midday mean irradiance reached in our control treatment) induced zeaxanthin biosynthesis. The high variability in antheraxanthin concentration shows the highly dynamic interconversion between VAZ pigments. Casazza and Mazzella (2002) analyzed pigment content in several seagrass species. They only detected traces of antheraxanthin in *P. oceanica*. Given the absence of zeaxanthin, variations in the de-epoxidation ratio $((A + Z)/(A + Z + V))$ are mainly driven by sole antheraxanthin concentration (it explains 77.3% of VAZ ratio variance ($p < 0.001$) whereas violaxanthin explains 0.2% of the variance, $p = 0.360$ (linear regression)).

The constant xanthophylls concentration (including $\beta\beta$-carotene and lutein, that are also involved in non photochemical quenching, Telfer (2002) and Jahns and Holzwarth (2011)) among shading treatments could suggest that non-shaded plants at 15 m already have a minimal pool of pigments because light intensity is low, even without experimental shading. Moreover, the whole VAZ pool is in the form of violaxanthin in our experiment. This makes sense at this depth since it is the least efficient VAZ pigments for light dissipation (Jahns and Holzwarth (2011)).

Even if pigments in samples harvested at dawn and those harvested at midday were considered together given the low number of significant differences among treatment/month combinations, there is a general trend for a higher content in pigments at dawn. Leaves harvested at dawn were kept in seawater during several hours to perform P/I curves whereas those sampled at noon were frozen faster. A higher degradation index is thus expected in dawn samples despite efforts to avoid this (samples transported in opaque bags then conservation in sea-temperature tanks).

In addition, a reflection about the circadian clock in plants could account for some observations. Many physiological events in plants are regulated by an endogenousa oscillator, the circadian clock (Taiz et al. (2015)), mainly regulated by photoperiod. It has been shown to regulate the expression of many genes in *Arabidopsis thaliana*, including some involved in photosynthesis and chlorophyll synthesis (Harmer et al. (2000)). The circadian clock is maybe modified among shading treatments ; it is possible that the plant detects a longer night (early and late day could be perceived as night in shaded plants). Besides, the daily variation in some genes expression driven by the circadian clock could explain the slight difference in pigments content between dawn and midday. For instance, Ralph et al. (2002) observed strong circadian variations in VAZ xanthophylls concentration (and in relative concentrations between them).

4.2.2 Photosynthesis

Diving-PAM technology has been used extensively on seagrass in the past decades. All PAM parameters recorded by the Diving-PAM (except F_v/F_m) are strongly influenced by temporal variations in light intensity, as shown by the close co-variation between PAR and RLC, PI and Yield data on fig. 3.3. N. Bouchachi (2017, nonpublished) measured $rETR_m$ in the same meadow, at 10 m (fig. 4.2). Her results follow approximately the same seasonal trend. Absolute values are similar to ours (if the same AF and 0.5 correcting factor are assumed).

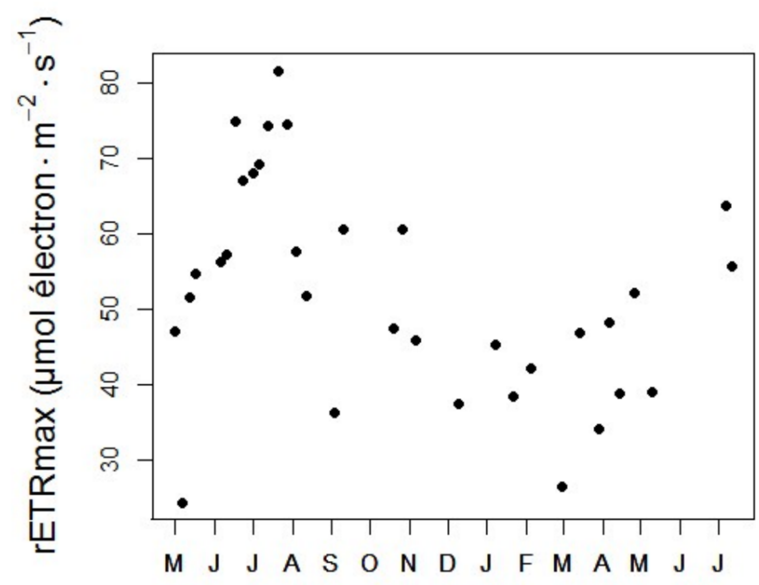

Figure 4.2: **rETR$_m$ results of N. Bouchachi (2017, nonpublished).**

Ralph and Gademann (2005) performed RLC on *Zostera marina* leaves, either experimentally acclimated to low irradiance (50 μmol photons m^{-2}.s^{-1}, lower than our most shaded treatment) or to high irradiance (300 μmol photons m^{-2}.s^{-1}; our control and 15% treatment reach this value in summer, and also in spring and autumn for the control, fig. 3.1). He showed strong differences in light curves shape between both experimental light expositions even though both plant materials were sampled at the same depth (fig. 4.3).

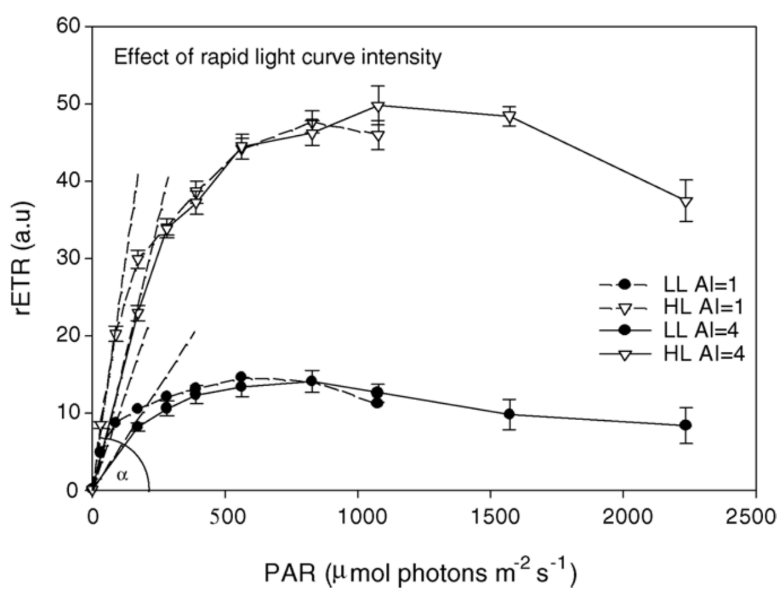

Figure 4.3: **RLC performed on high light adapted (HL) and low light adapted (LL) *Z. marina* leaves. From Ralph and Gademann (2005)**

Our RLC results show a strong temporal variation in RLC shape (fig. 4.4). When light is weak (e.g., t_0 in April), photosynthesis saturates quickly (see I_k, fig. 3.3), at a low rate (ETR_m, 3.3). The seasonal trend is marked whereas a decrease in ETR_m and I_k across the shading gradient is only slightly perceptible (more for I_k, showing that the plants become adapted to low-irradiance conditions). When light is more intense, the plant adapts itself to higher irradiances: I_k and ETR_m increase (fig. 3.3, $p < 0.001$ for temporal variations), despite a slight decrease in Y(II) ($p < 0.01$) since incident irradiance exceeds photosynthetic capacities. This pattern was expected to be observed along the shading gradient as well (as Ralph and Gademann (2005) observed on *Z. marina*), but it is not the case here. It is interesting to underline a coherent relationship between ETR_m and shading intensity, particularly in June. However, the relationship between RLC parameters and shading is far from always consistent over the whole shading period. For instance, PAR is lower in summer in the most shaded treatment than in April, control treatment. However, RLC under 60% shading in summer are more similar to RLC measured the same month, control treatment than to curves measured in April (fig. 4.4). This would suggest a part of plasticity to new light conditions (best observed in June) that is added to a strong undisturbed internal clock regulation.

P/I curves seasonal pattern, however, is not so strong (fig. 3.3). This suggest that *P. oceanica* photosynthesis apparatus was not deeply affected by light deprivation. It only keeps the capacity to dynamically react to light variations (as proved by RLC).

A decrease in F_v/F_m, given its relation to photoinhibition, is often interpreted as a stress symptom (Mishra (2018) and Silva et al. (2009)). The uniform F_v/F_m in this experiment indicates that *P. oceanica* is not significantly affected by light deprivation. (Beer et al. (2014)) makes the distinction between two kinds of F_v/F_m measurements depending on dark-adaptation duration. If it is measured after a long period of dark (e.g., a full night as for this experiment), there is enough time for photodamage-related degradations (e.g., destruction of D1 protein) to recover. This is particlulary adapted for the use of this parameter as a measure of stress. Otherwise, F_v/F_m measurement can be taken after only 10-15 minutes of darkness, which is not long enough for repair. However, photosystems can switch back to an oxidized state. The same authors recommend to discard yield values smaller than 0.1 because they are not reliable. No value is concerned in our data set. F_v/F_m was also associated to the content in chlorophyll, the latter

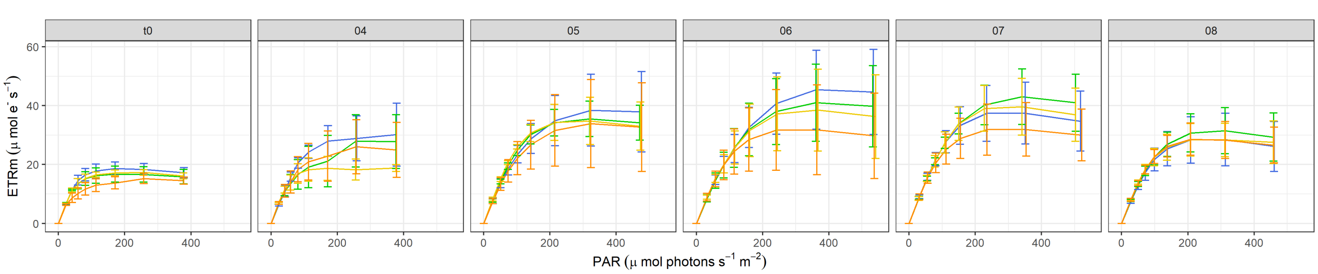

Figure 4.4: **RLC performed in this work. Error bars are mean ± standard deviation.**

being higher in low-light environments for an optimal light capture (hence the higher quantum yield) (Beer et al. (2014)). Our results are consistent with this hypothesis. It is assumed that RLCs do not reach photoinhibition because there is not enough time for that. It is however the case for P/I curves (Ralph and Gademann (2005)). Nevertheless, light curves were performed in such a way that it was stopped before an strong decrease in ETR_m.

G. Ghyselen (2017, nonpublished) investigated the temporal and bathymetric variations of Y(II). He observed a low variability at both scales but a high variability among repeated measurements. The latter observation is probably because Y(II) indicates the *current* state of PSII and can therefore vary within seconds (Ralph et al. (2002)). Here, a clear decrease of Y(II) in summer is observed in 15% shading and control, coinciding with maximal light intensity in summer (fig. 3.3). Indeed, the efficiency of photosystems is reduced in high light conditions because excessive light energy is quenched (Jahns and Holzwarth (2011)). However, there is much less temporal variability in 30% and 60% shading (fig. 3.3). This can be explained by lower light intensities, and therefore less requirements for light dissipation through NPQ. Moreover, the amplitude in light variations between April and summer is lower (fig. 3.1).

Standardization of the PAM protocol is of great importance for reliability and replicability of measurements. Indeed, a great variability in I_k and ETR_m – proportionnal to leaf age – has been observed along leaves, at a given moment (Alcoverro et al. (1998), Leonard 2012, unpublished). Our yield measurements and light curves were always performed on the epiphyte-free middle section of the 3^{rd} leaf. It is necessary to select leaf tissue, short-shoot location, and time of measurement for *in situ* determination of the photosynthetic activity parameters (Durako (2007)).

There is often a confusion between RLC-α and maximal photochemical yield, that are interpreted as the same value. This is however not true (Saroussi and Beer (2007)). This experiment confirms the absence of correlation between PI-α or RLC-α and F_v/F_m or Y(II), respectively (figs. 6.6 and 6.7). AF (absorption factor), the correction factor for the difference between incident and absorbed light irradiance, has been shown to change through time (Durako (2007)) and between species (Beer et al. (1998)), being for instance correlated to chlorophyll content, that displays strong temporal variations (fig. 3.2, Saroussi and Beer (2007)). When the AF is unknown or uncertain, ETR can be expressed as rETR = Y(II)*PAR. It is assumed to be proportional to ETR, but with a constant value of AF. Moreover, RLC and PI are analyzed with incident irradiance on the x-axis. However, it would be more reliable to use *absorbed* irradiance, namely incident irradiance corrected with AF (Beer et al. (2014)). This could provide more accurate estimates of ETR_m and I_k. Here, AF = 0.84 was used for every light curves. Ignoring these potential bias, it can be concluded that *P. oceanica* adapts its photosynthetic activity to a decrease in light intensity. Indeed, both I_k and ETR_m for RLC are lower in high shading treatments (fig. 3.3). It means that the photosystems become more efficient at lower irradiance levels (decrease in I_k) and decreases its activity (decrease in ETR_m).

It is difficult to predict growth on the basis of PAM measurements because *net* photosynthesis (or *true* photosynthesis) only is estimated with fluorescence, not *gross* photosynthesis (*apparent* photosynthesis), because of a lack of data about respiration (Silva et al. (2009) and Beer et al. (2014)). I_c – the compensating irradiance, that is not the same as I_k discussed earlier – is often used as an indicator of the balance between photosynthesis and respiration and is useful to assess the long-term effects of a stress (Alcoverro et al. (1998)). Our results do not give any explicit information about the impact of shading on respiration. A good correlation was found between PAM-based ETR_m estimation and rates of photosynthesis estimated with O_2-based light curves (discussed in Beer et al. (1998), on the basis of unpublished data), except sometimes at high irradiances (maybe because of photoinhibition not detected by PAM). But O_2-based P/I curves would be biased anyway because some oxygen produced by photosynthesis is sent to the roots/rhizome system where it reduces sulfides that are highly toxic for plants (Calleja et al. (2007)). Thus, sulfide concentration could be used as a proxy for oxygen production. Porewater was analyzed in this experiment (not in the framework of this work however) and does not show any impact of shading on sulfur concentration (fig. 6.5). Beer et al. (2014) underlines that chl *a* fluorescence analysis is nevertheless suitable for investigation of photosynthetic responses to environmental parameters, in part because it allows to investigate the response of true photosynthesis only, independently of respiration.

4.2.3 Genetic considerations

Several approaches, including *-omics* technologies, have been used to investigate the variability in gene expression along the bathymetric gradient, with a particular focus on light (Dattolo et al. (2013), Dattolo et al. (2014), Procaccini et al. (2017), and Bruno et al. (2010)). Differential expression and/or protein content differences were pointed out for genes involved in photosynthesis, photoprotection, energy metabolism, respiration and protein degradation. Glycolysis and electron transport chain genes are enhanced in high light whereas tricarboxylic acid cycle activity drops and respiration rate increases (Dattolo et al. (2013)). Moreover, it is suggested that deep-living plants are more exposed to oxidative stress because of more investment in basal metabolism. Analysis of gene expression along the bathymetric gradient (5 and 20 m) revealed a strong difference in translation and traduction in genes involved in photophysiology between both depths (Procaccini et al. (2017)). Given the strong differences in gene expression between shallow and deep plants, the authors suggest a genetic differentiation along the gradient. The same pattern was observed for heat shock resistance in *P. oceanica* and *C. nodosa* (Marín-Guirao et al. (2016)). In this kind of bathymetric gradient, results must be carefully interpreted and particularly linked to light because of the confusing temperature factor.

The existence of locally adapted genotypes hypothesis is put forward rather than sole physiological plasticity (which was also suggested for heat waves resistance, Marín-Guirao et al. (2016)). Furthermore, population genetics approaches indicate some genetic differentiation in meadows.

For instance, individuals from the meadow nearby STARESO, where this experiment was conducted, were distinclty discriminated by depth (fig. 4.5). Others results suggest that genetic patters are mainly the result of past historical events whereas current genetic flow is low, resulting in low genetic adaptation potential. (Jahnke et al. (2017)). Our results were obtained on plants with probably very similar local adaptations (screens were close to each others and at the same depth).

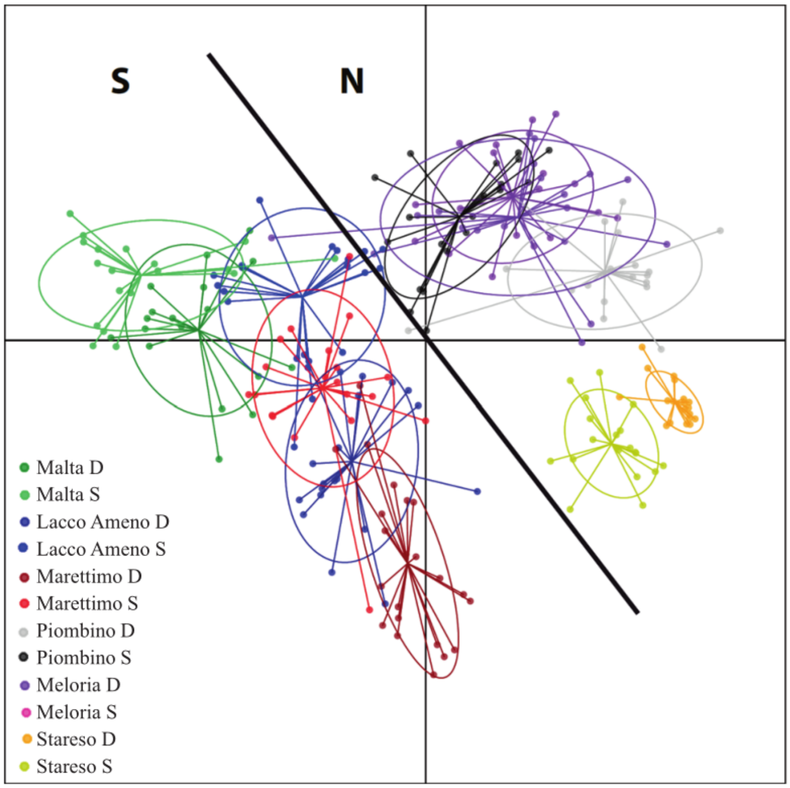

Figure 4.5: **Discrimination of *P. oceanica* shoots by latitude and depth (Jahnke et al. (2018)).** D: shoots sampled at a deep depth; S: shoots sampled at a shallow depth.

Evidence for bathymetric-related light adaptation explains the upwards shift of the meadow at its lower limit (in case of an overall light reduction) and at its upper limit (mainly because of heat waves, Boudouresque et al. (2009) and Marín-Guirao et al. (2016)). Our results support strong local adaptation of *P. oceanica* shoots, resulting in an inertia to changes in environmental conditions.

4.3 Carbohydrates and Biometry

4.3.1 Shoots mortality

At the end of the experiment, no mortality (namely dead matte) was observed, even in the most shaded treatment. Next year (observations in May and December 2019), the observations were the same. Shoot density is estimated to be around 330 shoots m^{-2} at 15 m in this meadow (J. Richir, personnal communication). Ruiz and Romero (2001), that conducted a shading experiment similar to this study but at 9.5 m, observed an important mortality rate under a 40% shading (resulting irradiance similar to our 30% treatment, fig. 1.1) treatment. Nearly 30% of the shoots were dead after 100 days of experiment and it increased up to 40% several hundreds of days after removal of the screens. Interestingly, they were roughly in the same conditions as in this work (healthy and wind-protected meadow, 9.5 m deep). Serrano et al. (2011) observed some mortality only from 99% shading (at 5 m).

4.3.2 Growth

Serrano et al. (2011) observed a reduction of net leaf production in all shading treatments (80%, 90%, 99% of surface irradiance, at 5 m). But all plants, except the most shaded ones (99%), kept an increasing leaf production throughout the shading period, reaching more than 3 mg_{DW} day^{-1} in control and 80% shading (fig. 4.6). Productivity of our meadow in Corsica is higer, with as much as 6 mg_{DW} day $^{-1}$; no increase throughout the season is observed. Ruiz and Romero (2001), however, observed a similar pattern to ours at 9.5 m: decrease throughout time from 6-7 mg_{DW} day $^{-1}$ in June to 1-2 mg_{DW} day $^{-1}$ in September. This difference is probably explained by a shallower depth in Serrano et al. (2011) and therefore a higher intrinsic productivity capacity, nearly undisturbed by shading.

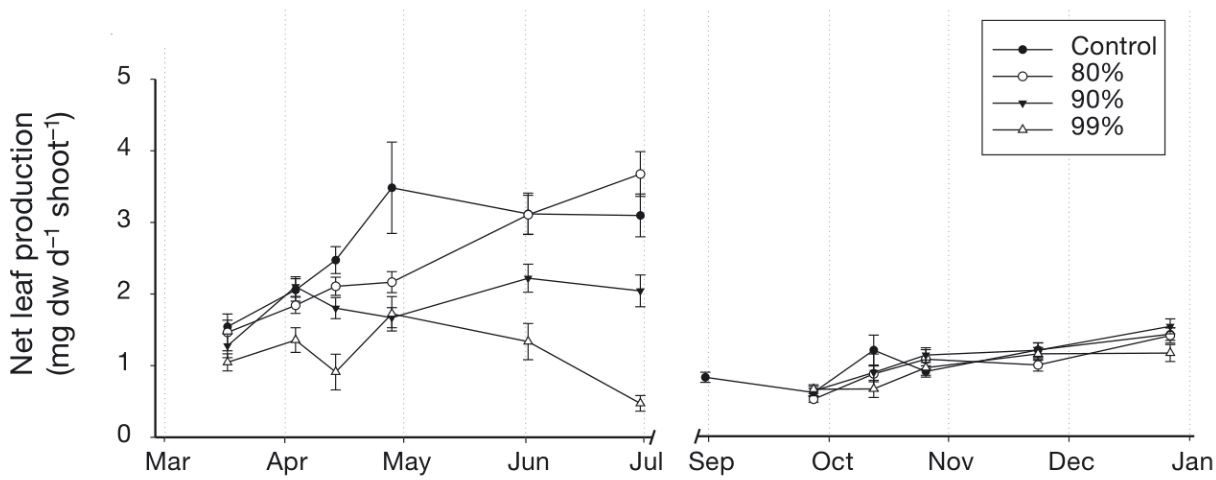

Figure 4.6: **Net leaf production in *P. oceanica* shaded by Serrano et al. (2011).**

N. Bouchachi (2017, nonpublished) conducted a bathymetric survey in summer. Her biometry results extrapolated to 15 m (her plants were sampled at 10 m and 20 m, not inside this interval) are much similar to our results, with the exception of total shoot weight. Is is much higher in her work (about 2 mg_{DW} whereas it ranges between 1-1.5 mg_{DW} here). It is probably explained by the sole inter-annual variability of the meadow productivity; shoot dry weight in this meadow ranges between 1 and 2 g_{DW} from one year to the next (Gobert (2002)).

Another shading experiment at 5 m revealed an interaction between shading treatment and season in *P. oceanica* (Serrano et al. (2011)). Light deprivation of 80% to 99% in autumn and winter, when photosynthesis rate is low and the plants relies mainly on carbohydrates storage accumulated during the previous year, did not prevent the plant from growing normally. Conversely, the same shading in spring and summer, when environmental conditions are optimal for growth, had detrimental consequences for the meadow. Net leaf production was reduced (fig. Serrano et al. (2011)). In our experiment, the meadow was shaded during the optimal period for photosynthesis and carbohydrates storage (April-August). Enough light is necessary during this period for plants to maintain a positive carbon balance over the whole season. On the basis of a experimental shading gradient, Gacia et al. (2012) estimated the threshold of irradiance for balanced metabolism (net primary production > 0) of a whole *P. oceanica* meadow at 6 m to 248 µmol photons s^{-1} m^{-2} (measured in May, at noon). This threshold is not reached in the two most shaded treatments (see fig. 3.1), for which the mean PAR in May are 193 and 151 μmol photons m^{-2} s^{-1} for 30% and 60% shading, respectively. It can be seen in carbohydrates results; starch concentration decreases in late summer in the two most shaded treatments and soluble sugar accumulation rate decreases with increasing shading (fig. 3.4). Extrapolation of this threshold irradiance must be interpreted with great caution because it has been measured on plants sampled at a shallow depth. The plants growing deeper could display local adaptation to lower light conditions resulting in another threshold irradiance.

The same authors did not detect any correlation between irradiance and the cell cycle dynamics in the shoot apical meristem. This could explain the absence of observed changes in growth dynamics of our plants, the plant producing its biomass as usually, regardless of ambient light conditions and compensating the light deficit with the catabolism of storage carbohydrates. Investigation of *P. oceanica* photoreceptors expression in response to light deprivation would be relevant to understand to which extent the seagrass responds to light at the molecular level. Dattolo et al. (nonpublished) detected some variations in gene expression across the day, including one phytochrome and both cryptochromes.

For obvious technical reasons, only nine square meters of meadow for each treatment were experimentally shaded here. However, *P. oceanica* is a clonal plant; ramets are often interconnected. Thus translocation of nutrients or other metabolites from plants exposed to full light to shaded plants could alleviate the consequences of the experimental light reduction. Samples were taken at the center of each screen to avoid this as much as possible. It is well known that translocation of carbon and nutrients occurs between rhizomes and leaves (within a given ramet) as well as between rhizomes of neighbouring ramets. Short-term experiments (a few hours) revealed a transfer of ^{14}C across rhizomes up to 15 cm away from the radioisotope injection site (Libes and Boudouresque (1987)) or 5 ramets further (Marbà et al. (2002)). Since this experiment was conducted at a much larger time scale, the transfer distance could be greater. Collier et al. (2010) shaded *Posidonia sinuosa* (50% light reduction with screens of about the same size as this study) and analyzed carbon and nitrogen translocation between shoots. They showed that nitrogen, unlike carbon, is more translocated from rhizomes to growing leaves in the shaded treatment. However, results of the current work in Corsica show a decrease in carbohydrates in rhizomes but no morphological or physiological modifications at the shoot level (carbohydrates concentration in leaves are not available yet). This would suggest a translocation of carbon as well between different ramets in *P. oceanica*, besides – maybe – nitrogen that will be investigated later in the framework of this experiment. This could explain, in combination with others factors discussed further, why biomass production was not hindered despite up to 60% shading.

Transplantation of shoots and rhizomes across the depth gradient has been performed (Genot et al. (1994)). Before moving shoots, an increase in total chlorophyll ($a + b$) content was observed with increasing depth, along the natural gradient. This content, however, did not change when shoots were transplanted from their origin depth to another. It would suggest a low plasticity of *P. oceanica* regarding pigment content regulation, as observed here. Shoots moved toward the surface from a greater depth did not face any stress. The carbohydrates content decreases proportionally with origin depth, but an efficient photosynthesis (necessary in low-light conditions) was enough to compensate the low reserves in shoot transplanted to lower depths. However, the reverse movement leads to a low survival rate and a strong carbohydrates depletion. The observations for chlorophyll content were replicated here with *in situ* shading (fig. 3.2). It would suggest that *P. oceanica* physiology is, at least partially, optimized for a given depth and not able to tolerate, in the long term, harsher environmental conditions because of low plasticity. The lack of plasticity could have been compensated by an increase in reserve carbohydrates use. This hypothesis is strenghten by genetic investigations, discussed earlier.

The important accumulation of carbohydrates in summer is similar to the results of Alcoverro et al. (2001), that observed a peak in summer. Fig. 4.7 shows total nonstrucutral carbohydrates in *P. oceanica* relative to dry weight, in the whole plant.

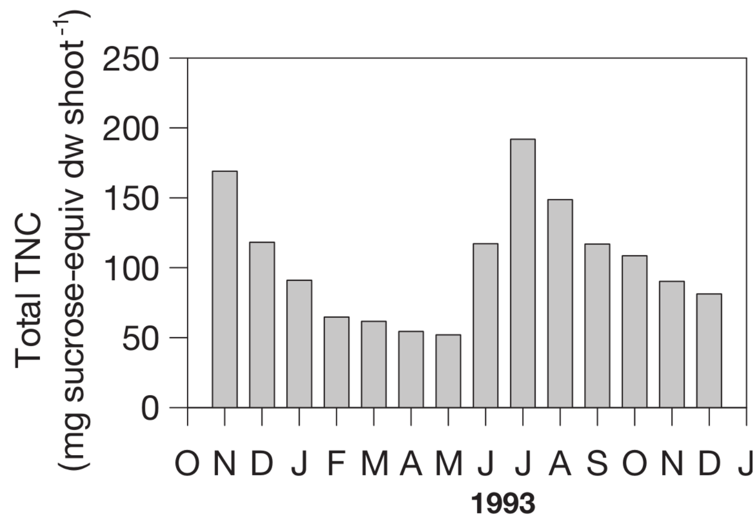

Figure 4.7: **Total nonstructural carbohydrates content in *P. oceanica*. From Alcoverro et al. (2001).**

They estimated the carbon balance to be positive between May and August. This carbon accumulation is necessary to compensate the negative balance observed between September and April (Alcoverro et al. (2001)). On this period, most of the biomass is underground and strictly net consumer of carbohydrates, but shows a low respiratory rate (Alcoverro et al. (2001)).

Interestingly, primary production dry weight decreases from April-May to August whereas light and temperature are growing (at least until July for light). Indeed, most of *P. oceanica* primary production is produced in winter and spring and not in summer (also shown by the low changes in shoot biomass, fig. 3.5), despite conditions often considered as optimal for plant growth (Pirc (1986)). The high photosynthetic rate in summer (fig. 3.3) produces carbohydrates reserves that accumulate in tissues (fig. 3.4). They are necessary, not only to sustain a basal metabolism in winter, but also to provide energy and carbon for a sustained growth in low-light and low temperature conditions. Conversely, O_2-based gross primary production estimation of meadows indicates a maximal primary production in June/July (Champenois and Borges (2018)). However, these values were estimated for the whole meadow ecosystem and not *P. oceanica* alone. A continuous recording of O_2 production, as did Champenois and Borges (2018), could have provided precious information but maybe would have require the use of closed and shaded incubation mesocosms for reliable measurements, given the diffusion of O_2 in water. Here, we estimated biomass and primary production for the plant and leaves-associated epiphytes only. An effect of shading on other components of the *P. oceanica* meadow ecosystem, all of which contribute to respiration and some to primary production, can not be excluded (Personnic et al. (2014)).

The absence of recorded effect of light deprivation on biometry parameters and primary production makes sense under the following hypothesis. The plants in all shading treatments have used their carbohydrates – soluble carbohydrates, and starch particularly – synthesized during the previous year (in full light conditions for all treatments). These storage metabolites were used at the beginning of the shading experiment to produce most of the biomass, as usual. Then, in summer, the accumulation of carbohydrates - that will be used next year – allowed by optimal light and temperature conditions is reduced in the most shaded treatments. This could be detrimental for the next year's growth.

The A coeffiicent (proportion of damages apexes) decreases in August because many intact juvenile leaves grow at this period (Pergent1991). When considering adult leaves only, leaves are decaying and therefore often torn away or at least seriously damaged. Apex degradation does not differ between treatments; it means that shading did not influence the presence of herbivores animals.

5

Conclusion

The main goal of this experiment was to study the short to long term effect of low to moderate experimental shading on *P. oceanica* physiology, morphology and production. Indeed, previous works were either short term studies, or used very strong thus little environmentally relevant shading treatments. Furthermore, *in situ* experimental shading is complementary to bathymetric surveys along the natural gradient of distribution of the plant, that also provides precious information about *P. oceanica* response to different environmental conditions.

We hightlighted no response of the plants regarding its pigments content (except little trends for chl *b* and the chl *a*/chl *b* ratio), primary production and phenology. However, the photosynthetic activity showed some dynamic responses to shading: saturation at lower irradiance, higher efficiency and lower total activity. Regarding carbohydrate concentrations, soluble carbohydrates and starch in rhizomes decreased over time when compared to control with increasing shading level.

The results of this experiment show that five months is not long enough to evaluate with certainty how *P. oceanica* shoots from an healthy and little disturbed meadow responds to low to moderate shading treatments. The decrease in carbohydrates content suggests however some harmful effects at long term for growth. This experiment should be replicated with less replicates (i.e. only one shading treatment) to alleviate the field work but on several years. New results from such a long study will probably refute the apparent good health plants still display over five months of shading. Furthermore, gene expression studies (even *-omics* approaches) should be used to understand the molecular mechanisms impacted by experimental *in situ* shading, with a particular focus on light reduction perception (i.e., analysis of photoreceptors expression). Nevertheless, this work underlines the strong capacity of healthy *P. oceanica* to resist local (nine m^2 surfaces) light stress and to maintain its usual primary production and pigments content, as well as to slightly adapt its photosynthesis for an optimal resilience. This is assumed to be possible because of a significant use of storage carbohydrates (in rhizomes), particularly starch (and some compensation process through translocation).

This work was carried out in the context of a larger study that aims to understand other physiological parameters as well. Organosulfur compounds DMSP and DMSO content will be measured in leaves. Carbohydrates concentration in leaves will be assessed as well. It would also be possible to investigate deeper the photosynthetic activity with other parameters recorded by the Diving-PAM (quenching parameters and reflectance for instance).

Bibliography

Abadie, Arnaud et al. (2016). “From mechanical to chemical impact of anchoring in seagrasses: The premises of anthropogenic patch generation in Posidonia oceanica meadows”. In: *Marine Pollution Bulletin* 109.1, pp. 61–71. DOI: 10.1016/j.marpolbul.2016.06.022. (Visited on 06/01/2019).

Ackerman, Josef Daniel (2006). “Sexual Reproduction of Seagrasses: Pollination in the Marine Context”. In: *Seagrasses: Biology, Ecology and Conservation*. Springer. Dordrecht: Larkum Anthony. W.D., Orth Robert J., Duarte Carlos M., pp. 89–109.

Alcoverro, Teresa, Carlos M. Duarte, and Javier Romero (1997). “The influence of herbivores on Posidonia oceanica epiphytes”. en. In: *Aquatic Botany* 56.2, pp. 93–104. DOI: 10.1016/S0304-3770(96)01098-4. (Visited on 02/09/2019).

Alcoverro, Teresa, Marta Manzanera, and Javier Romero (1998). “Seasonal and age-dependent variability of Posidonia oceanica (L.) Delile photosynthetic parameters”. In: *Journal of Experimental Marine Biology and Ecology* 230.1, pp. 1–13. DOI: 10.1016/S0022-0981(98)00022-7.

— (2001). “Annual metabolic carbon balance of the seagrass Posidonia oceanica: the importance of carbohydrate reserves”. en. In: *Marine Ecology Progress Series* 211, pp. 105–116. DOI: 10.3354/meps211105. (Visited on 05/28/2019).

Ballesteros, Enric et al. (2005). “Pseudovivipary, a new form of asexual reproduction in the seagrass Posidonia oceanica”. en. In: *Botanica Marina* 48.2. DOI: 10.1515/BOT.2005.026. (Visited on 05/31/2019).

Beer, Sven, Mats Björk, and John Beardall (2014). *Photosynthesis in the Marine Environment*. en. John Wiley & Sons. ISBN: 978-1-119-97958-6.

Beer, S et al. (1998). “Measuring photosynthetic rates in seagrasses by pulse amplitude modulated (PAM) fluorometry”. In: *Mar. Ecol. Prog. Ser.* 174, pp. 293–300. DOI: 10.3354/meps174293.

Blankenship, Robert E. and Roger C. Prince (1985). “Excited-state redox potentials and the Z scheme of photosynthesis”. In: *Trends in Biochemical Sciences* 10, pp. 382–383.

Borg, J. A. et al. (2006). “Wanted dead or alive: high diversity of macroinvertebrates associated with living and ‘dead’ Posidonia oceanica matte”. en. In: *Mar Biol* 149.3, pp. 667–677. DOI: 10.1007/s00227-006-0250-3. (Visited on 04/28/2019).

Boudouresque, Charles F. et al. (2009). “Regression of Mediterranean seagrasses caused by natural processes and anthropogenic disturbances and stress: a critical review”. In: *Botanica Marina* 52.5, pp. 395–418. DOI: 10.1515/BOT.2009.057. (Visited on 04/21/2019).

Boudouresque, Charles F. et al. (2016). “The necromass of the Posidonia oceanica seagrass meadow: fate, role, ecosystem services and vulnerability”. en. In: *Hydrobiologia* 781.1, pp. 25–42. DOI: `10.1007/s10750-015-2333-y`. (Visited on 06/07/2019).

Boudouresque, Charles-François et al. (2012). "Protection and conservation of Posidonia Oceanica meadows". en. In: *RAMOGE and RAC/SPA publisher, Tunis*, p. 202.

Bruno, A et al. (2010). "PoCHL P expression pattern in Posidonia oceanica is related to critical light conditions". In: *Mar. Ecol. Prog. Ser.* 415, pp. 61–71. DOI: `10.3354/meps08725`.

Buia, M. C. and L. Mazzella (1991). "Reproductive phenology of the Mediterranean seagrasses Posidonia oceanica (L.) Delile, Cymodocea nodosa (Ucria) Aschers., and Zostera noltii Hornem." In: *Aquatic Botany* 40.4, pp. 343–362. DOI: `10.1016/0304-3770(91)90080-O`. (Visited on 04/21/2019).

Buia, Maria Cristina, Valerio Zupo, and Lucia Mazzella (1992). "Primary Production and Growth Dynamics in Posidonia oceanica". en. In: *Marine Ecology* 13.1, pp. 2–16. DOI: `10.1111/j.1439-0485.1992.tb00336.x`. (Visited on 06/03/2019).

Burke, M.K., W.C. Dennison, and K.A Moore (1996). "Non-structural carbohydrate reserves of eelgrass Zostera marina". en. In: *Marine Ecology Progress Series* 137, pp. 195–201. DOI: `10.3354/meps137195`. (Visited on 05/28/2019).

Cade, Brian S and Barry R Noon (2003). "A gentle introduction to quantile regression for ecologists". In: *Front Ecol Environ* 1.8, p. 9.

Calleja, Maria Ll., Núria Marbà, and Carlos M. Duarte (2007). "The relationship between seagrass (Posidonia oceanica) decline and sulfide porewater concentration in carbonate sediments". In: *Estuarine, Coastal and Shelf Science* 73.3, pp. 583–588. DOI: `10.1016/j.ecss.2007.02.016`.

Campagne, Carole Sylvie et al. (2015). "The seagrass Posidonia oceanica: Ecosystem services identification and economic evaluation of goods and benefits". In: *Marine Pollution Bulletin* 97.1, pp. 391–400. DOI: `10.1016/j.marpolbul.2015.05.061`. (Visited on 05/19/2019).

Casazza, Gianna and Lucia Mazzella (2002). "Photosynthetic pigment composition of marine angiosperms: Preliminary characterization of Mediterranean seagrasses". In: 71.3.

Casola, E. et al. (1987). "Structure of the Epiphytic Community of Posidonia oceanica Leaves in a Shallow Meadow". en. In: *Marine Ecology* 8.4, pp. 285–296. DOI: `10.1111/j.1439-0485.1987.tb00189.x`. (Visited on 04/25/2019).

Cebrián, J. et al. (1999). "Epiphyte Accrual on Posidonia oceanica (L.) Delile Leaves: Implications for Light Absorption". en. In: *Botanica Marina* 42.2. DOI: `10.1515/BOT.1999.015`. (Visited on 02/09/2019).

Champenois, W. and A. V. Borges (2012). "Seasonal and interannual variations of community metabolism rates of a Posidonia oceanica seagrass meadow". en. In: *Limnology and Oceanography* 57.1, pp. 347–361. DOI: `10.4319/lo.2012.57.1.0347`. (Visited on 05/30/2019).

— (2018). "Inter-annual variations over a decade of primary production of the seagrass Posidonia oceanica". en. In: *Limnology and Oceanography* 64.1, pp. 32–45. DOI: `10.1002/lno.11017`. (Visited on 05/30/2019).

Collier, Catherine J., Patricia Prado, and Paul S. Lavery (2010). "Carbon and nitrogen translocation in response to shading of the seagrass Posidonia sinuosa". en. In: *Aquatic Botany* 93.1, pp. 47–54. DOI: 10.1016/j.aquabot.2010.03.003.

Collier, Cj et al. (2008). "Physiological characteristics of the seagrass Posidonia sinuosa along a depth-related gradient of light availability". In: *Mar. Ecol. Prog. Ser.* 353, pp. 65–79. DOI: 10.3354/meps07171.

Costa, Monya M. et al. (2015). "Epiphytes Modulate Posidonia oceanica Photosynthetic Production, Energetic Balance, Antioxidant Mechanisms, and Oxidative Damage". English. In: *Front. Mar. Sci.* 2. DOI: 10.3389/fmars.2015.00111. (Visited on 03/05/2019).

Croce, Roberta and Herbert van Amerongen (2014). "Natural strategies for photosynthetic light harvesting". In: *Nat Chem Biol* 10.7, pp. 492–501. DOI: 10.1038/nchembio.1555.

Dattolo, Emanuela et al. (2013). "Acclimation to different depths by the marine angiosperm Posidonia oceanica: transcriptomic and proteomic profiles". In: *Front. Plant Sci.* 4. DOI: 10.3389/fpls.2013.00195.

Dattolo, E. et al. (2014). "Response of the seagrass Posidonia oceanica to different light environments: Insights from a combined molecular and photo-physiological study". In: *Marine Environmental Research* 101, pp. 225–236. DOI: 10.1016/j.marenvres.2014.07.010. (Visited on 04/21/2019).

Dauby, Patrick and Mathieu Poulicek (1995). "Methods for removing epiphytes from seagrasses: SEM observations on treated leaves". en. In: *Aquatic Botany* 52.3, pp. 217–228. DOI: 10.1016/0304-3770(95)00500-5. (Visited on 02/09/2019).

Demmig-Adams, Barbara and William W. Adams (1996). "The role of xanthophyll cycle carotenoids in the protection of photosynthesis". In: *Trends in Plant Science* 1.1, pp. 21–26. DOI: 10.1016/S1360-1385(96)80019-7. (Visited on 04/10/2019).

Duarte, Carlos M. (2017). "Reviews and syntheses: Hidden forests, the role of vegetated coastal habitats in the ocean carbon budget". en. In: *Biogeosciences* 14.2, pp. 301–310. DOI: 10.5194/bg-14-301-2017. (Visited on 05/29/2019).

Duarte, Carlos M. et al. (2010). "Seagrass community metabolism: Assessing the carbon sink capacity of seagrass meadows". en. In: *Global Biogeochemical Cycles* 24.4. DOI: 10.1029/2010GB003793.

DuBois, Michel. et al. (1956). "Colorimetric Method for Determination of Sugars and Related Substances". en. In: *Analytical Chemistry* 28.3, pp. 350–356. DOI: 10.1021/ac60111a017.

Durako, Michael J. (2007). "Leaf optical properties and photosynthetic leaf absorptances in several Australian seagrasses". In: *Aquatic Botany* 87.1, pp. 83–89. DOI: 10.1016/j.aquabot.2007.03.005.

Eskling, Marie and Hans-Erik Åkerlund (1998). "Changes in the quantities of violaxanthin de-epoxidase, xanthophylls and ascorbate in spinach upon shift from low to high light". en. In: *Photosynthesis Research* 57.1, pp. 41–50. DOI: 10.1023/A:1006015630167. (Visited on 05/31/2019).

Esteban, Raquel et al. (2009). "Distribution and evolutionary trends of photoprotective isoprenoids (xanthophylls and tocopherols) within the plant kingdom". en. In: *Physiologia Plantarum* 135.4, pp. 379–389. DOI: 10.1111/j.1399-3054.2008.01196.x. (Visited on 05/20/2019).

Fisher, Brendan, R. Kerry Turner, and Paul Morling (2009). "Defining and classifying ecosystem services for decision making". In: *Ecological Economics* 68.3, pp. 643–653. ISSN: 0921-8009. DOI: 10.1016/j.ecolecon.2008.09.014. (Visited on 05/30/2019).

Fowler, Jim and Lou Cohen (1990). *Practical Statistics for Field Biology*. John Wiley & Sons Inc. New York, USA.

Gacia, E. et al. (2012). "Thresholds of irradiance for seagrass Posidonia oceanica meadow metabolism". en. In: *Marine Ecology Progress Series* 466, pp. 69–79. ISSN: 0171-8630, 1616-1599. DOI: 10.3354/meps09928. (Visited on 06/02/2019).

García-Plazaola, Jose I., Shizue Matsubara, and C. Barry Osmond (2007). "The lutein epoxide cycle in higher plants: its relationships to other xanthophyll cycles and possible functions". en. In: *Functional Plant Biol.* 34.9, pp. 759–773. DOI: 10.1071/FP07095. (Visited on 05/20/2019).

Gauthier, J., Q. V. Wu, and T. A. Gooley (2019). "Cubic splines to model relationships between continuous variables and outcomes: a guide for clinicians". In: *Bone Marrow Transplant*, s41409–019–0679–x. DOI: 10.1038/s41409-019-0679-x.

Genot, I. et al. (1994). "Role of chlorophyll and carbohydrate contents in survival of Posidonia oceanica cuttings transplanted to different depths". en. In: *Marine Biology* 119.1, pp. 23–29. DOI: 10.1007/BF00350102. (Visited on).

Giraud, G (1979). "Sur une méthode de mesure et de comptage des mesures foliaires de Posidonia oceanica (Linnaeus) Delile". In: *Bull. Mus. Hist. Nat. Marseille* 39, pp. 33–39.

Gobert, Sylvie (2002). "Variations spatiale et temporelle de l'herbier à Posidonia oceanica (L.) Delile (Baie de la Revellata-Calvi-Corse)". PhD Thesis. Université de Liège, Liège, Belgique.

Gobert, Sylvie, Noémie Laumont, and Jean-Marie Bouquegneau (2002). "Posidonia oceanica meadow: a low nutrient high chlorophyll (LNHC) system?" En. In: *BMC Ecology* 2.1, p. 9. DOI: 10.1186/1472-6785-2-9. (Visited on 04/21/2019).

Gobert, Sylvie et al. (2006). "Biology of Posidonia". In: *Seagrasses: Biology, Ecology and Conservation*. Springer. Dordrecht: Larkum Anthony. W.D., Orth Robert J., Duarte Carlos M., pp. 409–439.

Gobert, Sylvie et al. (2009). "Assessment of the ecological status of Mediterranean French coastal waters as required by the Water Framework Directive using the Posidonia oceanica Rapid Easy Index: PREI". en. In: *Marine Pollution Bulletin* 58.11, pp. 1727–1733. DOI: 10.1016/j.marpolbul.2009.06.012.

Guiry, M.D. and G.M. Guiry (2019). "Posidonia oceanica (Linnaeus) Delile". In: *AlgaeBase. World-wide electronic publication, National University of Ireland, Galway.* URL: http://www.algaebase.org.

Harmer, S. L. et al. (2000). "Orchestrated Transcription of Key Pathways in Arabidopsis by the Circadian Clock". In: *Science* 290.5499, pp. 2110–2113. DOI: 10.1126/science.290.5499.2110.

Harrel, Frank E. (2015). *Regression Modeling Strategies: With Applications to Linear Models, Logistic and Ordinal Regression, and Survival Analysis*. Springer. 598 pp.

Jacquemart, Julien and Vincent Demoulin (2006). “Inventaire des macroalgues épiphytes des feuilles de Posidonia oceanica (L.) Delile dans la baie de la Revelatta (Calvi, Corse)”. fr. In: *lejeunia*. (Visited on 05/30/2019).

Jahnke, Marlene et al. (2017). “Potential and realized connectivity of the seagrass *Posidonia oceanica* and their implication for conservation”. In: *Divers Distrib* 23.12. Ed. by Andrew Lowe, pp. 1423–1434. DOI: 10.1111/ddi.12633.

Jahnke, Marlene et al. (2018). “Adaptive responses along a depth and a latitudinal gradient in the endemic seagrass Posidonia oceanica”. In: *Heredity* 122.2, pp. 233–243. DOI: 10.1038/s41437-018-0103-0.

Jahns, Peter and Alfred R. Holzwarth (2011). “The role of the xanthophyll cycle and of lutein in photoprotection of photosystem II”. In: *Biochimica et Biophysica Acta (BBA) - Bioenergetics*. Photosystem II 1817.1, pp. 182–193. DOI: 10.1016/j.bbabio.2011.04.012. (Visited on 05/20/2019).

Jassby, Alan D. and Trevor Platt (1976). “Mathematical formulation of the relationship between photosynthesis and light for phytoplankton”. en. In: *Limnology and Oceanography* 21.4, pp. 540–547. DOI: 10.4319/lo.1976.21.4.0540. (Visited on 05/31/2019).

Jayathilake, Dinusha R. M. and Mark J. Costello (2018). “A modelled global distribution of the seagrass biome”. In: *Biological Conservation* 226, pp. 120–126. ISSN: 0006-3207. DOI: 10.1016/j.biocon.2018.07.009. (Visited on 05/30/2019).

Karydis, Michael and Dimitra Kitsiou (2012). “Eutrophication and environmental policy in the Mediterranean Sea: a review”. en. In: *Environ Monit Assess* 184.8, pp. 4931–4984. DOI: 10.1007/s10661-011-2313-2. (Visited on 06/02/2019).

Kennedy, Hilary et al. (2010). “Seagrass sediments as a global carbon sink: Isotopic constraints”. en. In: *Global Biogeochemical Cycles* 24.4. DOI: 10.1029/2010GB003848.

Kiparissis, Sotiris et al. (2011). “Illegal trawling and induced invasive algal spread as collaborative factors in a Posidonia oceanica meadow degradation”. en. In: *Biol Invasions* 13.3, pp. 669–678. ISSN: 1573-1464. DOI: 10.1007/s10530-010-9858-9. (Visited on 06/01/2019).

Koenker, Roger and Gilbert Bassett (1978). “Regression Quantiles”. In: *Econometrica* 46.1, p. 33. DOI: 10.2307/1913643.

Lepoint, Gilles et al. (1999). “Fauna vs flora contribution to the leaf epiphytes biomass in a Posidonia oceanica seagrass bed (Revellata Bay, Corsica)”. en. In: *Hydrobiologia* 394, pp. 63–67.

Libes, M and C-F Boudouresque (1987). “Uptake and long-distance transport of carbon in the marine phanerogam Posidonia oceanica”. en. In: *Mar. Ecol. Prog. Ser.* 38, pp. 177–186. DOI: 10.3354/meps038177.

Marbà, Núria, Elena Díaz-Almela, and Carlos M. Duarte (2014). “Mediterranean seagrass (Posidonia oceanica) loss between 1842 and 2009”. In: *Biological Conservation* 176, pp. 183–190. DOI: 10.1016/j.biocon.2014.05.024. (Visited on 05/28/2019).

Marbà, N et al. (2002). "Carbon and nitrogen translocation between seagrass ramets". en. In: *Mar. Ecol. Prog. Ser.* 226, pp. 287–300. DOI: 10.3354/meps226287.

Marín-Guirao, Lazaro et al. (2016). "Physiological and molecular evidence of differential short-term heat tolerance in Mediterranean seagrasses". In: *Sci Rep* 6.1, pp. 1–13. DOI: 10.1038/srep28615.

Marín-Guirao, L. et al. (2013). "Xanthophyll cycle-related photoprotective mechanism in the Mediterranean seagrasses Posidonia oceanica and Cymodocea nodosa under normal and stressful hypersaline conditions". In: *Aquatic Botany* 109, pp. 14–24. DOI: 10.1016/j.aquabot.2013.03.006.

Mascart, Thibaud et al. (2015). "Seasonal variability of meiofauna, especially harpacticoid copepods, in Posidonia oceanica macrophytodetritus accumulations". In: *Journal of Sea Research* 95, pp. 149–160. DOI: 10.1016/j.seares.2014.07.009. (Visited on 04/28/2019).

Mateo, Ma and J Romero (1997). "Detritus dynamics in the seagrass Posidonia oceanica:elements for an ecosystem carbon and nutrient budget". In: *Mar. Ecol. Prog. Ser.* 151, pp. 43–53. DOI: 10.3354/meps151043.

Mazzella, Lucia, Maria Beatrice Scipione, and Maria Cristina Buia (1989). "Spatio-Temporal Distribution of Algal and Animal Communities in a Posidonia oceanica Meadow". en. In: *Marine Ecology* 10.2, pp. 107–129. DOI: 10.1111/j.1439-0485.1989.tb00069.x. (Visited on 04/25/2019).

Mishra, Amarendra Narayan (2018). "Chlorophyll Fluorescence: A Practical Approach to Study Ecophysiology of Green Plants". en. In: *Advances in Plant Ecophysiology Techniques*. Ed. by Adela M. Sánchez-Moreiras and Manuel J. Reigosa. Cham: Springer International Publishing, pp. 77–97. DOI: 10.1007/978-3-319-93233-0_5. (Visited on 04/02/2019).

Muller, P. (2001). "Non-Photochemical Quenching. A Response to Excess Light Energy". en. In: *PLANT PHYSIOLOGY* 125.4, pp. 1558–1566. DOI: 10.1104/pp.125.4.1558. (Visited on 05/04/2019).

Nielsen, S (2010). "Phenol-Sulfuric Acid Method for Total Carbohydrates". en. In: *Food Analysis Laboratory Manual*. Ed. by S. Suzanne Nielsen. Boston, MA: Springer US, pp. 47–53. DOI: 10.1007/978-1-4419-1463-7_6.

Nordlund, Lina Mtwana et al. (2016). "Seagrass Ecosystem Services and Their Variability across Genera and Geographical Regions". en. In: *PLOS ONE* 11.10, e0163091. DOI: 10.1371/journal.pone.0163091. (Visited on 05/30/2019).

Pearson, R.K. (2001). "Exploring process data". In: *Journal of Process Control* 11.2, pp. 179–194. DOI: 10.1016/S0959-1524(00)00046-9.

Pergent, G., C. Pergent-Martini, and M. Cambridge (1997a). "Morphochronological variations in the genus Posidonia". en. In: *Mar. Freshwater Res.* 48.5, pp. 421–424. DOI: 10.1071/mf96100. (Visited on 04/28/2019).

Pergent, Gérard and Christine Pergent-Martini (1991). "Leaf renewal cycle and primary production ofPosidonia oceanica in the bay of Lacco Ameno (Ischia, Italy) using lepidochronological analysis". In: *Aquatic Botany* 42.1, pp. 49–66. DOI: 10.1016/0304-3770(91)90105-E. (Visited on 04/21/2019).

Pergent, Gérard, Valérie Rico-Raimondino, and Christine Pergent-Martini (1997b). "Fate of primary production in Posidonia oceanica meadows of the Mediterranean". In: *Aquatic Botany* 59.3, pp. 307–321. DOI: 10.1016/S0304-3770(97)00052-1. (Visited on 04/28/2019).

Pergent, Gérard et al. (1989). "Cyclic Changes along Posidonia oceanica Rhizomes (Lepidochronology): Present State and Perspectives". en. In: *Marine Ecology* 10.3, pp. 221–230. DOI: 10.1111/j.1439-0485.1989.tb00474.x. (Visited on 05/30/2019).

Personnic, Sébastien et al. (2014). "An Ecosystem-Based Approach to Assess the Status of a Mediterranean Ecosystem, the Posidonia oceanica Seagrass Meadow". en. In: *PLOS ONE* 9.6. DOI: 10.1371/journal.pone.0098994. (Visited on 08/03/2018).

Piazzi, Luigi, David Balata, and Giulia Ceccherelli (2016). "Epiphyte assemblages of the Mediterranean seagrass Posidonia oceanica: an overview". en. In: *Marine Ecology* 37.1, pp. 3–41. DOI: 10.1111/maec.12331. (Visited on 05/30/2019).

Pirc, Helmut (1986). "Seasonal aspects of photosynthesis in Posidonia oceanica: Influence of depth, temperature and light intensity". In: *Aquatic Botany* 26, pp. 203–212. DOI: 10.1016/0304-3770(86)90021-5.

Platt, T, C.L. Gallegos, and W. G. Harrison (1980). "Photoinhibition of photosynthesis in natural assemblages of marine phytoplankton". In: *Journal of Marine Research* 38, pp. 687–701.

Procaccini, Gabriele et al. (2017). "Depth-specific fluctuations of gene expression and protein abundance modulate the photophysiology in the seagrass *Posidonia oceanica*". en. In: *Scientific Reports* 7, p. 42890. DOI: 10.1038/srep42890. (Visited on 04/20/2019).

Ralph, Peter J. and Rolf Gademann (2005). "Rapid light curves: A powerful tool to assess photosynthetic activity". In: *Aquatic Botany* 82.3, pp. 222–237. DOI: 10.1016/j.aquabot.2005.02.006.

Ralph, P.J. (1999). "Light-Induced Photoinhibitory Stress Responses of Laboratory-Cultured Halophila ovalis". In: *Botanica Marina* 42, pp. 11–22. DOI: https://doi.org/10.1515/BOT.1999.003.

Ralph, P.J. et al. (2002). "Operation of the xanthophyll cycle in the seagrass Zostera marina in response to variable irradiance". In: *Journal of Experimental Marine Biology and Ecology* 271, pp. 189–207. DOI: https://doi.org/10.1016/S0022-0981(02)00047-3.

Richir, J. et al. (2013). "Experimental in situ exposure of the seagrass Posidonia oceanica (L.) Delile to 15 trace elements". en. In: *Aquatic Toxicology* 140-141, pp. 157–173. DOI: 10.1016/j.aquatox.2013.05.018.

Ruiz, J. M. et al. (2017). "Experimental evidence of warming-induced flowering in the Mediterranean seagrass Posidonia oceanica". In: *Marine Pollution Bulletin*. Securing a future for seagrass 134, pp. 49–54. DOI: 10.1016/j.marpolbul.2017.10.037. (Visited on 04/21/2019).

Ruiz, Juan Manuel and Javier Romero (2001). "Effects of in situ experimental shading on the Mediterranean seagrass Posidonia oceanica”. In: *Marine Ecology Progress Series* 215, pp. 107–120.

Saroussi, Shai and Sven Beer (2007). “Alpha and quantum yield of aquatic plants derived from PAM fluorometry: Uses and misuses”. In: *Aquatic Botany* 86.1, pp. 89–92. DOI: 10.1016/j.aquabot.2006.09.003.

Schober, Patrick, Christa Boer, and Lothar A. Schwarte (2018). “Correlation Coefficients: Appropriate Use and Interpretation”. In: *Anesthesia & Analgesia* 126.5, pp. 1763–1768. DOI: 10.1213/ANE.0000000000002864.

Schreiber, Ulrich (2004). “Pulse-Amplitude-Modulation (PAM) Fluorometry and Saturation Pulse Method: An Overview”. en. In: *Chlorophyll a Fluorescence*. Ed. by George Christos Papageorgiou and Govindjee. Vol. 19. Dordrecht: Springer Netherlands, pp. 279–319. DOI: 10.1007/978-1-4020-3218-9_11. (Visited on 04/02/2019).

Serrano, O., M. A. Mateo, and P. Renom (2011). “Seasonal response of Posidonia oceanica to light disturbances”. en. In: *Marine Ecology Progress Series* 423, pp. 29–38. DOI: 10.3354/meps08955. (Visited on 06/02/2019).

Silva, J and R Santos (2003). “Daily variation patterns in seagrass photosynthesis along a vertical gradient”. In: *Mar. Ecol. Prog. Ser.* 257, pp. 37–44. DOI: 10.3354/meps257037.

Silva, J et al. (2009). “Measuring seagrass photosynthesis: methods and applications”. en. In: *Aquat. Biol.* 7, pp. 127–141. DOI: 10.3354/ab00173. (Visited on 06/07/2019).

Taiz, Lincoln, Eduardo Zeiger, and Ian Max Møller, eds. (2015). *Plant physiology and development*. 6th ed. Sunderland: Sinauer associates. ISBN: 978-1-60535-255-8.

Telesca, Luca et al. (2015). “Seagrass meadows (*Posidonia oceanica*) distribution and trajectories of change”. en. In: *Scientific Reports* 5. DOI: 10.1038/srep12505. (Visited on 05/30/2019).

Telfer, Alison (2002). “What is β–carotene doing in the photosystem II reaction centre?” In: *Phil. Trans. R. Soc. Lond. B* 357.1426. Ed. by J. Barber and J. M Anderson, pp. 1431–1440. DOI: 10.1098/rstb.2002.1139.

The Angiosperm Phylogeny Group (2016). “An update of the Angiosperm Phylogeny Group classification for the orders and families of flowering plants: APG IV”. en. In: *Botanical Journal of the Linnean Society* 181.1, pp. 1–20. DOI: 10.1111/boj.12385. (Visited on 04/19/2019).

Tomasello, Agostino et al. (2016). “Reference growth charts for Posidonia oceanica seagrass: An effective tool for assessing growth performance by age and depth”. In: *Ecological Indicators* 69, pp. 50–58. DOI: 10.1016/j.ecolind.2016.04.005. (Visited on 05/30/2019).

Tussenbroek, Brigitta I. et al. (2006). “The Biology of Thalassia: Paradigms and Recent Advances in Research”. In: *Seagrasses: Biology, Ecology and Conservation*. Springer. Dordrecht: Larkum Anthony. W.D., Orth Robert J., Duarte Carlos M., pp. 409–439.

Vassallo, Paolo et al. (2013). “The value of the seagrass Posidonia oceanica: A natural capital assessment”. In: *Marine Pollution Bulletin* 75.1, pp. 157–167. DOI: 10.1016/j.marpolbul.2013.07.044. (Visited on 05/19/2019).

Via, Josef Dalla et al. (1998). “Light gradients and meadow structure in Posidonia oceanica:ecomorphological and functional correlates". en. In: *Marine Ecology Progress Series* 163, pp. 267–278. DOI: `10.3354/meps163267`.

White, Anthony J and Christa Critchley (1999). "Rapid light curves: A new fluorescence method to assess the state of the photosynthetic apparatus". en. In: *Photosynthesis Research* 59.1, pp. 63–72.

Zar, Jerrold H. (2010). *Biostatistical Analysis*. Prentice Hall. 966 pp.

Zieman, Joseph C. (1974). "Methods for the study of the growth and production of turtle grass, Thalassia testudinum König". In: *Aquaculture* 4, pp. 139–143. DOI: `10.1016/0044-8486(74)90029-5`. (Visited on 04/21/2019).

6

Supplemental data

6.1 Carbohydrates protocols comparaison

6.1.1 Material and Methods

Several protocols for quantification of carbohydrates concentrations were compared. Three parameters (extraction temperature and duration, use of activated coal or not and coloration method) were tested in a nested design (table 6.1) on *P. oceanica* samples. Furthermore, efficiency of starch hydrolysis with 1M HCl was assessed with lugol (I_2/KI).

Extraction	**Coal**	**Coloration**	**n**
5', room temp.	Yes	Phenol	8
5', room temp.	Yes	Anthrone	8
5', room temp.	No	Phenol	8
5', room temp.	No	Anthrone	8
30', 80°C	Yes	Phenol	8
30', 80°C	Yes	Anthrone	8
30', 80°C	No	Phenol	8
30', 80°C	No	Anthrone	8

Table 6.1: **Experimental nested degin for protocols comparaison**

About 5 g of leaves were cut into small pieces and pooled together. For each sample, 100-150 mg of these leaf fragments were grinded (30 HZ, 4x30" runs with freezing in liquid nitrogen between each run). Soluble carbohydrates were extracted twice in 70% ethanol (in 10 mL first, then in 6 mL), either 5' at room temperature or 30' at 80°C, then centrifugated (8000 rpm, 10'). For half of the samples, 30 mg of powdered activated coal was added, then shaked for 2 hours and centrifugated (5000 rpm, 8'). 200 µL of each sample were colorized either with 1 mL of an anthrone/H_2SO_4

method (0.5 g anthrone in 250 mL H_2SO_4 95% and 10 mL water) or with 1 mL of a phenol/H_2SO_4 solution (H_2SO_4 95% and 200 µL of phenol 5%). Phenol/H_2SO_4 samples were homogenized, left 10' at room temperature, homogenized again and left 30' in the same situation. Anthrone/H_2SO_4 samples were incubated 10' in a boiling water bath (100°C) and immediately cooled in ice. Absorbance at 490 nm and 625 nm for phenol/H_2SO_4 and anthrone/H_2SO_4 coloration, respectively, was measured spectrophotometrically after a calibration with D-glucose.

Powder activated coal was also tested on pure D-glucose samples. D-glucose solutions were prepared (20-40-60 µg/L, 1.5 mL) and half of them were shaked two hours with 30 mg of powered activated coal. After centrifugation (8000 rpm, 10'), samples were colorized with phenol/H_2SO_4 method.

6.1.2 Results and Discussion

Activated coal should not be used to remove pigments given its strong effect on carbohydrates as well (fig. 6.1(b)). Extraction at a higher temperature seems to increase carbohydrates extraction efficiency (fig. 6.1(d)). However, it could be the consequence of heat-induced depolymerization of complex carbohydrates (e.g. starch). The difference between warm and cold extraction is weak, therefore a cold extraction will be selected. There is no difference between coloration methods (fig. 6.1(c)), which is not surprising since each absorbance measurement is based on a calibration prepared with the same coloration method.

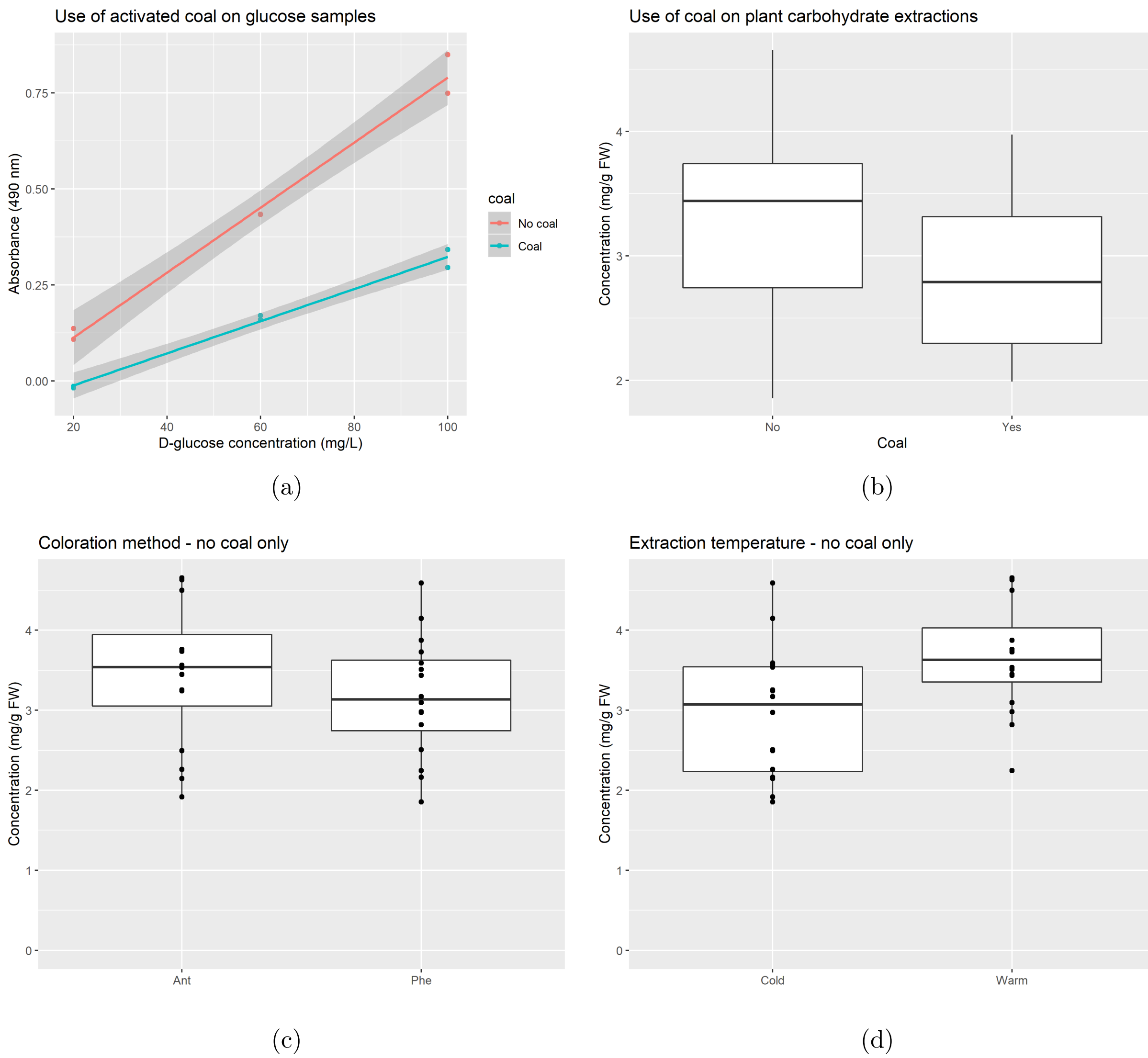

Figure 6.1: **Comparaison of protocols for quantification of carbohydrates in *P. oceanica*.** (a) Powdered activated coal strongly decreases glucose concentration. 200 µL of three glucose solutions (20-40-60 mg/L) were colorized with 200 µL phenol and 1 mL H_2SO_4 95%; absorbance was read at 490 nm. (b) Powdered activated coal decreases measured carbohydrate concentration at the spectrophotometer. (c) Coloration method effect on measured carbohydrate concentration at the spectrophotometer. (d) Extraction temperature effect on absorbance measurement. P-values are from three-factor anova tests.

6.2 Carbohydrates

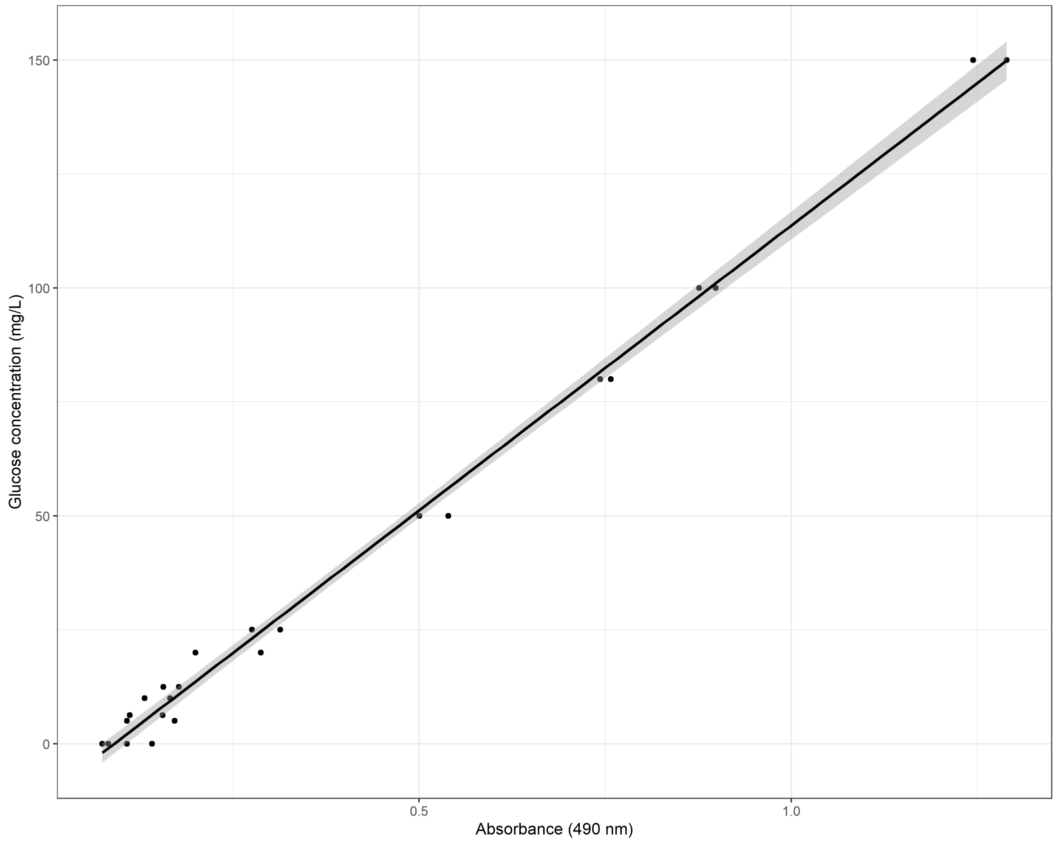

Figure 6.2: **Calibration the spectrophotometer with D-glucose. R^2=0.9936 (linear regression)**

6.3 Biometry

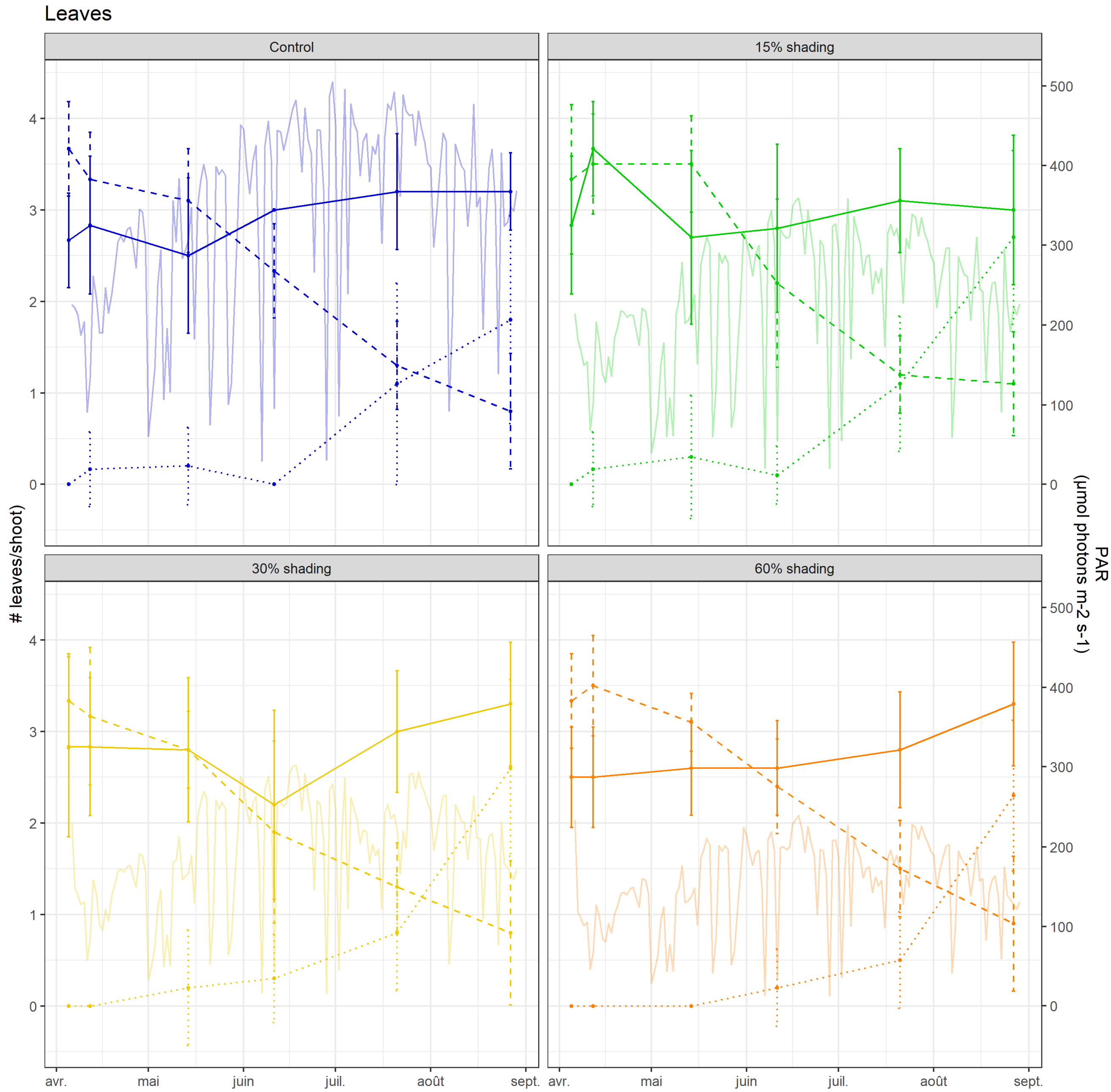

Figure 6.3: **Leaf developmental stage. Adult leaves (solid lines), intermediate leaves (dashed lines) and juvenile leaves (dotted lines).**

Figure 6.4: **Total shoot surface**

6.4 Porewater chemistry

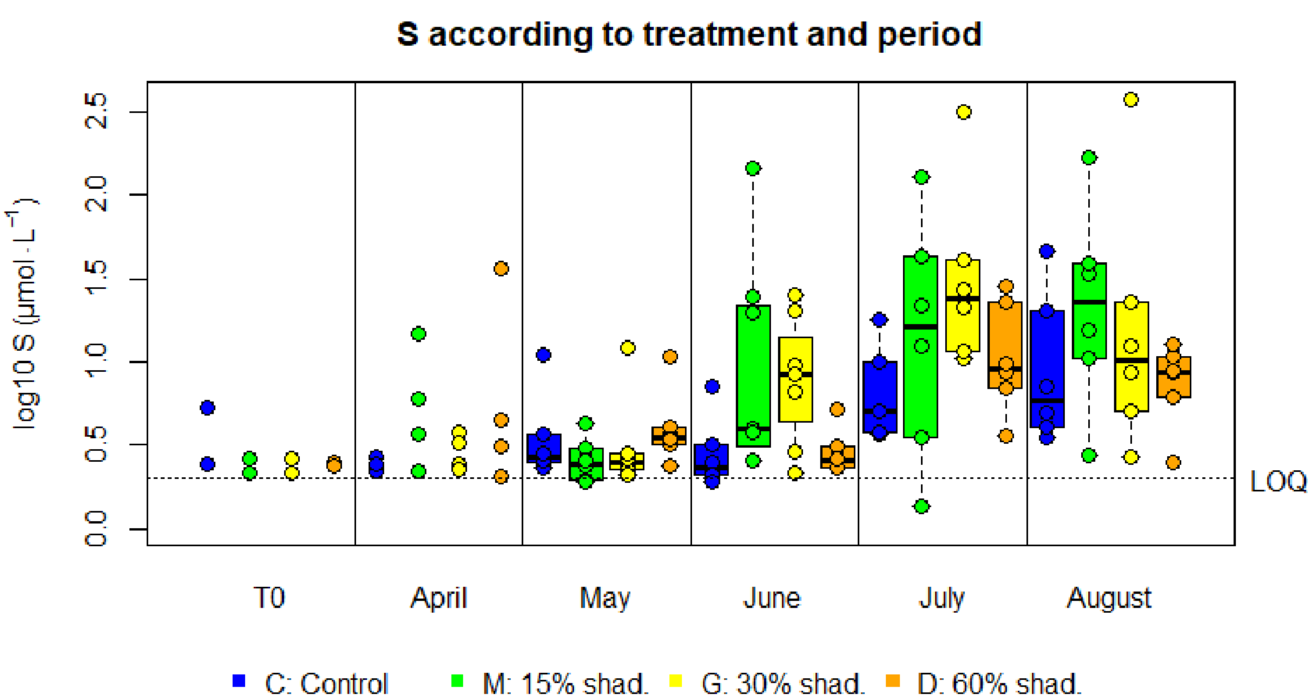

Figure 6.5: **S concentration in porewater.**
Work of J. Richir.

6.5 Statistics

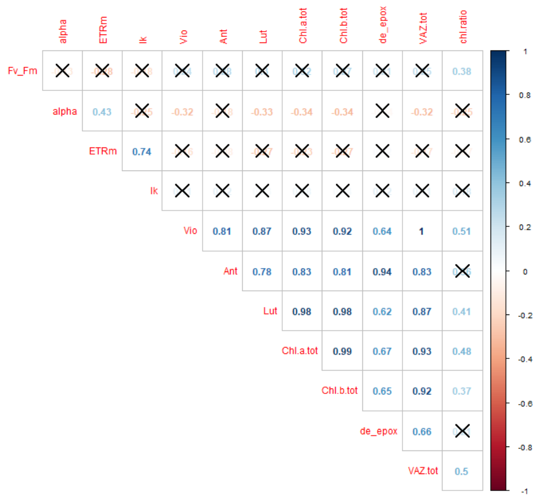

Figure 6.6: **Correlation matrix (Spearman's rho coefficient) of mean pigments and PI curves parameters on dark-adapted samples for each date/shading combination. Non significant correlations (p > 0.05) are crossed.**

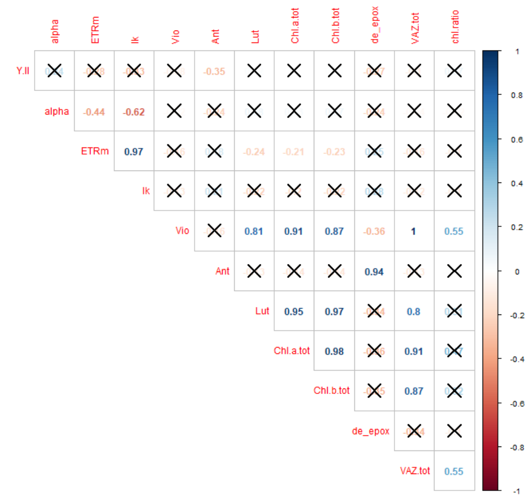

Figure 6.7: **Correlation matrix (Spearman's rho coefficient) of mean pigments and RLC curves parameters on light-adapted samples for each date/shading combination.**

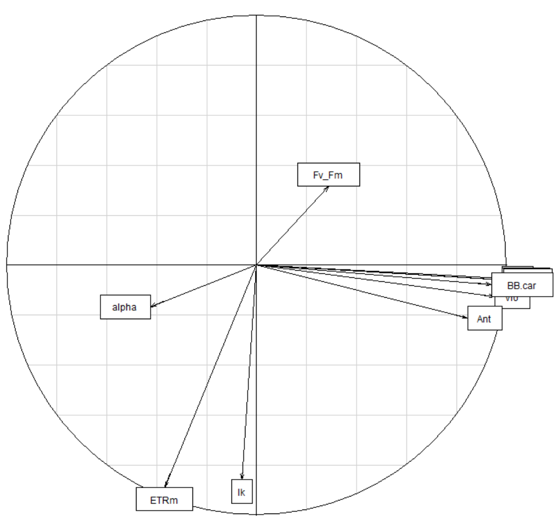

Figure 6.8: **PCA correlation circle for dark-adapted samples.**

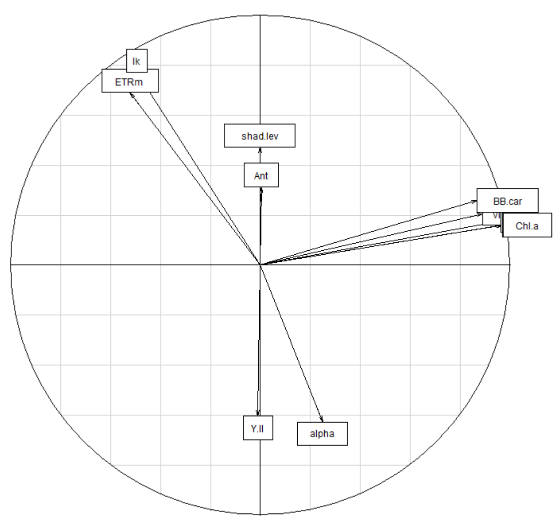

Figure 6.9: **PCA correlation circle for light-adapted samples.**

Parameter	Surf/shoot DW	Epiphytes DW	Epiphytes DW/surface	Max. length	A coefficient
Intercept	0.2828	0.2780	0.8331	0.0001	0.0238
date.num	0.2643	0.2700	0.8159	0.0001	0.0234
date.num'	0.0503	0.0113	0.0580	0.1762	0.2555
treat=M	0.8654	0.5447	0.9493	0.9142	0.9570
treat=G	0.5488	0.0496	0.2382	0.8230	0.6311
treat=D	0.8088	0.4450	0.5499	0.3056	0.8441
date.num * treat=M	0.8654	0.5445	0.9500	0.9115	0.9573
date.num' * treat=M	0.7838	0.6822	0.7750	0.9549	0.8654
date.num * treat=G	0.5475	0.0494	0.2373	0.8231	0.6318
date.num' * treat=G	0.3776	0.0615	0.2922	0.7576	0.7111
date.num * treat=D	0.8083	0.4443	0.5490	0.3054	0.8434
date.num' * treat=D	0.7984	0.5619	0.6763	0.3214	0.7150

Table 6.2: **Biometry - p-values for ols model**

Parameter	Chl a	Chl b	VAZ	Lutein	$\beta\beta$-carotene
Intercept	0.0000	0.0000	0.0000	0.0000	0.0000
date.num	0.0000	0.0000	0.0000	0.0000	0.0000
date.num'	0.0062	0.0080	0.0041	0.0060	0.0001
treat=M	0.7076	0.6717	0.6226	0.7440	0.3336
treat=G	0.8466	0.9415	0.6959	0.6269	0.1313
treat=D	0.1532	0.0945	0.0214	0.3248	0.2026
date.num * treat=M	0.7078	0.6720	0.6211	0.7443	0.3334
date.num' * treat=M	0.9760	0.9436	0.3748	0.9903	0.2293
date.num * treat=G	0.8462	0.9412	0.6971	0.6265	0.1317
date.num' * treat=G	0.5982	0.6368	0.9466	0.4236	0.3794
date.num * treat=D	0.1536	0.0947	0.0214	0.3255	0.2029
date.num' * treat=D	0.2504	0.1719	0.0196	0.4804	0.2509

Table 6.3: **Pigments - p-values for ols models**

Parameter	Soluble carbohydrates	Starch
Intercept	0.5478	0.0559
date.num	0.5527	0.0550
date.num'	0.0001	0.8286
treat=M	0.9534	0.5663
treat=G	0.2212	0.2556
treat=D	0.4435	0.6530
date.num * treat=M	0.9541	0.5658
date.num' * treat=M	0.3162	0.7083
date.num * treat=G	0.2207	0.2545
date.num' * treat=G	0.0197	0.0057
date.num * treat=D	0.4438	0.6524
date.num' * treat=D	0.5656	0.0936

Table 6.4: **Carbohydrates - p-values for ols models**

Parameter	Y(II)	RLC-ETRm	RLC-Ik	RLC-α	PI-ETRm	PI-Ik	PI-α
Intercept	0.0010	0.0001	0.0003	0.8136	0.2967	0.0824	0.0001
date.num	0.0012	0.0001	0.0003	0.8549	0.2817	0.0877	0.0000
date.num'	0.0026	0.0000	0.0002	0.9918	0.3110	0.3380	0.0033
treat=M	0.6840	0.2176	0.1974	0.1072	0.0068	0.0049	0.2619
treat=G	0.0357	0.3662	0.4150	0.1097	0.1351	0.3858	0.8064
treat=D	0.0592	0.5083	0.4158	0.8719	0.1078	0.0345	0.1839
date.num * treat=M	0.6831	0.2180	0.1979	0.1073	0.0067	0.0049	0.2628
date.num' * treat=M	0.6414	0.4707	0.4468	0.1562	0.0074	0.0195	0.6995
date.num * treat=G	0.0353	0.3673	0.4168	0.1104	0.1346	0.3853	0.8058
date.num' * treat=G	0.0859	0.6376	0.7602	0.2183	0.0990	0.4008	0.5862
date.num * treat=D	0.0586	0.5059	0.4135	0.8718	0.1081	0.0346	0.1841
date.num' * treat=D	0.0803	0.2303	0.1919	0.9894	0.1757	0.1397	0.4817

Table 6.5: **Photosynthetic activity - p-values for ols model**

Parameter	Chl a/Chl b ratio	F_v/F_v	Shoot DW	Primary production DW
Intercept	0.0000	0.0673	0.1321	0.0805
date.num	0.0000	0.3228	0.1207	0.0852
treatM	0.6481	0.0081	0.1553	0.6545
treatG	0.2435	0.0043	0.4051	0.7820
treatD	0.9605	0.5827	0.2068	0.4802
date.num:treatM	0.6494	0.0080	0.1548	0.6541
date.num:treatG	0.2433	0.0044	0.4035	0.7847
date.num:treatD	0.9566	0.5869	0.2065	0.4823

Table 6.6: **p-values for quantile regression models**

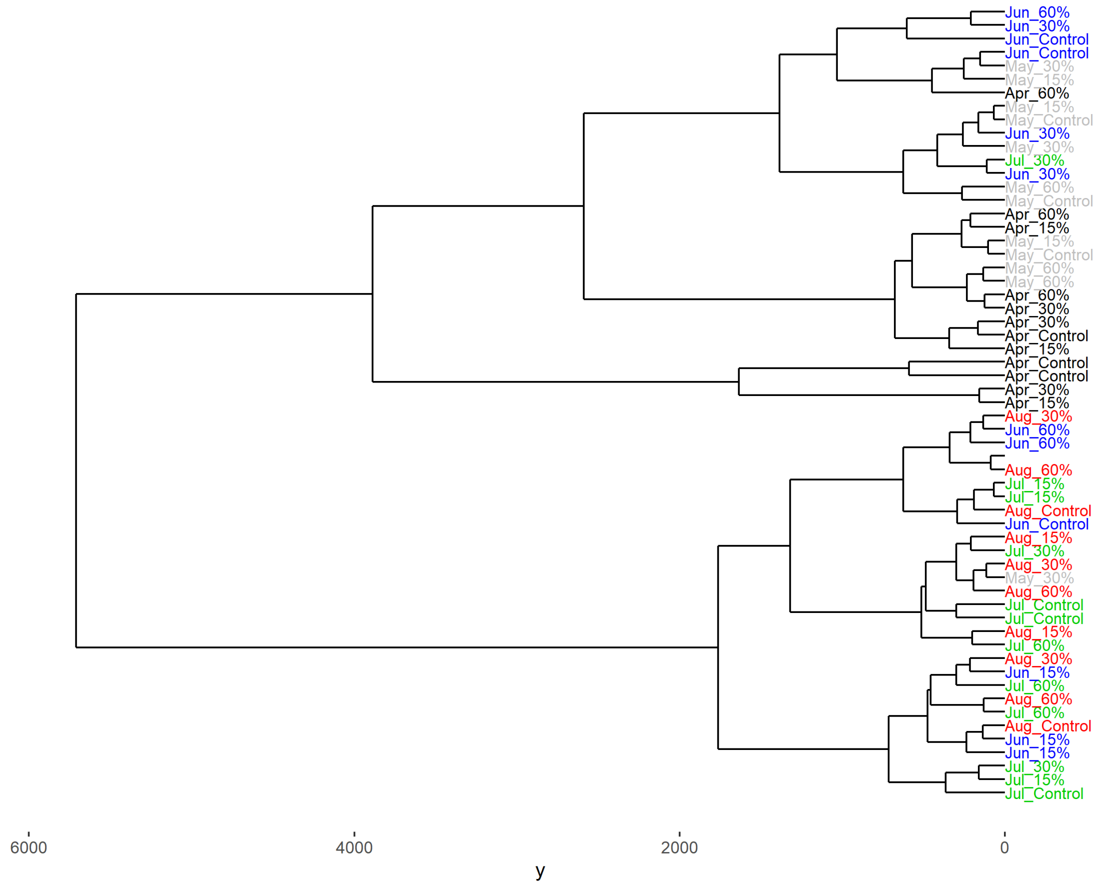

Figure 6.10: **Global cluster analysis including all investigated variables, averaged over dates and treatments.**

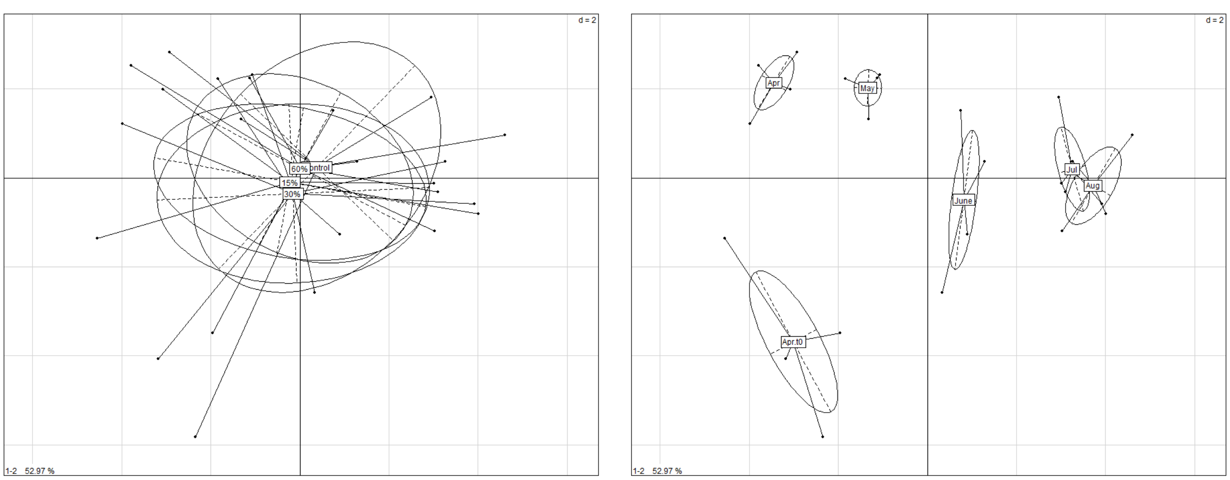

(a) (b)

Figure 6.11: **Principal component analyses with all investigated variables. (a) Observations (i.e. means over monthes and treatments) are grouped by treatment; (b) Observations are grouped by month. The two first axes are presented, that explain 52.97% of total variance.**

UNIVERSITE CATHOLIQUE DE LOUVAIN
Faculté des Sciences
Place des Sciences, 2 bte L6.06.01, 1348 Louvain-la-Neuve, Belgique | www.uclouvain.be/sc